Title

Breaking Schistosomiasis Transmission: Challenges, Opportunities, and a Path Forward

Author

Hoover, Christopher M

Publication Date

2020

Peer reviewed|Thesis/dissertation

Breaking Schistosomiasis Transmission: Challenges, Opportunities, and a Path Forward

by

Christopher M Hoover

A dissertation submitted in partial satisfaction of the

Requirements for the degree of

Doctor of Philosophy

in

Environmental Health Sciences

in the

Graduate Division

of the

University of California, Berkeley

Committee in charge:

Professor Justin Remais, Chair
Professor Jay Graham
Professor Joe Lewnard

Fall 2020

Breaking Schistosomiasis Transmission: Challenges, Opportunities, and a Path Forward

by

Christopher M Hoover

Abstract

Breaking Schistosomiasis Transmission: Challenges, Opportunities, and a Path Forward

by

Christopher M Hoover

Doctor of Philosophy in Environmental Health Sciences

University of California, Berkeley

Professor Justin Remais, Chair

Schistosomiasis is the second most debilitating parasitic disease of humans in the world, trailing only malaria in terms of its harmful effects on global human health. Schistosomiasis is caused by infection with trematode parasites of the genus *Schistosoma* that are transmitted via intermediate host snails and thrive in areas of the world which lack adequate access to safe water, sanitation, and hygiene. One of many neglected tropical diseases (NTDs), schistosomiasis is slated for elimination in the coming decades due to the availability of cheap and effective drugs to cure the disease. Like other diseases caused by helminthic parasites, schistosomiasis transmission is hypothesized to be limited by positive density dependent mate limitation, giving rise to a transmission breakpoint below which elimination becomes inevitable. This breakpoint represents a logical target for elimination campaigns, but there has been little effort devoted to empirically estimating the breakpoint population size of schistosomes. Furthermore, there has been limited investigation of the implications of breakpoints for elimination strategies.

This dissertation seeks to fill these research gaps, using mathematical modeling and statistical analysis to investigate the breakpoint dynamics of schistosomiasis for the first time. Chapter 1 contextualizes schistosomiasis transmission, providing background on associated pathology and global burden, the schistosome life cycle, and the influence of positive density dependence on schistosomiasis transmission. Chapter 2 explores the dynamics of schistosome aggregation, a key determinant of the strength of positive density dependence, and its implications for the breakpoint. Chapter 3 proposes a novel intervention, the use of prawn aquaculture as a biocontrol agent and a source of revenue in impoverished areas, to combat schistosomiasis. Chapter 4 introduces a modeling framework and a novel, individual-based model of schistosomiasis to estimate schistosomiasis transmission breakpoints and to simulate intervention strategies including mass drug administration, snail control, snail habitat reduction, sanitation, and education to identify strategies that most effectively suppress transmission below the breakpoint. Chapter 5 concludes with commentary on the future of schistosomiasis control and elimination, some reflections on the strengths and limitations of the work, and future directions for the ideas introduced here.

Table of Contents

Acknowledgments

Having completed more than twenty years of education, it appears as though I am now worthy of the honorific “doctor”, which feels quite strange. I have been fortunate to grow up in the presence of other doctors, my parents and grandfather being doctors of the veterinary variety, but the term did not carry so much resonance for me until the past few months. It now carries the weight of long hours and many years spent in the pursuit of knowledge, and none of it would have been possible without the help of many other doctors.

Although they never said it explicitly, my parents made it abundantly clear that I was free to pursue whatever I wanted in life and they made it possible for me with little apparent effort. Except I know now that it required herculean effort and immense sacrifice. This dissertation does not grant me a PhD in economics or physics, but I am quite certain that loving parents are the single most valuable resource and the strongest force in the universe. Mike and Diane, Dr. Bruner and Dr. Hoover, Mom and Dad: thank you, I love you, none of this would have been possible without you.

As a middle child, I like to think I am a blend of the attributes that make my elder brother and younger sister the incredible people they are. Daniel, you are the most knowledgeable dude I know, and my career in academia will be a constant struggle to know a little bit more about a small part of the world than you. McKenna, you are the most caring and creative person I know and I hope to be half as decent a teacher as you in my career.

Once my family handed me off to Emory University, Donal Bisanzio, Gonzalo Vazquez-Prokopec, and JR McMillan were kind enough to invest their time molding me into a scientist when I still was not quite sure what it meant. I joined Emory’s vector ecology group as a kid who wanted to be outside and get some class credit for it, but I left it as someone with ideas and passion for a career that they continue to exemplify today.

From the vaguely workable chunk of Georgia clay that emerged from the vector ecology group, Justin Remais next took over and molded me into a passable piece of California pottery. As my first boss, my impetus for moving across the country on a whim, and my dissertation advisor, there are few individuals who have shaped my life more, and I am a better person and far better scientist because of his guidance these past six years.

My time at Berkeley has also been made more enjoyable and productive by the world class faculty I have gotten to meet. Ellen Eisen, John Balmes, Carl Boettiger, Joe Lewnard, Jay Graham, Kirk Smith, and Maya Petersen loaded more into my brain than I thought was possible, and I look forward to learning yet more from them. In addition, Giulio de Leo and Sanna Sokolow (from that other University) went from being names on papers that I admired to close collaborators and friends.

Speaking of friends, I could not have made it through the classes, setbacks, and frustrations and I would have had far less fun without the comradery and shenanigans of Phil Collender, Tomás León, Nick Skaff, Carly Hyland, Jackie Ferguson, Jennifer Head, Qu Cheng, Karina Cucchi, Andrea Lund, Isabel Jones, and anyone else who was always down to find a table at Triple Rock

on Friday afternoon. It is an incredible privilege to know a group of such incredibly smart, genuine, and fun people.

Finally, to my partner, Heather. We thought we would be a few months into our marriage together right now, but here we are in 2020. If there is a silver lining to this year, it's that I have gotten to spend nearly every waking minute of every day with you. Thank you for moving to California for me, thank you for keeping me grounded, for being my best hiking partner, my sous chef, my study buddy, and my best friend. Living every day with you, Bullet, and Moose brings me endless joy and I cannot wait to spend the rest of my life with you.

Chapter 1: Introduction: Schistosomiasis transmission, pathology, global burden, and current control strategies

1.1 Structure and significance of dissertation

This dissertation is organized as five chapters. Chapter 1 provides an introduction to key concepts that run through the dissertation including schistosome parasites, the disease schistosomiasis, the global burden of schistosomiasis, and breakpoints. Chapter 2 explores the influence of schistosome aggregation dynamics on breakpoints as human populations are treated and other control efforts are implemented; drawing on data from one of the largest randomized control trials assessing schistosomiasis interventions ever conducted in an elimination setting. Chapter 3 draws on models and theory from ecology, epidemiology, and economics to evaluate the potential of a novel intervention to combat schistosomiasis and the conditions which facilitate its spread. Chapter 4 incorporates theory, dynamic model simulations, and data from ongoing studies in the lower Senegal River basin—the site of one of the largest known outbreaks of schistosomiasis ever—to suggest a shift in focus from purely pharmaceutical interventions to intervention strategies that explicitly alter the breakpoint, making sustainable control and elimination more feasible. Chapter 5 places Chapters 2-4 in the broader context of global and environmental health and provides some conclusions and reflections on the work and process presented herein.

1.2 Transmission, Pathology, and Diagnosis

Schistosomiasis, also known as Bilharzia, is a parasitic disease caused by trematodes of the genus *Schistosoma* that undergo a complex lifecycle involving passage through the environment between definitive human hosts and intermediate host snails. Intestinal schistosomiasis is caused by schistosome species, including *S. mansoni*, *S. japonicum*, *S. mekongi*, and *S. intercalatum*, that reside in the mesenteric vasculature surrounding the intestines while urinary schistosomiasis is caused by *S. haematobium* which live in the vasculature surrounding the bladder. Humans become infected when exposed to freshwater infested with free-living, aquatic schistosome larvae called cercariae that penetrate the skin and mature into adult worms. These adult worms mate sexually within the human host and begin laying eggs that are shed in the urine or feces of infected individuals. Miracidia, another free-living aquatic larval stage, hatch from these eggs, infect specific species of intermediate host snails, and develop into sporocysts which begin shedding cercariae to infect humans and complete the transmission cycle.

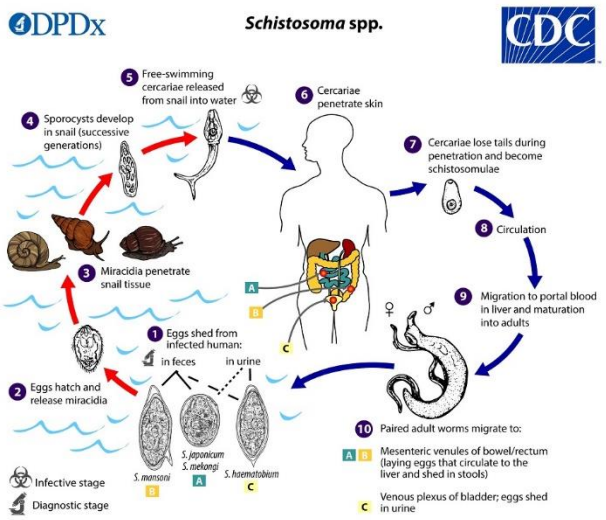

Figure 1.2.1 Schistosome lifecycle (https://www.cdc.gov/parasites/schistosomiasis/biology.html)

Pathology associated with schistosomiasis can be caused by an acute Th-1 type immune response to schistosomulae that enter circulation following cercarial penetration.[1] Symptoms associated with acute infection include fever, abdominal pain, and diarrhea.[1] The presence of eggs that lodge in the intestine, bladder, and other tissues can also cause more severe outcomes.[1] Because adult schistosomes can live for five years or more, chronic infections that go untreated can lead to large numbers of eggs enclosed in granulomas which cause fibrosis of the liver, spleen, intestines, bladder, and other organs.[1] Children who are chronically infected can also experience developmental delays caused by anemia and malnutrition.[1] Urinary schistosomiasis in particular may also cause genital pathology and has been associated with increased risk of HIV infection.[2,3]

Diagnosing schistosomiasis has generally relied on identifying eggs in the urine or feces of infected individuals or by hematuria in the case of urinary schistosomiasis. Because pathology is associated with the intensity of infection, (i.e. number of egg-laying worm pairs) egg-based diagnostics are essential to identify high-burden infections characterized by large amounts of eggs detected in stool or urine samples. Two key metrics are used to determine the community-level infection intensity: the mean egg burden and the prevalence of egg shedding. However, egg-based diagnostics suffer from low sensitivity, particularly at low infection intensities where samples may not contain eggs despite active infection. Recently, cheap and effective point of care molecular diagnostics that detect circulating antigens to adult schistosomes have been developed and found to improve case-identification in low-transmission settings.[4–6]

1.3 Global Burden, Epidemiology, and Control

Schistosomiasis is the second most debilitating parasitic disease of humans behind malaria.[7] There are currently more than 200 million people that require treatment, and more than 700 million people live in areas that put them at risk for schistosomiasis.[8] More than 90% of schistosomiasis cases occur in sub-Saharan Africa where *S. mansoni* and *S. haematobium* are most common.[8] In South America, *S. mansoni* remains endemic in some areas of Brazil, Suriname, and Venezuela. A recent outbreak of schistosomiasis associated with *S. mansoni* was

also identified in Corsica, and it appears that local endemicity may have been established.[9] In China and Southeast Asia, *S. japonicum* and, to a lesser extent, *S mekongi* are transmitted.

Schistosomiasis is one of many neglected tropical diseases (NTDs) slated for elimination in the coming decades. The WHO recommends control strategies focused on preventive chemotherapy with the anthelminthic drug Praziquantel. These control strategies are generally implemented in annual mass drug administration (MDA) campaigns to school-aged children (SAC; ages 5-14 years old) due to the relative logistical ease of school-based administration and the high infection intensities commonly observed in children.[8] National control programs across sub-Saharan Africa, large philanthropic donations from national, international, and private organizations, and donations of Praziquantel from Merck have made such MDA campaigns a success in many areas, greatly reducing morbidity associated with schistosomiasis infection.[8,10,11]

However, challenges in the global control of schistosomiasis remain. Implementation of MDA is difficult in remote areas of sub-Saharan Africa and in areas where political conflict or other disturbances such as the 2015 Ebola outbreak in West Africa and the 2020 global pandemic of COVID-19 affect healthcare infrastructure.[11,12] Even in areas where MDA is successfully implemented according to WHO recommendations, transmission sometimes remains stable after multiple years of MDA, with infection intensity and prevalence rebounding to pre-MDA levels prior to the next round of treatment.[10,13–15] For example, in a large group of studies conducted by the Schistosomiasis Consortium for Operational Research and Evaluation (SCORE; https://score.uga.edu/), multiple community- and school-based MDA strategies with different frequencies and "drug holiday years" were tested. Across these strategies, many communities experienced substantial reductions in prevalence between baseline surveys and reassessment at five years. Still other communities, termed "persistent hot-spots", experienced only minor decreases or even increases in prevalence.[15,16] Fine-scale variation between so-called "responder" communities and persistent hot-spots also suggests that highly local factors determine the success or failure of MDA-based control.

Meanwhile, China since 2004 has embarked on a mission to eliminate schistosomiasis using an "integrated" control strategy that focuses on non-pharmaceutical interventions (NPIs) in addition to MDA to treat infected individuals. These NPIs include environmental transmission controls such as reducing snail habitat, molluscicide, and treating or removing zoonotic reservoirs as well as developmental improvements including improving sanitation practices and educating exposed populations to avoid water contact.[17–19] This strategy has been extremely successful, with incidence rates of acute schistosomiasis cases decreasing to 0 in some areas, implying successful interruption of transmission.[17] Translating these successful strategies from China into control programs in sub-Saharan Africa represents a major opportunity.[20] However, progress along this front remains elusive due to challenges implementing the kinds of infrastructural and behavioral improvements that were successful in China in other areas. Furthermore, a theoretical understanding of the interactions between these types of interventions and common MDA-based strategies is lacking.

1.4 The breakpoint: evidence and implications

Positive density dependent (+DD) processes increase the rate of growth of a population as the population size increases. A key consequence of +DD is the emergence of ecological or demographic Allee effects, also commonly referred to as tipping points or breakpoints. Allee effects were first described in 1932 by Walter Clyde Allee, who observed that individual fish had increased fitness in larger, less isolated populations.[21] These processes have important implications for a variety of fields and have been particularly well studied in conservation ecology, where avoiding tipping points that result in population extinction is the goal.[22]

Mate limitation is a source of +DD that produces an Allee effect in a number of large mammal species due to a critical decline in the frequency of encounters between individuals of opposite sexes in a population, or because of a decline in genetic diversity which leaves the population vulnerable to other sources of extinction such as environmental change or disease.[22] Helminthic parasites that mate sexually within definitive human hosts are expected to experience mate limitation at small population sizes as a result of declining encounters between male and female parasites within definitive human hosts. This source of +DD affects the transmission of a variety of helminthic parasites that infect humans, including *Schistosoma*, *Wuchereria*, *Brugia*, and *Onchocerca* parasites as well as those commonly referred to as soil-transmitted helminths (STHs).

Mate limitation is important to global efforts to control and eliminate parasitic diseases because it gives rise to a transmission breakpoint where the number of mated female worms producing viable offspring that carry on the parasite's lifecycle becomes insufficient to sustain transmission. The breakpoint therefore provides a logical target for intervention campaigns that decrease parasite burden, e.g., through the use of MDA, as reducing the parasite population below its breakpoint should result in elimination even without further resources devoted to intervention, assuming no additional external introductions of the parasite in any form. Conceptually, the breakpoint is similar to the herd immunity threshold common to vaccine-preventable diseases in that it represents a key threshold between disease endemicity and elimination; an outbreak or successful control. However, breakpoints are not considered when planning or implementing control and elimination efforts targeting schistosomiasis or other helminthic diseases. This is likely due to suggestions that breakpoints are too small to be relevant to control efforts,[23] but there has never been a concerted effort to estimate schistosomiasis breakpoints from empirical data or explore how they may be manipulated or achieved via efforts to control schistosomiasis.

Schistosomes are unique among helminthic parasites in that they monogamously mate for life, therefore transmission is dependent on schistosomes of opposite sexes successfully infecting the same host, surviving to sexual maturity, and locating each other within the host vasculature. Positive density dependent mate limitation as a result of this process has been hypothesized for schistosomes for more than four decades.[23] This also makes schistosomes more prone to the effects of positive density dependence than other helminths that are polygamous or hermaphroditic.[24] Mate limitation among schistosomes and other helminths is generally

expressed as the mating probability, ϕ, which describes the probability that a given female parasite in a population is successfully mated.[23] This quantity is a function of the parasite population size and the aggregation of parasites among hosts. For schistosomiasis, high transmission intensity and high degrees of parasite aggregation (that lead to individual hosts with very large parasite burdens) both increase the mating probability. At lower transmission intensities, ϕ tends to decrease due to the lower probability that male and female parasites will infect the same individual. However, this decrease is predicated on a common assumption that aggregation remains constant as transmission decreases. If aggregation increases as transmission decreases, the response of ϕ becomes less certain due to the opposing effects of increased aggregation and reduced transmission.

Despite the importance of parasite aggregation and the resulting effects of mate limitation on transmission and elimination thresholds, there is remarkably little empirical investigation of these phenomena among macroparasitic organisms such as schistosomes. A notable exception is the parasitic salmon louse, *Lepeophtheirus salmonis*, which has been found to experience mate limitation that limits its establishment and further proliferation among salmon host populations.[25] An additional study which directly estimated the mating probability of sea lice among salmon also found a negative relationship between parasite abundance, aggregation, and the number of mated female parasites.[26]

Because of the global health importance of helminthic parasites, it is convenient to explicitly define Allee effects in more epidemiological terms. For these parasitic diseases, population growth of the parasite is intrinsically linked to transmission or force of infection and therefore may be estimated by the incidence of the disease in a human population or by estimating the change in infection intensity over time, particularly as intervention efforts such as MDA perturb transmission. The bounce back rate is one such measure of the change in infection intensity derived from epidemiological data collected over the course of routine (e.g. annual) MDA that I have proposed previously.[27] Parasite population size at a given time is related to prevalence, but is often estimated via cross-sectional estimates of infection intensity based on egg diagnostics. Combining longitudinal measures of infection intensity with mathematical models of transmission or using recently developed statistical methods to detect and respond to the presence and strength of +DD [28–30] therefore provides the opportunity to derive empirical evidence of Allee effects in the transmission of a helminthic parasitic disease for the first time.

Because adult schistosomes are not directly observable in human hosts, direct measurement of the parasite population is not possible in epidemiological studies. Laboratory studies suggest that single-sex infections are common and that unmated male schistosomes may manipulate host characteristics to subsequently increase their mating probability.[31,32] Male *S. mansoni* cercariae may also be more infective than female cercariae, and subsequently increase the infectivity of female cercariae once established.[33] Furthermore, unpaired male worms are able to establish and mature, waiting for a female mate, whereas unpaired females may not mature, and may die within 8 weeks due to starvation.[31,33,34] Other experimental studies with *S. japonicum* suggest that immature female worms may survive for up to a year, and single-sex *S. japonicum* infections were common among sentinel mice used to estimate cercarial concentrations in China.[34]

Similarly, a field study of wild rats in Guadeloupe, found that 80% of *S. mansoni* infected rats had dual-sex infections, 18% had single adult male infections, and only 2% had single adult female infections.[35]

There may also be variability in the efficacy of praziquantel to unmated and mated worm pairs. Higher doses of praziquantel are required to kill unmated worms of either sex than mated pairs.[36] Since mated females reside within the groove of males, females may also be shielded from the effects of praziquantel exposure and survive treatment, a potential explanation for observed variability in cure rates over the course of multiple praziquantel administrations.[37] More recently, genotyping miracidia hatched from eggs shed by infected individuals has enabled the study of schistosome population structure over the course of MDA interventions. These studies have produced mixed results, with some finding evidence for decreases in the number of reproducing females, as evidenced by reduced genetic diversity of miracidia following MDA,[38–40] and others finding no such reductions in genetic diversity.[41,42] These discrepancies may be explained by variability in transmission intensity, as high transmission areas are likely to have a more diverse genetic pool than low transmission areas where schistosome populations are more likely to experience mate limitation, thus reducing genetic diversity.

1.5 Data used in the dissertation

The Schistosomiasis Consortium for Operational Research and Evaluation (SCORE) is a Gates Foundation funded project tasked with identifying schistosomiasis intervention strategies that most effectively achieve control and elimination goals.[1] Most of SCORE's operations are in sub-Saharan Africa and focus on *S. mansoni* and *S. haematobium*. In collaboration with local governments and NGOs, SCORE has conducted community randomized trials of different school-based MDA, community-wide MDA, and combined interventions that implement MDA in addition to snail control and WASH improvements. These trials aim to evaluate the most effective strategies for achieving transmission control in high and medium prevalence areas, or for achieving elimination in low transmission areas. I use data from a community-randomized control trial in Zanzibar as part of the Zanzibar Elimination of Schistosomiasis Transmission (ZEST) study that compared biannual MDA to biannual MDA plus snail control and biannual MDA plus a behavioral intervention.[43,44] Zanzibar is a semi-autonomous archipelago of Tanzania off the southeastern coast of Africa, making it a unique area to study schistosomiasis transmission. The ZEST study was conducted in 90 small administrative units called shehias, 45 each on the main islands of Pemba and Unguja. Data collected in these trials include annual evaluations of individual infection burdens measured with egg assays that provide an estimate of infection intensity. These longitudinal estimates of infection intensity are used to estimate aggregation as quantified via the aggregation parameter of a negative binomial distribution, κ, in Chapter 2 and further called upon in Chapter 2 to investigate a novel data-generating distribution to explore underlying mechanisms in schistosome acquisition and their implications for mating dynamics, breakpoints, and elimination feasibility.

In addition to the ZEST data, I draw on data from ongoing studies led by collaborators at Stanford University and the University of Notre Dame in the lower Senegal River basin. These studies include evaluation of novel interventions such as the introduction of aquatic macroarthropod predators of snails, further explored in Chapter 3, and removal and composting of aquatic vegetation that serves as snail habitat. These studies have been described extensively in previous publications.[45–48] I utilize data collected in pre-treatment surveys of school-aged children in twelve of the unmanipulated communities (Fig 1.5.1) enrolled in these studies in the control group to fit and parameterize the dynamic mathematical models described in Chapters 3 and 4.

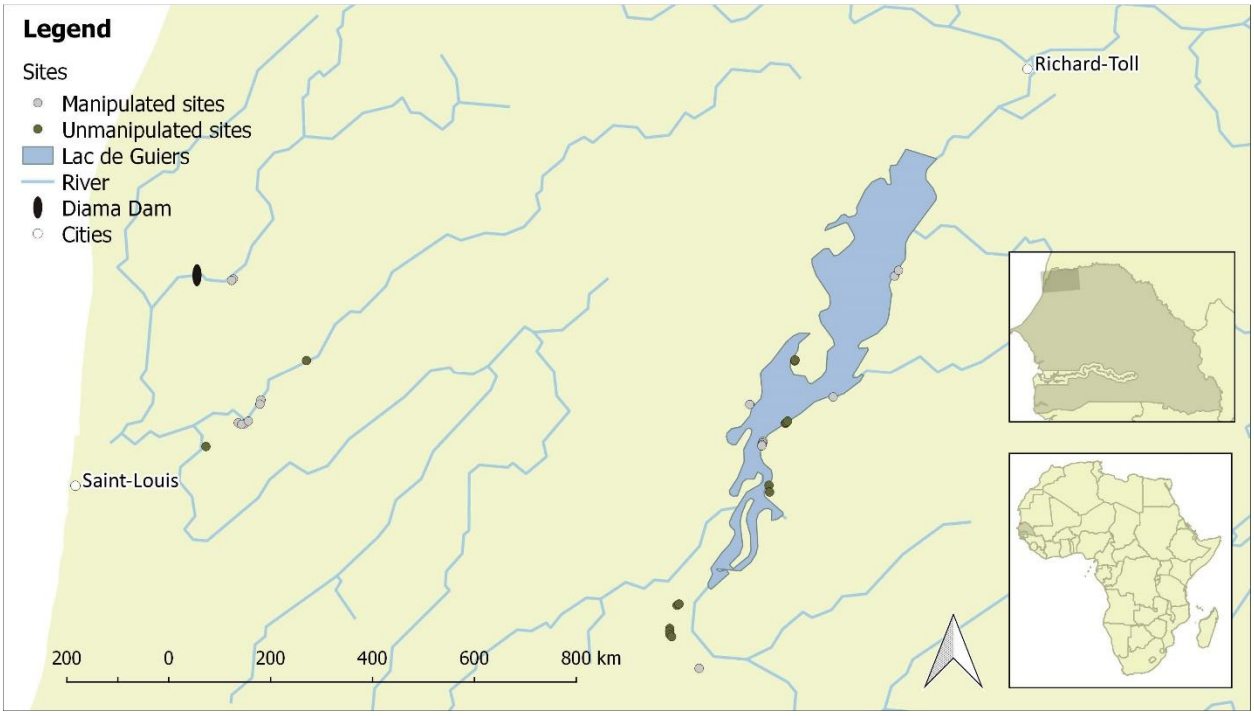

Figure 1.5.1: Study area and sites in the lower Senegal River basin, taken from [47]

Both the ZEST and Senegal data consisted of de-identified records of previously collected data and therefore did not require institutional review board (IRB) approval. I played no role in collecting the original data, but am extremely grateful for the international collaborations that have enabled the following analyses.

Chapter 2: Aggregation dynamics under intense control efforts and implications for schistosomiasis control and elimination

2.1 Practical and theoretical importance of aggregation

Decades of mass drug administration (MDA) have drastically reduced the prevalence and burden of neglected tropical diseases, particularly helminthiases including schistosomiasis, onchocerciasis, lymphatic filariasis (LF), and soil transmitted helminths (STHs). National control programs supported by organizations such as the Gates Foundation and World Health

Organization and drug companies which donate necessary drugs for treatment, have made substantial progress reducing the burden of helminthiases. [49] More recently, the global conversation has shifted towards elimination. China, for instance, has made substantial progress towards elimination of schistosomiasis with an integrated control approach that utilizes MDA in addition to environmental and behavioral controls. [19,20,50] Globally, progress towards elimination is mixed and many areas of sub-Saharan Africa where the vast majority of schistosomiasis and other helminthiases occur have struggled to achieve transmission control and progress towards elimination.

Under sufficient coverage and frequency, elimination using MDA alone is believed to be possible in low and moderate transmission settings. [51] From a practical standpoint, achieving these necessary treatment conditions is challenging due to the programmatic limitations of many control campaigns. School-based interventions, for instance, are often the primary method of drug delivery in communities since they are straightforward to implement and reach school-aged children, widely considered the most vulnerable and most heavily infected segment of the population. However, school-based strategies, and even those that seek to reach all members of the broader community, often miss infected individuals that contribute to transmission. [52,53]

Because of this, control efforts are likely to have profound implications for parasite aggregation: the distribution of parasites among the human host population. While the dynamics of parasite burden following MDA and other interventions have been studied extensively, the corresponding dynamics of aggregation are largely unexplored. Aggregation is measured by the aggregation parameter, κ (also frequently referred to as "dispersion parameter") of a negative binomial distribution. While κ is often considered constant in models and other forward-looking analyses of control efforts, there is reason to believe that it is itself a dynamic variable that is positively correlated with transmission intensity. More transmission leads to less-skewed distributions of infection, while reductions in transmission from interventions such as MDA lead to more skewed distributions in which fewer individuals host larger proportions of the total parasite population. Individuals that remain infected in these scenarios may be those who miss treatment, are heavily exposed, are particularly susceptible to infection, or have parasite strains that are resistant to praziquantel. [54–58]

Aggregation dynamics approaching elimination are important from a number of practical and theoretical vantages. As parasite burden is reduced, so too is the number of individuals contributing to and sustaining transmission—a realization of the "20/80 rule" in which 20% of individuals contribute 80% of the transmission potential. [54] Identifying and treating these individuals through control efforts will therefore be essential to achieving elimination, but is complicated by systematic non-adherence to treatment, treatment failures, and insensitive diagnostics. [54,59–61] A better understanding of aggregation dynamics could aid the planning and implementation of surveillance and control efforts in low transmission and elimination settings. [59]

From a theoretical standpoint, the conditions under which MDA alone can achieve elimination is dependent on reducing the parasite population below its breakpoint. Breakpoints in helminth

transmission are expected to arise from mate limitation in low transmission settings whereby the probability of individuals being infected with fecund worms decreases as parasite burden and transmission decrease. Mate limitation in helminth populations is generally quantified in terms of the probability that a given female parasite in a population is successfully mated, $\phi(W, \kappa)$, which is estimated as a function of the mean parasite burden, W, and aggregation parameter, κ. [23,62] In endemic settings, parasite distributions among a population of definitive human hosts are well-represented by a negative binomial distribution with κ below 1. This implies a heavily right-skewed distribution in which most parasites are aggregated in a few human hosts.

For constant dispersion parameter, κ, in the range $[0.01,1.0]$ as has been widely observed previously, $\phi \to 0$ as $W \to 0$, giving rise to the hypothesized breakpoint at which worm mating becomes insufficient to sustain transmission. [24] As transmission decreases, the response of the dispersion parameter could have profound implications for the breakpoint. For instance, if $\kappa \to 0$ as $W \to 0$, implying increasingly skewed distributions that can be realistically interpreted as all parasites being harbored by one individual, ϕ remains large and the breakpoint is vanishingly small. [62] However, derivations of the mating probability based on the negative binomial distribution of adult parasites are derived from endemic settings, and stochasticity in worm acquisition at low transmission intensities is likely to play an increasingly important role on the distribution of adult parasites as elimination is approached. [23,62]

Here, we examine evidence for dynamic aggregation from the Zanzibar Elimination of Schistosomiasis Transmission (ZEST) study, a randomized control trial with the aim of eliminating schistosomiasis as a public health problem and halting schistosomiasis transmission on the two main islands of the Zanzibar archipelago off the coast of Tanzania. [43,44] We revisit classic assumptions of how adult schistosomes are distributed among human hosts and propose a novel, mechanistic data-generating process for worm acquisition and resulting mating dynamics. We then explore how these assumptions and underlying data-generating process affect estimation of the mating probability and discuss implications for ongoing control and elimination efforts for schistosomiasis and other helminthiases.

2.2 Aggregation estimation

The ZEST project enrolled 45 administrative regions called shehias on the island of Pemba with the goal of eliminating urogenital schistosomiasis as a public health problem (defined as reducing the prevalence of heavy infections below 1%) and 45 Shehias on the island of Unguja with the goal of interrupting *S. haematobium* transmission (defined as reducing the number of incident cases to zero). [43,44] On each island, shehias were randomly assigned to receive biannual MDA, biannual MDA plus snail control, or biannual MDA plus a behavioral intervention. [43,63,64] Cross-sectional parasitological surveys were conducted annually from 2012-2017 in each shehia. Data used here were acquired via a formal data request to the Schistosomiasis Consortium for Operational Research and Evaluation (SCORE) and are comprised of 27,626 observations of parasite burden among adults and 75,039 observations of parasite burden among school-aged children, each measured as *S. haematobium* eggs per 10mL urine.

The likelihood of the inverse negative binomial aggregation parameter, $\alpha_{st}^{\mathcal{E}}$, and mean community egg burden, $\mathcal{E}_{st}$, can be estimated for each shehia, s, and year, t, from individual, i, egg counts, e_{ist}, as:

$$L(\mathcal{E}_{st}, \alpha_{st}) = \prod_{i=1}^{n_{st}} \frac{\Gamma(e_{ist} + \alpha_{st}^{-1})}{e_{ist}!\,\Gamma(\alpha_{st}^{-1})} \left(\frac{\alpha_{st}\mathcal{E}_{st}}{1 + \alpha_{st}\mathcal{E}_{st}}\right)^{e_{ist}} (1 + \alpha_{st}\mathcal{E}_{st})^{-1/\alpha_{st}}$$

While aggregation is most frequently reported and discussed in terms of κ, its inverse, $\alpha = 1/\kappa$ has more desirable properties for statistical estimation and inference (see e.g.[65]). Therefore results are presented in terms of $\kappa_{st}^{\mathcal{E}}$ following trivial transformation from estimates derived using $\alpha_{st}^{\mathcal{E}}$.

The maximum likelihood estimate of $\mathcal{E}_{st}$ is simply the empirical mean of individual egg counts, and maximum likelihood estimates of $\alpha_{st}^{\mathcal{E}}$ were estimated using the Brent method within the `optim` function in R. [66] Uncertainty in estimates of $\alpha_{st}^{\mathcal{E}}$ were derived from the Hessian matrix. Both $\mathcal{E}_{st}$ and $\alpha_{st}^{\mathcal{E}}$ were estimated among the adult (A), child (C), and total (T) populations in each shehia-year.

Weighted generalized estimating equations (GEE) with unstructured correlation matrices of the form:

$$\mathbb{E}(\alpha_{st}|\mathcal{E}_{st}) = \exp[\beta_0 + \beta_1 \log(\mathcal{E}_{st})]$$

were used to estimate the relationship between aggregation and parasite burden. Weights were assigned as the inverse of the standard error of $\alpha_{st}^{\mathcal{E}}$. Models stratifying by population (child, adult, or total), by intervention type (MDA only, behavioral, or snail control), and by island (Pemba or Unguja) were also estimated. Results are reported for each stratum as the change in κ associated with an interquartile range increase in mean egg burden, $\Delta\kappa_{IQR}$. Clustered nonparametric bootstrapping was used to estimate uncertainty in estimates of $\Delta\kappa_{IQR}$ with $B = 10{,}000$ bootstrapped samples.

There were 93 shehia-years in which no individuals had positive egg counts and 16 shehia-years in which the maximum individual egg count was 1 and therefore variance estimates for $\alpha_{st}^{\mathcal{E}}$ could not be derived. This left 447 observations of $\alpha_{st}^{\mathcal{E}}$ and $\mathcal{E}_{st}$, shown in Figure 1A along with the marginal estimate of $\mathbb{E}(\kappa_{st}^{\mathcal{E}}|\mathcal{E}_{st})$ from the fitted GEE. We estimate a median 0.011 (Bootstrapped IQR: 0.01-0.013) increase in $\kappa_{st}^{\mathcal{E}}$ associated with an IQR increase in $\mathcal{E}_{st}$, implying a negative relationship between mean egg burden and aggregation. This relationship appears to be driven by dynamics in children, as there was weak evidence for a relationship between $\kappa_{st}^{\mathcal{E}}$ and $\mathcal{E}_{st}$ among adults (Fig 1B). Egg burden in adults ($IQR^A = 1.36$) was substantially lower than in children ($IQR^C = 4.65$), however. Shehias receiving the MDA+snail control and MDA+behavior change interventions appeared to have a stronger burden-aggregation relationship (larger $\Delta\kappa_{IQR}$, Fig 1B). An additional GEE model including main effects of intervention arm and island showed that reductions in $\kappa_{st}^{\mathcal{E}}$ were significantly larger in shehias receiving the MDA+snail control and MDA+behavioral change interventions ($p = 0.01$ and $p = 0.016$, respectively).

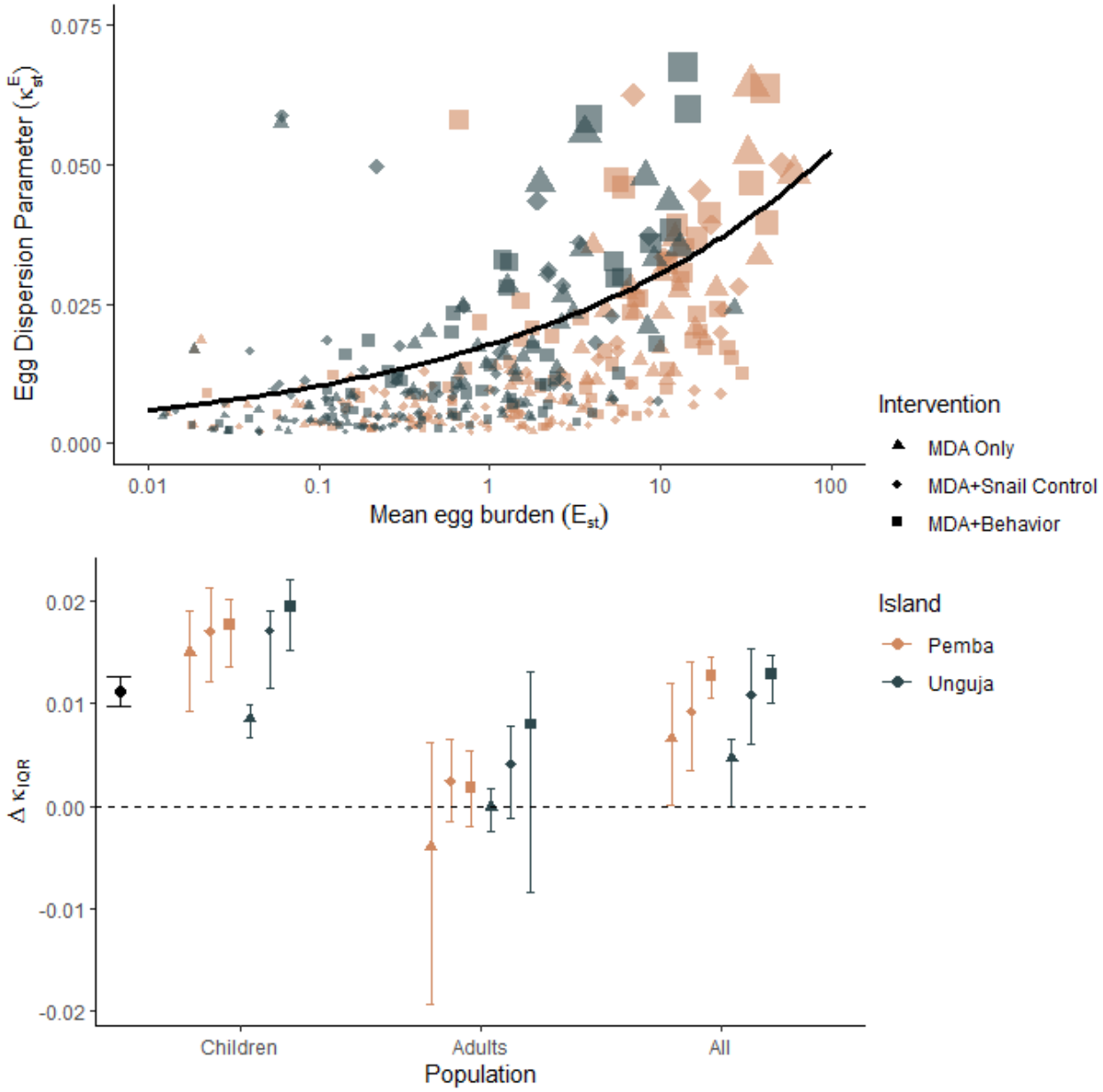

Figure 2.2.1: Relationship between community egg burden and dispersion. Panel A shows the scatterplot of all estimates of $\kappa_{st}^{\mathcal{E}}$ and $\mathcal{E}_{st}$ where each point is sized according to its weight, derived as the inverse of the standard error of α_{st}. Points are also symbolized according to their assigned intervention group—MDA only (▲), MDA+snail control (♦), or MDA+behavioral intervention (■)—and the island of the shehia. The solid black line in panel A represents the marginal estimate of $\mathbb{E}(\kappa_{st}^{\mathcal{E}}|\mathcal{E}_{st})$ from the fitted GEE. Panel B shows estimates of $\Delta\kappa_{IQR}$, the change in aggregation for an interquartile range increase in community egg burden stratified by population, treatment group, and island. The black point and error bars correspond to the unstratified marginal estimate of $\Delta\kappa_{IQR}$ as in panel A. Error bars correspond to the interquartile range of estimates derived from B=5000 bootstrapped samples.

2.3 Translating egg counts to worm burdens using approximate Bayesian computation

Because egg counts are an indirect estimate of parasite burden, are prone to undercounts at low burdens, and may change non-linearly with parasite burden [67], we next seek to determine if changes in aggregation as measured by egg counts are indicative of changes in aggregation of the adult parasite population. We use approximate Bayesian computation (ABC) to estimate mean community parasite burden and dispersion, denoted $W_{st}^{\mathcal{D}}$ and $\kappa_{st}^{W_{\mathcal{D}}}$, respectively, under three proposed data-generating mechanisms, $\mathcal{D} \in \{1,2,3\}$ (described below). Briefly, ABC proceeds by: 1) sampling $i = 1, \ldots, n$ parameter sets from a prior distribution, $\theta^{\mathcal{D}}$; 2) simulating datasets, $y_i^{\mathcal{D}}$, from the priors under the given data generating mechanism; 3) deriving summary statistics, $\mathcal{S}(y_i^{\mathcal{D}})$, from the generated data to compare to the observed data, $\mathcal{S}(y_O)$; 4) generating distance metrics, $d(\mathcal{S}(y_i^{\mathcal{D}}), \mathcal{S}(y_O))$, to assess the fit of the generated data to the observed data; and 5) accepting parameter sets that fall within a provided distance tolerance. [67] The accepted parameter sets thus represent an approximation of the posterior distribution of $\theta^{\mathcal{D}}$, but the estimation procedure does not require exact calculation of the likelihood of every proposed prior. Here, ABC was preferred to MCMC methods due to the number of estimates needed combined with the complexity of the likelihood function of the parasite population estimated from observed egg counts (see e.g. [68,69]).

The three data-generating mechanisms considered correspond to the "distributed together" and "distributed separately" assumptions (Cases 1 and 2) from Robert May's seminal work on schistosome mating dynamics [23] and a third mechanism (Case 3) that considers susceptibility and exposure as independent parameters. Prior parameter distributions and data generating processes that connect simulated worm burdens and egg counts to observed egg burdens are delineated in Table 1. Briefly, Case 1 assumes worms are distributed among human hosts according to a single negative binomial distribution with 1:1 sex ratio. Case 2 assumes male, w^m, and female, w^f, worms are distributed according to separate negative binomial distributions, each with mean $0.5W$. Case 3 assumes susceptibility, S, interpreted as the probability a given cercarial exposure will result in an adult worm, follows a gamma distribution, and cercarial exposures follow a negative binomial distribution independent of susceptibility. Worm pairing in individual hosts is then determined from a hypergeometric distribution that incorporates individual susceptibility, cercarial exposure, and 1:1 sex ratio among cercarial exposures (Table 1). The susceptibility distribution parameters are fixed, with parameters derived from previous work on *S. japonicum* [57,58], such that Case 3 estimation is based on the same number of parameters (3) as Case 1 and 2, and estimates of the mean worm burden and dispersion parameter can be estimated from the expectation and combined variances of the Case 3 susceptibility and exposure parameters. The number of eggs shed per mated worm pair per day is assumed to follow a negative binomial distribution with mean m and dispersion r for all three cases (Table 1).

The observed data, $\mathcal{S}(y_O)$, used in the ABC procedure consists of the mean community egg burden, $\mathcal{E}_{st}$; standard error of individual egg counts, $\mathrm{SE}_{st}^{\mathcal{E}}$; and an adjusted egg-prevalence measure—the number of egg positive individuals squared over the number of individuals—for every shehia-year among separate child and adult populations in which at least one individual

had an egg count > 1. The distribution of this adjusted prevalence measure—as opposed to the prevalence (bounded between 0 and 1) or raw number of individuals infected (an integer)—aligns better with the ABC estimation procedure. We used the default standardized distance metric in the R package `ABC` [70] to compare the observed data to $n = 100{,}000$ simulated datasets for each Case in each eligible shehia-year, and accepted the 100 parameter sets with the smallest estimated distance for each simulation (e.g. tolerance of 0.001). Posterior parameter sets were then adjusted and weighted based on their distance from the observed data using the ridge regression routine in `ABC`. Relative fits to the observed data foor each data-generating case were compared using the Bayes factor. Posterior distributions of W_{st} and κ_{st}^{W} were examined as described above for $\mathcal{E}_{st}$ and $\kappa_{st}^{\mathcal{E}}$. In addition, the mating probability was estimated for every simulated dataset as the number of mated worms per worm ($2W_{st}^{\Phi}/W_{st}$). These estimates were then compared to analytic estimates of the mating probability derived from the mean worm burden and worm dispersion parameter as derived previously. [23]

Table 2.3.1: Priors and data-generating processes for approximate Bayesian computation estimation of community parasite burden and aggregation. Data generation proceeds by first drawing from the multivariate prior, $\theta^{\mathcal{D}}$, containing shehia-year level summaries of parasite burden and aggregation (for Cases 1 and 2) or of individual susceptibility and exposure (for Case 3), then generating individual worm burdens, worm pairs, and finally egg burdens. Summaries of individual egg burdens for each shehia-year are then compared to observed summaries from ZEST to derive a posterior estimate of model parameters.

	Case 1 (Males and females distributed together)	Case 2 (Males and females distributed separately)	Case 3 (Explicit susceptibility and exposure)
Priors	$\theta^1 = \{W_{st}, \kappa_{st}^W, m, r\}$ $W_{st} \sim \mathcal{U}(1\times10^{-6}, 1\times10^{3})$ $k_{st}^W \sim \mathcal{U}(1\times10^{-5}, 1\times10^{5})$ $m \sim \mathcal{U}(3{,}30)$ $r = 1$	$\theta^2 = \{W_{st}, \kappa_{st}^W, m, r\}$ $W_{st} \sim \mathcal{U}(1\times10^{-6}, 1\times10^{3})$ $k_{st}^W \sim \mathcal{U}(1\times10^{-5}, 1\times10^{5})$ $m \sim \mathcal{U}(3{,}30)$ $r = 1$	$\theta^3 = \{C_{st}, \kappa_{st}^C, \alpha_S, \beta_S, m, r\}$ $C_{st} \sim \mathcal{U}(1{,}1\times10^{6})$ $\kappa_{st}^C \sim \mathcal{U}(1\times10^{-5}, 1\times10^{5})$ $\alpha_S = 1\,;\, \beta_S = 500$ $m \sim \mathcal{U}(3{,}30)$ $r = 1$
Worms	$w_{ist} \sim \mathrm{NB}(W_{st}, \kappa_{st})$	See below	$S_{ist} \sim \Gamma(\alpha_S, \beta_S)$ $c_{ist} \sim \mathrm{NB}(C_{st}, \kappa_{st}^C)$ $w_{ist} \sim \mathrm{Pois}(c_{ist} s_{ist})$
Pairs	$w_{ist}^f \sim \mathrm{Pois}(0.5 w_{ist})$ $w_{ist}^m = w_{ist} - w_{ist}^f$ $w_{ist}^{\Phi} = \min(w_{ist}^m, w_{ist}^f)$	$w_{ist}^f \sim \mathrm{NB}(0.5 W_{st}, \kappa_{st})$ $w_{ist}^m \sim \mathrm{NB}(0.5 W_{st}, \kappa_{st})$ $w_{ist}^{\Phi} = \min(w_{ist}^m, w_{ist}^f)$	$c_{ist}^f \sim \mathrm{Pois}(0.5 c_{ist})$ $w_{ist}^f \sim \mathrm{Hypergeo}(c_{ist}, c_{ist}^f, w_{ist})$ $w_{ist}^m = w_{ist} - w_{ist}^f$ $w_{ist}^{\Phi} = \min(w_{ist}^m, w_{ist}^f)$
Eggs	$e_{ist} \sim \mathrm{NB}(m w_{ist}^{\Phi}, r)$		

$\theta^{\mathcal{D}}$: multivariate prior for data-generating case, $\mathcal{D}$
W_{st}: mean worm burden in shehia, s, and year, t
w_{ist}: individual, i, worm burden in shehia, s, and year, t
k_{st}: aggregation parameter in shehia, s, and year, t
C_{st}: mean cercarial exposure in shehia, s, and year, t
α_S: shape parameter of gamma-distributed susceptibility, S
β_S: rate parameter of gamma-distributed susceptibility, S

m: mean eggs produced per mated worm pair
r: aggregation parameter of negative binomially distributed daily egg release

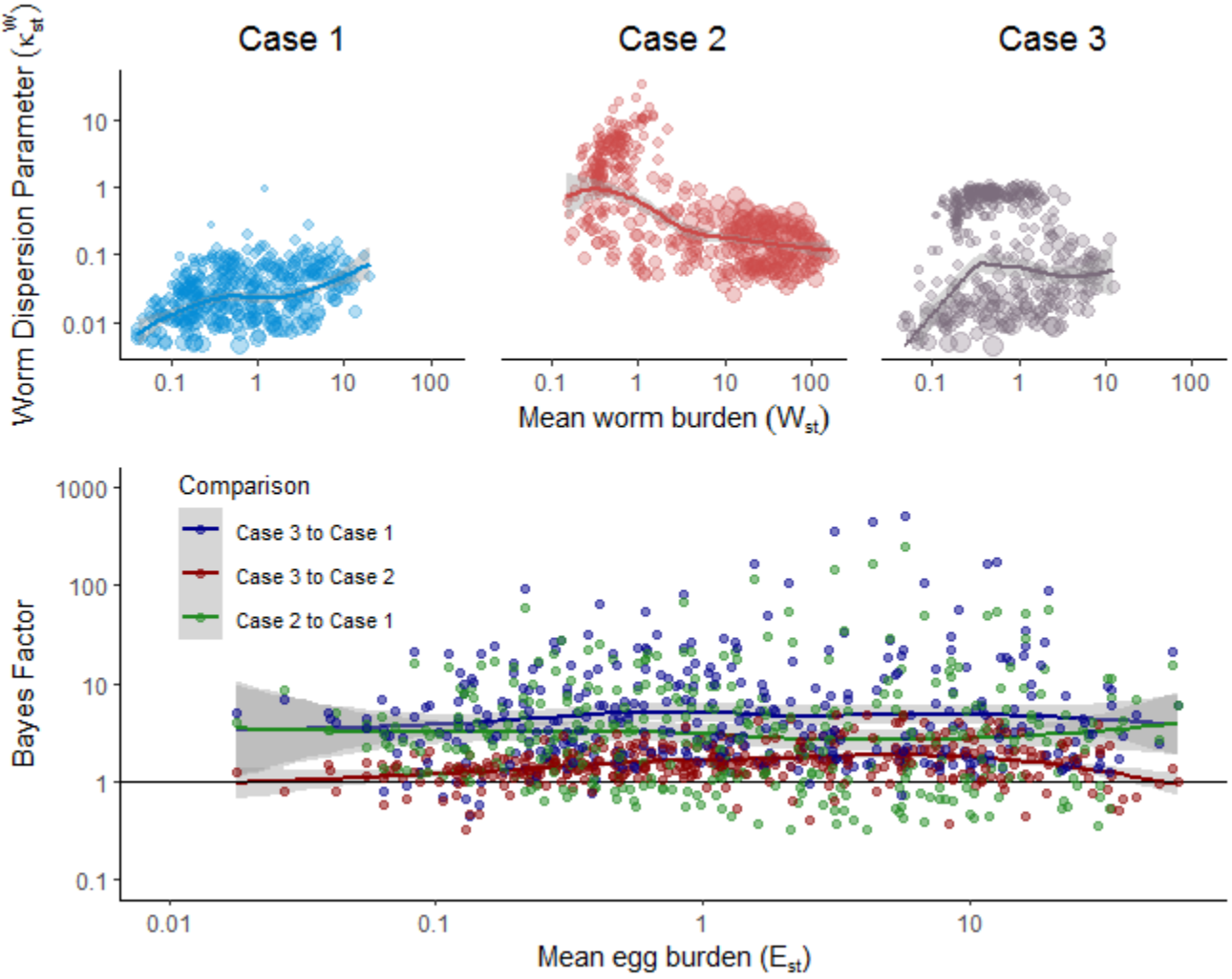

Figure 2.3.1: Summary of approximate Bayesian computation estimates of community worm distributions among children. Across the top are posterior estimates of the mean community worm burden (W_{st}) and worm dispersion parameter (k_{st}^{W}) from ABC estimation for Case 1 (Together, top left in blue), Case 2 (Separate, top middle in red), and Case 3 (Generalizable, top right in purple). The bottom panel shows comparisons of model fit for each case across the measured community egg burden (E_{st}) using the Bayes Factor, a ratio of model likelihoods in which higher values imply better fits to the observed data. All axes are log-transformed and smoothed averages are shown for figure clarity. Points in the top panels are sized in proportion to the inverse of the interquartile range of the posterior estimate of k_{st}^{W}.

Results of ABC estimation of the mean worm burden, aggregation parameter and mating probability are shown for children in figures 2 and 3. The same figures for estimation among adult populations can be found in the chapter supplement (Supp Figures 4-6). All three data-generating mechanisms considered produced summary statistics that matched the observed summary statistics from ZEST well (Supp Fig 1). Examination of the Bayes factors comparing

the fit of each Case shows that the generalizable Case 3 performs better than both the canonical Case 1 and Case 2, though Case 2 does appear to perform about as well (Bayes Factor ≈ 1) at lower parasite burdens (Fig 2). Case 1 estimates of W_{st} and κ_{st}^{W} exhibited a similar pattern to $\mathcal{E}_{st}$ and $\kappa_{st}^{\mathcal{E}}$, namely increasing aggregation (indicated by decreasing κ) with decreasing measures of burden (Fig 1 and Fig 2). However, Case 2 estimates showed the opposite effect of decreasing aggregation with decreasing worm burden (Fig 2). Finally, Case 3 estimates appear similar to a mixture of Case 1 and Case 2 results, with one cluster of estimates appearing to exhibit Case 1-like dynamics and another exhibiting Case 2-like dynamics (Fig 2). Further examination of each of these clusters reveals that Case 1-like dynamics recovered from Case 3 estimation occur more frequently in shehia-years with higher egg burdens, prevalences, and standard errors, while Case 2-like dynamics are recovered at lower egg burdens, prevalences, and standard errors (Supp Fig 2). Additionally, comparison of the estimated mean worm burden from each data-generating case to the observed mean egg burden shows that Case 3 estimates are more similar to Case 1 estimates at higher burdens, but closer to Case 2 estimates at lower burdens (Supp Fig 2.3).

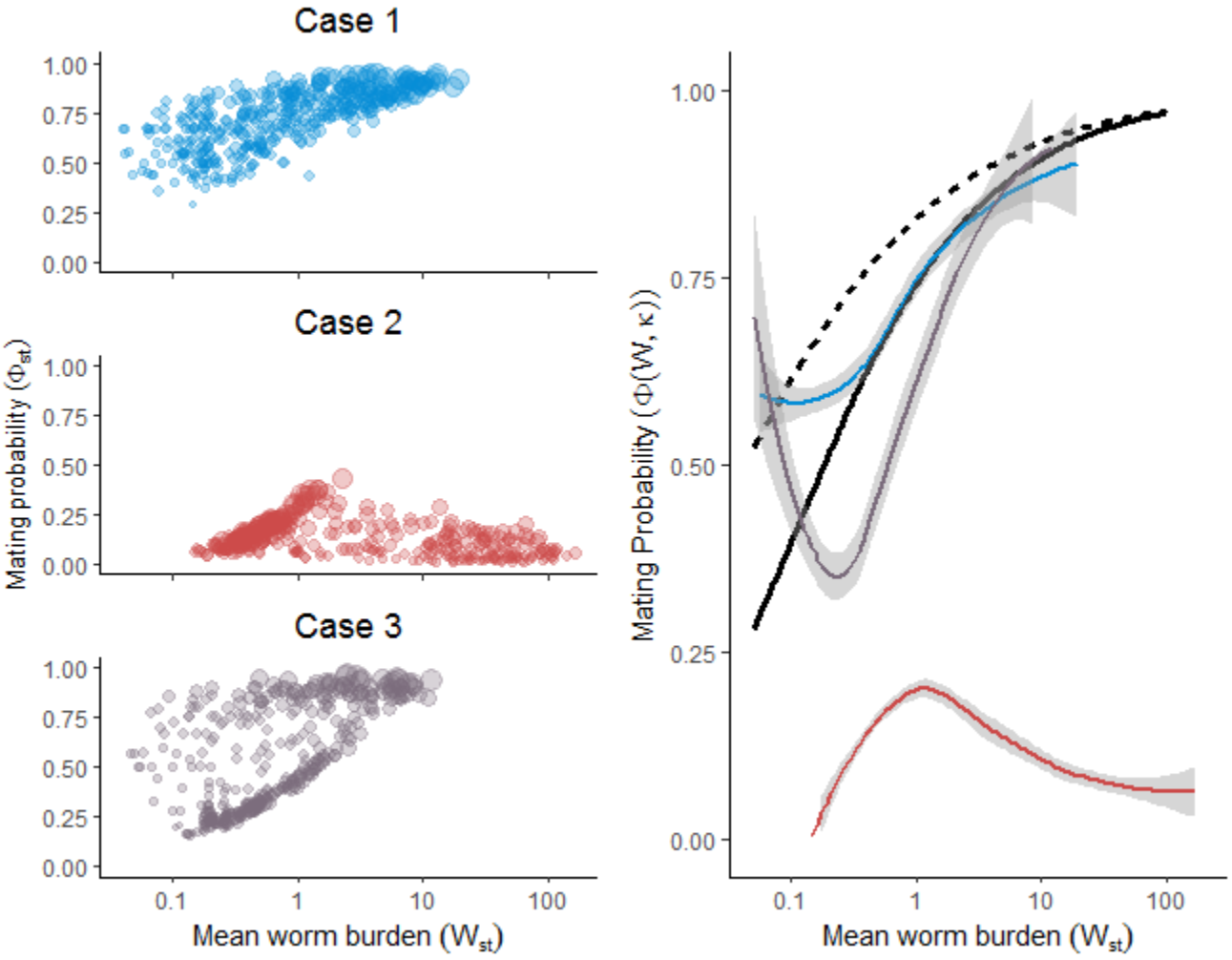

Figure 2.3.2: Comparison of predicted and estimated mating probabilities. Along the left side are estimates of the mating probability extracted from the best fit datasets generated in approximate Bayesian computation for every Shehia-year across the three cases. Case 1 (Together, top left in blue) estimates produce a high mating probability at high worm burdens that steadily decreases with decreasing mean worm burden. Case 2 (Separate, middle left in red) estimates produce a low mating probability across all mean worm burdens, with a subtle peak in mating probability at intermediate mean worm burdens. Case 3 (Generalizable, bottom left in purple) again appears to show hybridization with mating probability estimates at high mean worm burdens appearing similar to Case 1 and mating probability estimates at low mean worm burdens appearing similar to Case 2. The right panel compares loess-smoothed estimates of the mating probability from ABC estimation for each case to analytical predictions of the mating probability for static ($\kappa = 0.05$, solid black line) and dynamic aggregation ($\kappa(W)$, dashed black line). Analytic predictions of the mating probability are accurate at high mean worm burdens, but diverge from the empirical estimates as the mean worm burden decreases, indicating analytic predictions that assume constant Case 1 "distributed together" dynamics may be inaccurate in elimination settings.

Figure 2.3 shows the mating probability generated by all three data-generating cases from the best fit datasets in ABC estimation for every Shehia-year. These estimates are also compared to analytic predictions of the mating probability for both static aggregation ($\kappa = 0.05$, Fig 2.3 black solid line) and dynamic aggregation ($\kappa = f(W)$, Fig 2.3 black dashed line). These analytic predictions align well with empirical Case 1 and Case 3 estimates at high mean worm burdens, but underestimate the mating probability at lower mean worm burdens. Hybridization of Case 1 and Case 2 like dynamics recovered from Case 3 estimates are apparent once again, with Case 3 mating probability estimates similar to Case 1 estimates at high mean worm burdens, and resembling Case 2 estimates at lower mean worm burdens. This leads to uncertain mating probability estimates as the main determinant appears to be whether Case 1 or Case 2 like dynamics are dominant, rather than the mean worm burden or aggregation parameter from which analytic estimates are derived.

All analyses were performed in R version 4.0.2 utilizing the `geepack` [71], `tidyverse` [72], and `ABC` [70] packages. All code and derived data files necessary to reproduce the analysis can be found at https://github.com/cmhoove14/DynamicAggregation.

2.4 Implications of dynamic aggregation for breakpoints, control, and elimination

Here we use data from the ZEST study to explore how parasite aggregation dynamics change as elimination is approached due to intense control efforts. We find that parasite aggregation as measured directly by community egg distributions and through estimation of adult parasite distributions likely increases as elimination is approached. In addition, the classic (Case 1) assumption that male and female parasites are distributed together appears to hold at large mean community worm burdens. However, as proposed previously, this assumption appears to break down at smaller worm burdens as elimination is approached. [23]

The distribution of individual egg counts from ZEST was highly overdispersed, with $\kappa^{\mathcal{E}}$ in the range 0.001-0.067. Community egg dispersion was found to significantly decrease as the community worm burden decreased, and this effect was driven by children. As children frequently have the highest exposure and may be most susceptible to infection due to lack of acquired immunity, [70] this is not surprising. We also found that the relationship between the dispersion parameter and mean community egg burden was significantly greater in shehias from the ZEST study that received snail control or behavioral interventions in addition to biannual

MDA. This could be driven by higher starting prevalence and burden among these intervention arms, [43] though could also have theoretical underpinnings that will be the topic of future analyses.

We propose a novel, mechanistic data-generating process (Case 3) that explicitly models the interaction of individual susceptibility and exposure to allow the data to determine the most likely distribution of male and female parasites. Using approximate Bayesian computation to estimate mean parasite burdens and parasite dispersion, we find that this Case 3 data-generating process provides a better fit to the observed ZEST data across all values of parasite intensity. Due to the flexibility and superior fit of the proposed Case 3 mechanism, we believe it represents a superior theoretical basis for analyzing the dynamics of parasite aggregation and mating.

Case 3 estimation supports the hypothesis that male and female parasites are distributed together (Case 1) at high transmission intensities that result in high worm burdens. Case 3 estimates of worm burden and aggregation were more similar to estimates recovered from Case 1 estimation at higher worm burdens. As mean worm burden estimates decreased, Case 3 estimates became more irregular, with some similar to Case 2 estimates and others similar to Case 1. This supports previous hypotheses that the distribution of male and female parasites among a population of definitive human hosts is likely dependent on local transmission intensity and previous

This finding provides evidence supporting the hypothesis of Robert May that the distribution of male and female parasites is not strictly "together" (Case 1) or "separate" (Case 2), but is rather a blend of both that is dependent on the worm burden itself. [23] In particular, male and female parasites appear more likely to be distributed together at high burdens, and separate at low burdens. This reflects the higher likelihood that individuals are exposed to large numbers of cercariae more likely to contain a mix of males and females that will ultimately pair when transmission intensities are greater. At lesser transmission intensities, the probability of exposure events containing only male or female cercariae increases.

Variability in susceptibility as proposed previously [57] and considered as part of Case 3 estimates here plays a similar moderating effect on those cercariae that successfully infect the human host and mature into adult worms. This suggests that identifying individuals who are particularly susceptible to infection could be extremely valuable for control efforts, since these individuals are both most susceptible to pathology associated with infection and are most likely contributing to sustaining transmission. These individuals could be identified through a sufficiently accurate biomarker or simply by taking note of individuals who are most heavily infected. This information could then be used in targeted drug administration campaigns that prioritize treatment of such high-risk individuals, rather than prioritizing broad coverage of the population regardless of individuals' susceptibility or exposure. Such strategies will be the topic of subsequent modeling analyses that build on the results presented here.

Such strategies should also be pursued with caution if relying on diagnostics such as haematuria or egg-assays that are known to have low sensitivity for light infections. Indeed, reliance on these diagnostics represents a limitation of this analysis as sensitivity in egg counts is not explicitly considered in analysis of the community egg burdens or in the data-generating Cases

considered. However, high variability in daily egg counts produced by even heavily infected individuals [68] is a part of the data-generating processes of the ABC estimation, meaning that generated egg distributions would be expected to match observed ones if diagnostic sensitivity in the real world were perfect. Future analyses using more sensitive diagnostics such as circulating cathodic antigen (CCA) could be pursued to confirm these findings.

Heterogeneity in susceptibility and exposure (and their joint distribution) are not the only processes that could explain the dynamics of parasite burden and aggregation identified here, though they most likely play a significant role. Recent analyses have found that mated pairs may survive praziqauntel treatment and resume egg-laying shortly after treatment. [54] This would lead individuals harboring such resistant pairs to maintain their high worm burden following treatment, while others are cleared of adult worms, thus increasing aggregation as is seen in these analyses. Similarly, individuals who miss treatment due to absence, pregnancy, or non-compliance would also maintain their high worm burdens as others are treated and cleared of adult worms, leading to increased aggregation as the mean community burden decreases.

Regardless of the exact mechanism or combination of mechanisms that give rise to increased aggregation, the practical implications are noteworthy. [73] Because some individuals maintain high worm burdens and egg output, they are more likely to maintain transmission among the snail population, which could contribute to infection rebound in the entire community. From a theoretical perspective, this can be expressed in terms of the mating probability. Our results show that increased aggregation coupled with shifts in the distribution of male and female parasites leads to mating probabilities higher than are commonly predicted assuming Case 1 dynamics with constant aggregation. This implies that the hypothesized breakpoint in schistosomiasis transmission could be exceedingly small or non-existent. Widespread resilience to elimination [13,27,74–76] and the recent outbreak of schistosomiasis in Corsica that appears to have been introduced by a single egg-shedding individual [9] also provide evidence to this finding. Breaking schistosomiasis transmission to achieve elimination may therefore be more dependent on reducing environmental transmission through snail control, sanitation improvements, and behavioral interventions and on identifying and successfully treating the few individuals who remain infected and maintain transmission as elimination is approached. [77–79]

A renewed focus on snail control as an important component of schistosomiasis elimination is encouraging. Heterogeneities in susceptibility, exposure, and sex differentiation—and resulting aggregation dynamics—are just as complex in intermediate host snail populations as in human hosts. [80] Additional focus on even more integrated strategies that incorporate snail control, MDA, environmental remediation, sanitation, and behavioral changes could prove even more successful, as they were in bringing about widespread elimination of schistosomiasis transmission in China. [17,19] Emerging evidence that zoonotic components of transmission such as hybrid *S. bovis* and *S. haematobium* [9,81] strains and infected rodents [82] are capable of sustaining transmission even in the presence of widespread MDA make such integrated strategies even more important. Identifying such integrated intervention strategies that result in the highest probability of successful elimination, particularly in the context of resistance to elimination due

to dynamic aggregation as described here, is the subject of an ongoing modeling analyses that will be presented separately.

In conclusion, we have identified dynamic aggregation as an important aspect of schistosomiasis transmission in elimination settings. We propose a novel, generalizable quantitative framework for modeling parasite acquisition and subsequent mating dynamics among the human host population that suggests the canonical Case 1 assumption that male and female parasites are distributed together is only accurate at high parasite burdens. This implies that the mating probability of adult worms remains high as elimination is approached, and the feasibility of achieving elimination using MDA alone may be overestimated. We suggest more targeted treatment strategies and a focus on integrated intervention strategies that target other components of the schistosome lifecycle to combat this source of resilience and maintain global progress towards the elimination of schistosomiasis.

2.5 Appendix

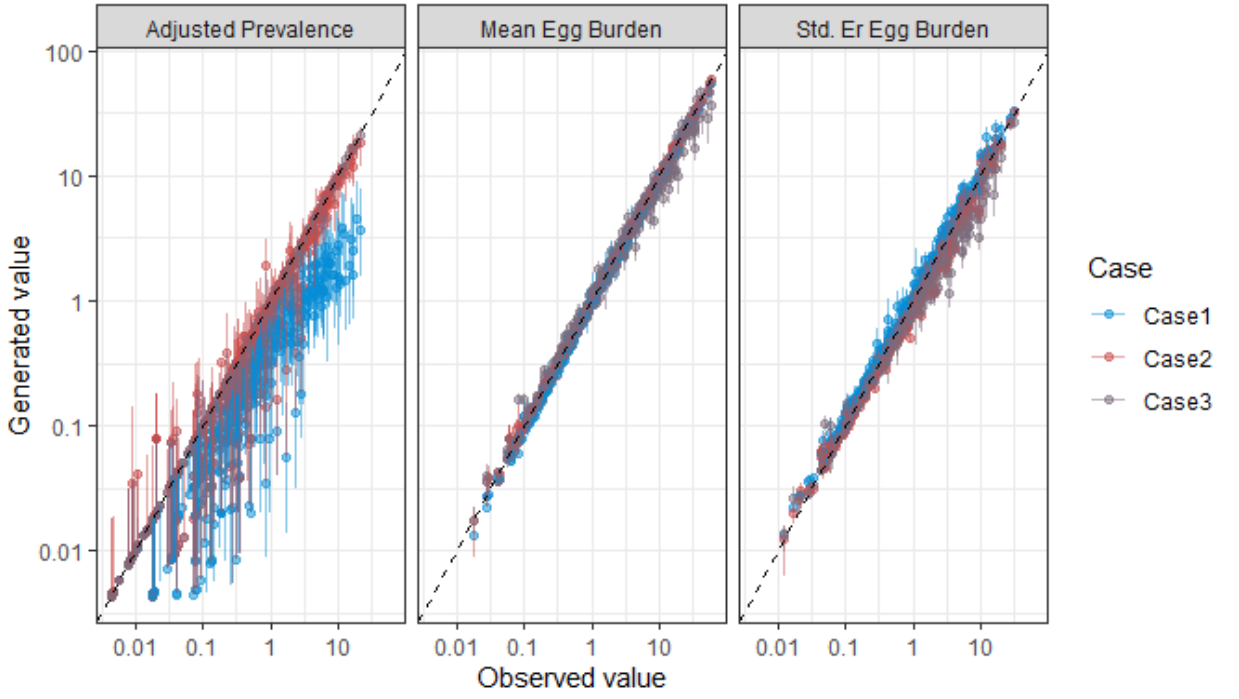

Figure 2.5.1: Comparison of generated to observed summary statistics used in approximate Bayesian computation estimation of community parasite burdens. Colors indicate the data generating Case and the 1:1 line implying perfect agreement between observed and generated data is shown. Error bars correspond to interquartile ranges of the generated summary statistics from parameter sets included in the posterior distribution.

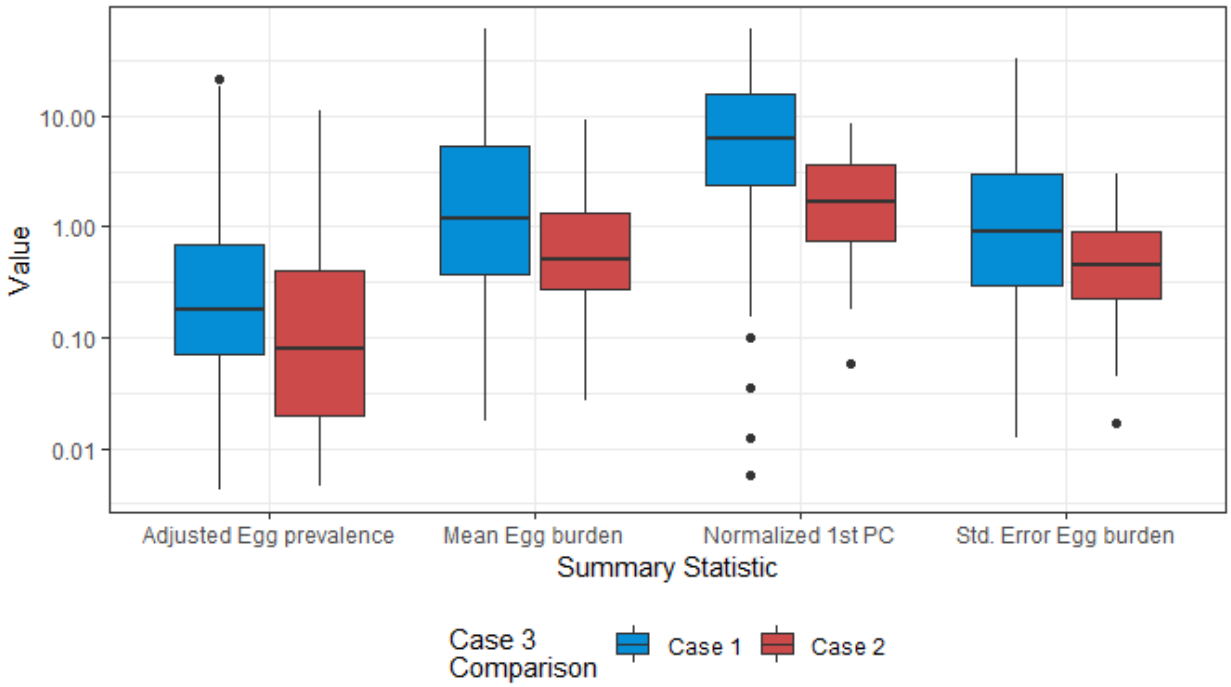

Figure 2.4.2: Distribution of summary statistics used in approximate Bayesian computation estimation of worm burdens from egg burdens and their first principle component, stratified by whether the Case 3 worm burden estimates were closer to the Case 1 (blue) or Case 2 (red) estimates. This demonstrates that Case 2 dynamics are more likely to be estimated at lower parasite burdens, prevalences, and standard errors—indicative of lower overall transmission—while Case 1 dynamics are recovered in higher transmission settings

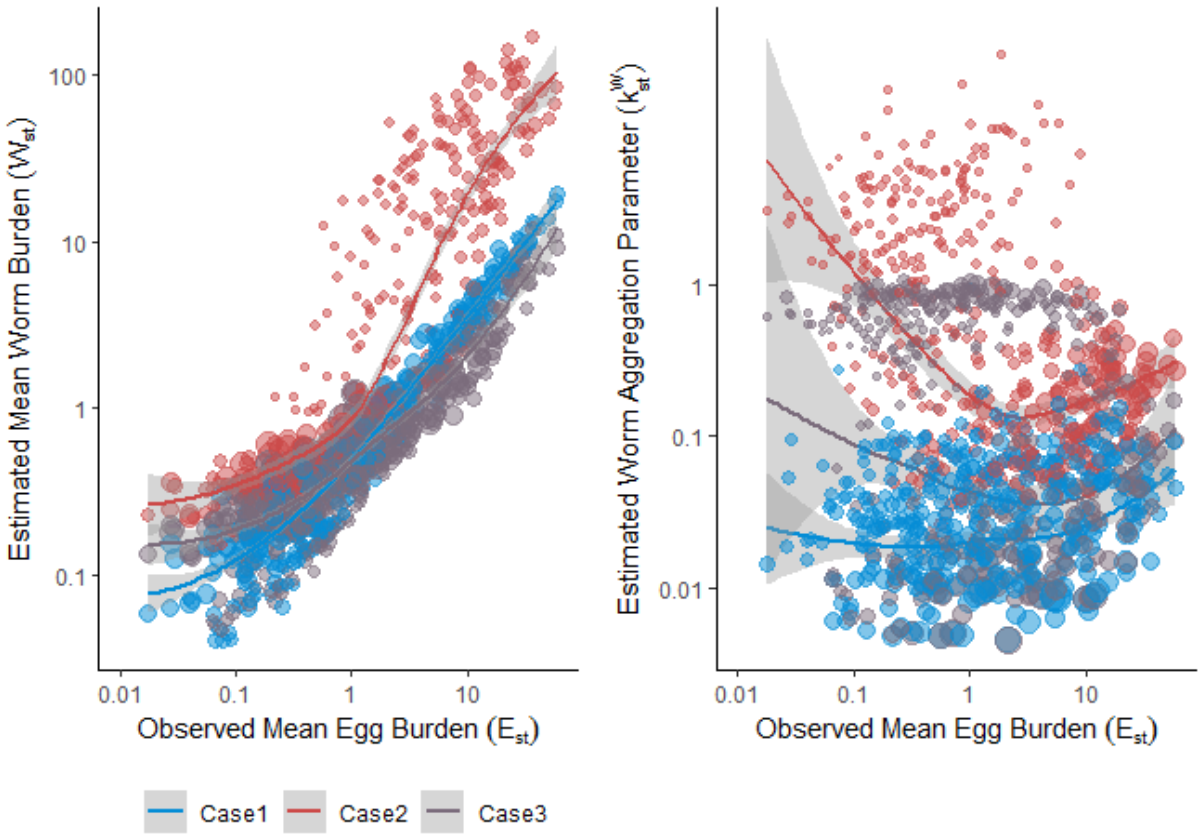

Figure 2.5.3: Comparison of mean worm burden and worm aggregation parameter estimates to observed egg burdens in every Shehia_year from ZEST for three data-generating cases. At high observed egg burdens, Case 3 estimates are more similar to Case 1 estimates, while at lower egg burdens, Case 3 estimates appear to stray from Case 1 and towards Case 2 estimates.

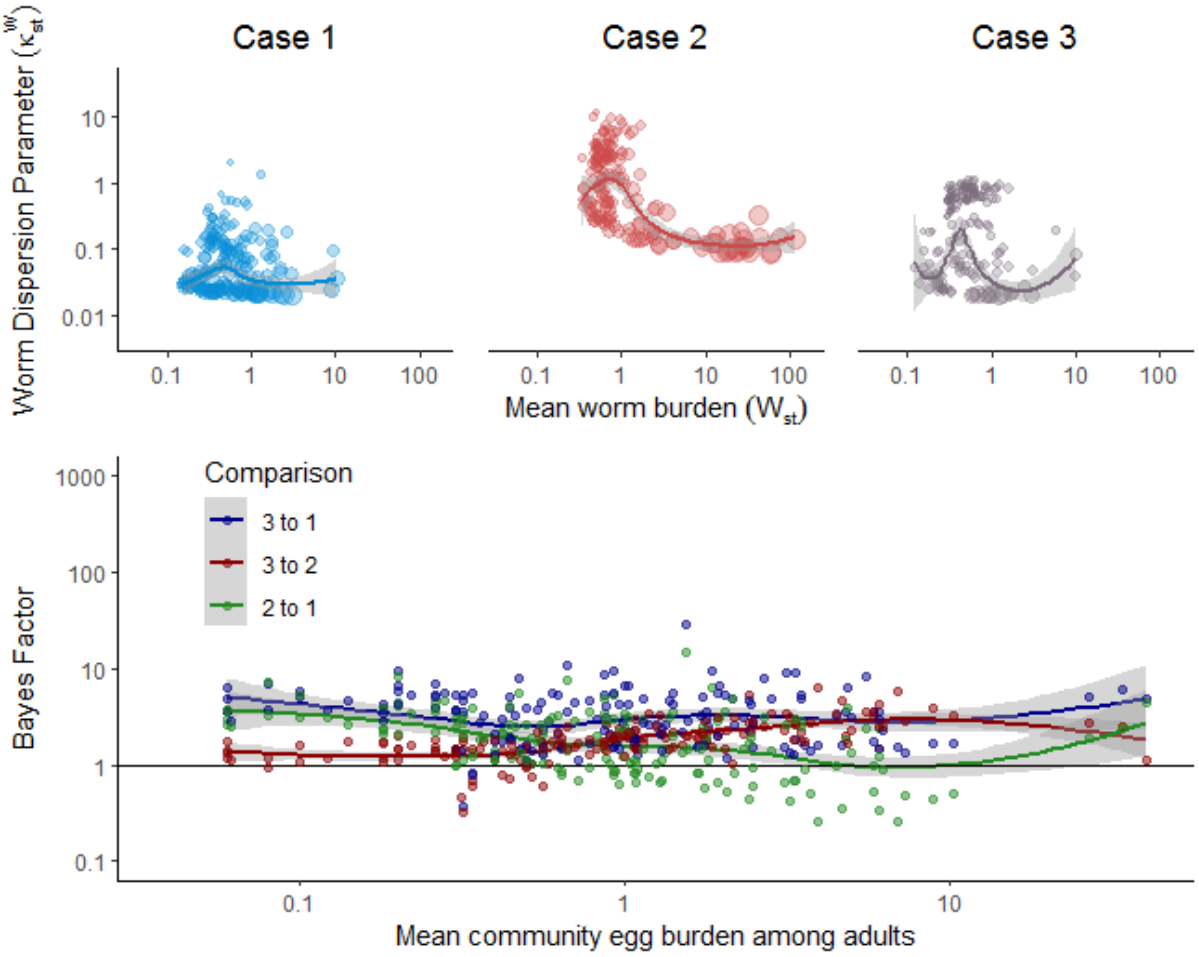

Figure 2.5.4: Mean community worm burden by aggregation parameter estimated via approximate Bayesian computation for all three data-generating cases among adults. Bayes factors comparing worm burden and dispersion fits among adult populations.

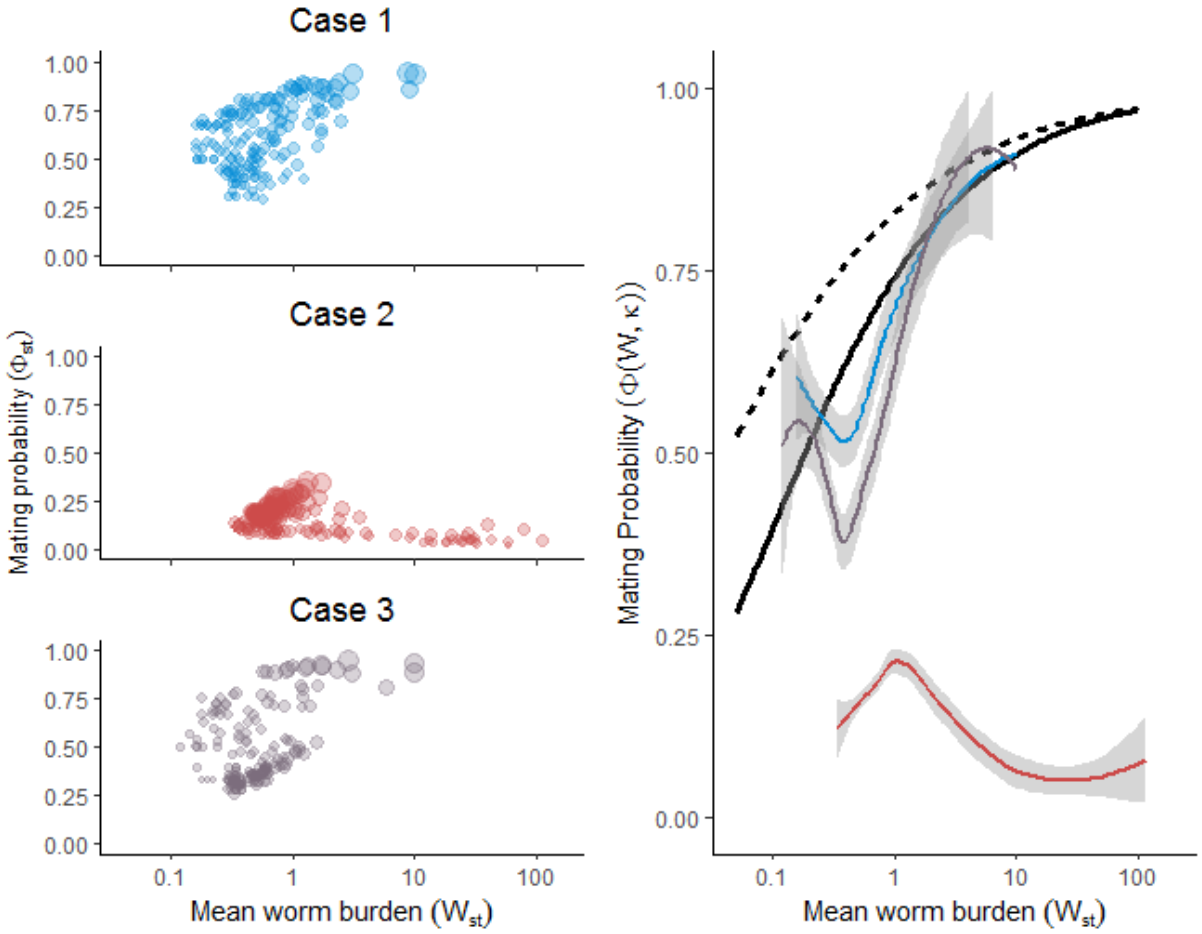

Figure 2.5.5: Mating probability observations and comparison to predictions for adult populations.

Chapter 3: A novel intervention: Modelled effects of prawn aquaculture on poverty alleviation and schistosomiasis control

3.1 Snail predators and schistosomiasis control

There is a rich history of environmental interventions for schistosomiasis that target the intermediate snail hosts [77]. Molluscicides are effective in reducing snail populations and have been used in integrated campaigns to control schistosomiasis in areas of South America, Northern Africa, and Southeast Asia [77,78,83]. However, these approaches generally require repeated applications of chemicals that may negatively affect non-target species in addition to *Schistosoma*-bearing snails [84,85].

Another option for reducing transmission is cultivating snail predators, such as river prawns, via aquaculture. Such snail predators have been shown to reduce schistosomiasis transmission associated with *S. haematobium* infection by consuming *Bulinus* snails in the aquatic environment where people contact infested water [45,86].

In addition to being voracious predators of snails [87,88], river prawns are a valuable food commodity [89,90]. The giant freshwater prawn *Macrobrachium rosenbergii* has been domesticated and widely used in commercial hatchery-based aquaculture [91], providing a key source of protein and encouraging local economic development [92]. Furthermore, advances in the production of nonbreeding *M. rosenbergii* monosex populations reduces the risk of prawn invasion in areas this species is not native, suggesting safe use of this biological control agent globally [46,93].

In sub-Saharan Africa, where at least 90% of schistosomiasis cases occur [94,95], the native African river prawn *M. vollenhovenii* has been proposed as an alternative to *M. rosenbergii* for aquaculture [46]. Furthermore, extensive prawn aquaculture—consisting of large enclosures, low prawn densities, and no use of supplemental feed, substrate, or additional oxygenation—is increasingly common in developing countries [89–91]. It can also be easily integrated into rice agriculture, which is increasingly an important part of food production and is already present in many schistosomiasis endemic areas [96,97].

Given that schistosomiasis is a disease of poverty, combining the nutritional and economic benefits of prawn aquaculture with disease control via prawn predation on snails may offer a sustainable approach to combat schistosomiasis and improve well-being and economic development in endemic areas. Here, an integrated model, consisting of 1) a bio-economic production model of *Macrobrachium* spp. aquaculture, 2) an epidemiologic model of *S. haematobium* transmission dynamics, and 3) a size- and density-dependent prawn predation model, is developed and parameterized via results of previous laboratory, modeling, and field-based empirical studies (Fig 3.1) [45,87]. The model is used to investigate whether extensive prawn aquaculture (using either endemic *M. vollenhovenii* or domesticated *M. rosenbergii*) can be managed at schistosome transmission sites such as rice paddies or enclosed points of water contact where people are exposed [45] to simultaneously maximize profit and control schistosomiasis. Estimates of the disability adjusted life years (DALYs) lost due to *S. haematobium* infection derived from the integrated model are used to compare reductions in disease burden achieved via aquaculture-based prawn interventions with conventional MDA interventions, and to estimate the benefits of utilizing both MDA and prawn aquaculture for schistosomiasis control.

3.2 Integrated bioeconomic model of prawn aquaculture and schistosomiasis transmission

The integrated model has three components: a) a bio-economic aquaculture component, simulating yields and accounting for density-dependent mortality and somatic growth of *Macrobrachium* spp. prawns over a range of initial stocking densities; b) an epidemiologic component to simulate the dynamics of mean *S. haematobium* worm burden in humans and the population and infection dynamics of intermediate-host snails through a size structured, Susceptible-Exposed-Infected compartmental model; and c) a predation function that links the epidemiologic and aquaculture models and estimates the rate at which prawns consume snails as a function of snail density and of snail and prawn body sizes.

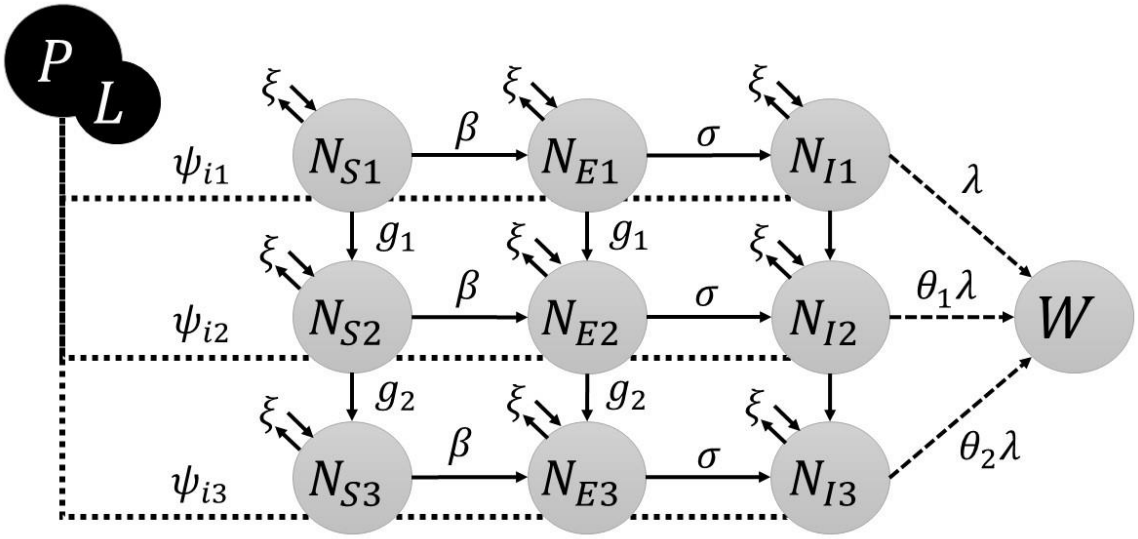

Figure 3.2.1: Model schematic representing the three components of the integrated bioeconomic model of prawn aquaculture and schistosomiasis transmission. Model schematic representing the three components of the integrated aquaculture-epidemiologic model. Prawn aquaculture is modeled via state variables *P* and *L*. The epidemiologic model consists of the size- and age-structured snail population state variables (N_{ij}) in grey circles and the mean worm burden in the human population, *W*. These two components are linked via size- and density-dependent prawn predation on snails estimated as ψ_{ij}. Parameters governing transitions between snail classes and migration into and out of each class are shown: ξ is the rate of migration between the external snail population and the population at the modeled intervention site, β is the man-to-snail transmission parameter, σ is the inverse of the pre-patent period of snails, g_1 and g_2 are the growth rates of snails in size class 1 and 2 respectively, λ is the snail-to-man transmission parameter, and θ_1 and θ_2 represent increased contribution of larger snails to human infection.

Aquaculture model

The dynamics of a cohort of P_0 juvenile prawns of initial mean length, L_0 [mm], stocked at time $t = 0\ days$ in an enclosure of $1{,}000\ m^2$—a size consistent with either a large water contact site or a typical rice field in small-scale, subsistence agriculture settings—are simulated over time as a function of density-dependent and size-dependent growth and mortality. Hatchery and nursery infrastructure is not explicitly considered in the model, but is assumed to supply juvenile prawns to stock at desired transmission sites.

Although prawns exhibit quite heterogeneous growth patterns depending upon sex (with males growing larger than females) and social structure [98], an average growth rate through the population is simulated here. In addition, growth of individual crustaceans is typically stepwise and occurs through a sequence of molting events, but here the population-average growth of prawns is modeled as somatic growth with the von Bertalanffy growth equation (VBGE) [99]:

$$\frac{dL}{dt} = k^*(L_\infty - L) \qquad (1)$$

VBGE produces a classic increasing-and-saturating growth curve with length *L* at time *t* (days after stocking) eventually approaching the mean asymptotic length, L_∞. Based on experimental stocking trials showing reduced growth rates of *M. rosenbergii* at high stocking densities [98], a

modified Brody growth coefficient, k^*, was estimated as a decreasing function of total population biomass, Ω:

$$k^*(\Omega) = \frac{k_{max}}{1 + \gamma\Omega(t)} \quad (2)$$

where k_{max} is the maximum value of the Brody coefficient at low densities and γ a coefficient parameterized to produce a density-dependent reduction in somatic growth qualitatively resembling that observed in experimental trials [98].

Total population biomass, $\Omega(t)$, is computed as the product of mean prawn body size in grams, $B(t)$, and the number of individuals, $P(t)$, t days after stocking:

$$\Omega(t) = B(t)P(t) \quad (3)$$

Body size $B(t)$ is derived as an allometric function of prawn length, $L(t)$, from *M. rosenbergii* grow-out data [100,101]:

$$B(t) = a_P L(t)^{b_P} \quad (4)$$

As prawns are generalist consumers with a wide range of invertebrate fauna and organic detritus in their diet [102], growth as described by equations (1-4) is assumed independent from snails' density and the corresponding predation rates.

After stocking, the total number of prawns in the enclosure decreases over time, with *per-capita* mortality rate modeled as an additive function of two components: (*i*) an exponentially decreasing function of body size, $B(t)$, as large prawns exhibit lower mortality than small prawns [103]; and (ii) a linearly increasing function of total population biomass, $\Omega(t)$, which accounts for density-dependent competition for resources and cannibalism at high population densities [98]. Accordingly, the dynamics of a cohort of initial size P_0 is described as follows:

$$\frac{dP}{dt} = -P(\mu_P B^{-d} + \omega\Omega) \quad (5)$$

with parameters μ_P and d derived from previous studies [103,104] and ω parameterized to produce density-dependent mortality outcomes qualitatively similar to those observed in the experimental trials by Ranjeet and Kurup [98]. Natural recruitment is excluded from the aquaculture model, as new prawns enter the system only in discrete, exogenously controlled events, when P_0 prawns of initial average body size L_0 are stocked from nurseries and grown out to market size. Natural, size- and density-dependent mortality are assumed to be the only causes of prawn population decline, though additional sources of mortality or loss such as predation by e.g. seabirds, escape from enclosures or rice fields, disease outbreaks, or declines in water quality are considered in sensitivity analyses described below.

It is assumed that all prawns are harvested at the end of a production cycle of length $t = T$, however, prawns weighing <30g are generally not of commercial interest. Experimental trials by

Ranjeet and Kurup with *M. rosenbergii* [98] showed the fraction of retrievable, market-size (>30g) prawns decreases linearly with increasing prawn stocking density. Accordingly, commercial yield at time $t = T$ is only a fraction of the total biomass:

$$Y(T, P_0) = \zeta(P_0) \cdot \Omega(T) \quad (6)$$

where ζ, the fraction of marketable size prawns in the population, is a decreasing function of initial stocking density P_0 estimated from data in the Ranjeet and Kurup experiments [98].

Cumulative profits over a finite time horizon are determined by the profit produced per cycle and the number of cycles completed within the given time period. In a time period of T_{max} days, the number of aquaculture cycles completed for each *Macrobrachium* species (sp) is $n^{sp} = \text{round}(\frac{T_{max}}{T})$. Cumulative discounted profit for each species, CP^{sp}, is then estimated as the sum of net discounted revenue for every cycle completed by T_{max}:

$$CP^{sp}(P_0, T, T_{max}) = \sum_{n=1}^{n^{sp}} \left(-cP_0 + \wp Y(T, P_0)\right) e^{-\delta nT} \quad (7)$$

where $\wp$ is the price per unit weight (USD/kg), c the per capita cost of stocked juvenile prawns, and δ the discount rate to account for the time lag between initial stocking costs and delayed revenues of commercial size prawns. Following the price analysis by Dasgupta and Tidwell [105], $c = \$0.10/P$ for a juvenile prawn of $L_0 = 40mm$ (corresponding to $\sim 0.35g$ juvenile prawns) and $\wp = \$12/kg$ harvested [105]. For simplicity, it is assumed that prawns of various sizes are all sold at the same weight-based rate, whereas larger prawns are likely to fetch a higher price in real markets. The discount rate is set to 7%, which is likely on the low end for sub-Saharan African countries endemic with schistosomiasis but higher than the 3-4% rate used for discounting long term government projects in the United States [106]. Other costs such as maintaining nurseries to produce juvenile prawns are considered external to the aquaculture scenario considered here and are therefore not included in the profit estimation. The influence of such costs as well as uncertainty in the cost of juveniles and the market price of harvested adults are considered in additional sensitivity analyses described below.

Cumulative discounted profits are maximized by jointly choosing the rotation length, T, and the initial stocking density, P_0. Given the rotation length, the number of rotations in the time period is determined, as T_{max} is given. Equation (7) has its basis in the optimal rotation models in forestry (see, e.g., [107]) and commercial aquaculture operations (see, e.g., [108,109]), which balance the marginal benefits of further growth against the opportunity costs of waiting to harvest. The resulting optimal rotation length is therefore shorter than a simple rule of when to harvest based solely on maximizing growth dynamics. Here, the same trade-off between benefits from waiting to harvest the prawns at a larger size and the opportunity costs of delaying the economic returns from future harvests is expected.

Parameters used in the prawn aquaculture model simulations are listed in Table S1. All results are expressed in USD to match the cost and price information identified in the literature and because of the common use of USD as an international reference currency.

Epidemiologic model

Building on our previous modeling of *S. haematobium* [45,110], the infection dynamics of the intermediate host *Bulinus* snail population, $\boldsymbol{N}$, are modeled as snails transition between $i \in \{S, E, I\}$ infection compartments corresponding to susceptible (S), exposed (E, pre-patent), and infected (I, patent) states. Furthermore, the growth dynamics of snails are modeled as they move through $j \in \{1, 2, 3\}$ size classes corresponding to $4mm$, $8mm$, and $12mm$ mean snail diameter (Figure 4). The model is further extended to include snail migration with a constant migration rate, ξ, to and from an external population, $\boldsymbol{N}^E$, that is not affected by prawn interventions. For simplicity, the external population is conceptualized to originate from an identical transmission site to the one in which interventions are modeled, though in reality, multiple sites with heterogeneous transmission dynamics may contribute differentially to the intervention site [111].

New snails enter the population as susceptible juveniles, i.e. in infection class $i = S$ and size class $j = 1$. Logistic snail population growth is modeled with *per-capita* recruitment, f, and carrying capacity, K. Neither small snails ($j = 1$) nor infectious snails ($i = I$) contribute to recruitment due to sexual immaturity and parasitic castration, respectively [112]. Pre-patent snails' contribution to recruitment is reduced by a fraction $0 < z < 1$ [113]. Snails of each size class are subject to both size-dependent natural mortality, μ_j, and predation mortality, ψ_j, a function of both prawn and snail body size and density described in the next section. Small and medium snails grow and transition to the next size class at the per capita rate g_1 (from size class 1 to 2) and g_2 (from class 2 to 3), respectively.

New snail infections occur at the rate βM, where β is the per-capita transmission rate and $M = 0.5\phi(W)WHm$ is an estimate of the overall number of *S. haematobium* miracidia (free living larvae that infect snails) produced by mated adult *S. haematobium* female worms and shed in the urine of infected individuals. This estimate is the product of the size of definitive human host population, H, the mean parasite burden, W, (i.e., mean number of adult worms per person), the rate at which mated adult female worms shed eggs that hatch into infectious miracidia, m, and the function $\phi(W)$ representing the density-dependent mating probability of adult worms [24]. The coefficient 0.5 accounts for the assumed 1:1 sex ratio of adult worms. For simplicity, a constant human population and no density-dependent fecundity of female worms are assumed. Following infection, pre-patent snails, E, transition to the patent class, I, at rate σ, with σ^{-1} being the mean time necessary for sporocyst development following snail infection with a miracidium.

The adult parasite population harbored by definitive human hosts is modeled as the mean parasite burden in the human population, W, assuming a negative binomial distribution with clumping parameter, φ [23,24]. Humans acquire adult worms as a result of contact with cercariae (free living larvae that infect humans) shed from patent snails. Worm acquisition occurs at rate λ, an aggregate parameter accounting for the *per capita* shedding rate of cercariae by infected

snails, cercariae mortality, contact rate, and probability of infection, as described in previous work [45]. The cercarial shedding rate of medium (N_{I2}) and large (N_{I3}) snails is assumed to exceed that of small (N_{I1}) snails by a factor θ_1 and θ_2, respectively [114].

Total DALYs lost over a given simulation period of T_{max} days is estimated as a function of: 1) disability weights associated with heavy and light infection (DW_{hi} and DW_{lo}, respectively) normalized to a daily estimate to match the dynamics of the model and 2) the number of individuals in each burden class at each time step of the epidemiological model (H_{hi_t} and H_{lo_t}):

$$\sum_{t=1}^{T_{max}} \frac{\boldsymbol{DW_{hi}}}{\boldsymbol{365}} \boldsymbol{H_{hi_t}} + \frac{\boldsymbol{DW_{lo}}}{\boldsymbol{365}} \boldsymbol{H_{lo_t}} \quad (10)$$

Additional information regarding the epidemiologic model including the full system of differential equations, epidemiologic model parameters (Table S2), and the process for estimating the number of individuals with heavy and light infection from the model can be found in the supplementary information.

Prawn predation model

As in previous work [110], the per-capita prawn predation rate on *Bulinus* snails of each class, ψ_{ij}, is modeled as a type III functional response, described by a generalization of Holling's disk equation [115]. This produces a sigmoid-shaped function, which increases and saturates at high prey densities and decreases to approach zero at low prey densities. Previous experiments by Sokolow et al [87] show that prawn predation of snails changes predictably as a function of the ratio of prawn biomass to snail body mass, r_j. Using these experimental data, the attack rate, α, is estimated as a log-linear function of the biomass ratio: $\alpha = \alpha_m * \log(r_j(t))$. The handling time, T_h, is estimated as a reciprocal function of the biomass ratio: $T_h = \left(T_{h_m} r_j(t)\right)^{-1}$, where α_m and T_{h_m} are coefficients estimated from Sokolow et al [87], and r_j is the ratio between prawn body size and mean snail body size in each class. Laboratory experiments presented in Sokolow et al [87] show that small prawns are unable to feed on large snails ($j = 3$), accordingly, $\psi = 0$ when $r_j < 3$. In addition, the attack rate, α, derived by Sokolow et al. [87] in controlled laboratory conditions in $1m^{-2}$ tanks, is penalized by a factor $0 < \epsilon < 1$ to account for the reduction in searching efficiency caused by the morphological complexity of foraging in wild settings.

The biomass ratio for each snail size class is estimated as:

$$r_j(t) = \frac{B(t)}{a_N L_{N_j}^{b_N}} \quad (8)$$

where $B(t)$ is prawn body size derived with eq. (4) and the denominator represents snail mass in each class *j*, derived as a simple allometric function of snail shell diameter in each size class. The *per-capita* attack rate of prawns on snails of size *j* and infection class *i* is then estimated as:

$$\psi_{ij} = \begin{cases} \frac{\alpha\left(r_j(t)\right)\epsilon N_{ij}^n}{1+\sum_{i=S}^{I}\sum_{j=1}^{3}\alpha\left(r_j(t)\right)\epsilon T_h\left(r_j(t)\right)N_{ij}^n}, & r_j \geq 3 \\ 0, & r_j < 3 \end{cases} \quad (9)$$

Prawn stocking at the considered densities is assumed to have no negative effects on water quality that may affect prawn survival, growth, predation of snails, or snail population dynamics, though ongoing field experiments in the lower Senegal River basin show that water quality may be negatively affected by nets installed to contain prawns introduced at transmission sites.

Parameters of the snail predation component of the combined model are listed in Table S3.

The model was coded in R version 3.5.0 and simulated using the deSolve package [116]. To address concerns regarding reproducibility, all model code and data are provided as a supplementary folder to the manuscript and are freely available online at https://github.com/cmhoove14/Prawn_fisheries_Public_health.

Model Simulations

A time horizon of $T_{max} = 10$ years is used for comparability to similar analyses investigating different schistosomiasis intervention strategies [78,117]. The aquaculture component of the model is first used to simulate growth and mortality dynamics for each *Macrobrachium* species (*sp*) in a $1{,}000m^2$ enclosure. Because prawn body size increases and levels off with time, but prawn abundance decreases in time due to size- and density-dependent mortality, both stock biomass and cumulative profit are unimodal functions of time for any given initial stocking density, P_0. Additionally, harvesting prior to peak profit may afford the opportunity to increase the number of aquaculture cycles, n^{sp}, and therefore sacrifice short term profits to maximize long term profit. The stocking density, P_0, and harvest time, T, that maximize cumulative profit for each species, CP^{sp}, are identified via numeric simulation. The surface of values (P_0, T, CP^{sp}) is related to the eumetric curve used in fishery science to identify the stocking density or fishing effort that maximizes profit [118]. As stocking costs increase linearly with stocking density, P_0, while revenues increase less than linearly as a consequence of density-dependent growth and mortality, the surface is unimodal and its peak represents the maximum achievable cumulative profit, $CP_{opt}^{sp} = \max(CP^{sp})$. Therefore, it is possible to identify the stocking density, ${P_0}_{opt}^{sp}$, and harvest time, T_{opt}^{sp}, that maximize cumulative profit, CP_{opt}^{sp}, here collectively defined as *optimal management*. Optimal management for each prawn species is identified using a grid search over initial stocking densities, P_0, ranging between $0.5 - 7.5\ Pm^{-2}$ and potential harvest times, T, on each day between $1 - 730$ days.

The epidemiologic model of schistosomiasis transmission is an extension of the model presented in Sokolow et al. 2015 [45]. It describes the growth and infection dynamics of the intermediate host snail population as snails move from small to intermediate and then large size classes and transition from susceptible (*S*) to exposed (*E*) and then infective (*I*, implying active shedding of larval cercariae which infect humans) infection classes. It also tracks human infection via a state variable representing the mean worm burden, W, in the human population. Finally, the

epidemiologic and aquaculture models are linked via a predation function parameterized via results from Sokolow et al 2014 [87], representing the prawn population's size-and density-dependent rate of snail consumption, penalized for wild foraging conditions as described above. This linked model is subsequently referred to as the *integrated model* which is used for additional simulations of potential prawn- and MDA-based interventions.

In the integrated model, prawn stocking and harvesting are simulated at regular intervals of T_{opt}^{sp} days as instantaneous events that reset the values of prawn density, P, and mean prawn body size, L, to match the initial conditions at the beginning of each stocking cycle (i.e. $P_{0_{opt}}^{sp}$ and L_0). This assumes that all prawns—regardless of marketability—are harvested and replaced with $P_{0_{opt}}^{sp}$ juveniles in a single day. Mass drug administration is implemented as an instantaneous 85% reduction in the mean worm burden, W, of the epidemiologic model and is assumed to affect the same 75% of the human population, corresponding to assumptions of 85% drug efficacy and 25% systematic non-compliance to treatment [117,119].

The integrated aquaculture-epidemiologic model is run under the following scenarios: (1) 10 years of annual MDA with no prawn intervention; (2) and (3) 10 years of prawn stocking and harvesting under optimal aquaculture management for *M. rosenbergii* and *M. volenhovenii*, as described above, with no MDA; and (4) and (5) 10 years of integrated intervention with both annual MDA and prawn stocking and harvesting under optimal management for each species. In all scenarios, the system is simulated for an additional 10 years without intervention to explore rebound in the community mean worm burden, *W*, in the case the intervention program is ceased.

To compare the effects of different interventions, disability associated with schistosomiasis is modeled using the disability adjusted life year (DALY) as in previous analyses [78,120]. Disability weights measuring the disability associated with a condition for a single year of life—where 0 is perfect health and 1 is death—were distributed among individuals with heavy (> 50 eggs per 10mL urine, H_{hi}) and light ($0 <$eggs per 10mL urine ≤ 50, H_{lo}) *S. haematobium* burdens as defined by WHO guidelines. Total DALYs lost are then estimated cumulatively over each simulation period (see methods).

All simulations are performed across 1,000 candidate parameter sets derived from latin hypercube sampling of the parameters and ranges listed in Tables S1-S3 to determine variability in model outputs arising from parametric uncertainty. These same parameter sets are used in global sensitivity analyses using partial rank correlation coefficients in addition to specific sensitivity analyses to explore the influence of increased prawn mortality and fixed costs associated with stocking or harvesting prawns.

3.3 Profit-optimal stocking densities and schistosomiasis control efficacy

With parameters reported in Table S1, stocking *M. rosenbergii* at $P_0 = 2.6\ Pm^{-2}$ and harvesting at $T_{opt}^{ros} = 165\ days$ maximizes cumulative ten-year profit, while stocking at $P_0 = 2.4\ Pm^{-2}$ and harvesting at $T_{opt}^{vol} = 260\ days$ maximizes cumulative profit for *M. vollenhovenii*. These stocking densities and harvesting times were used to simulate aquaculture cycles for each

species. Figure 2 shows the dynamics of each species run continuously through two years with vertical dashed lines indicating the optimal time of harvest, T_{opt}^{sp}. Prawns grow in length, L, and weight over time (Fig 2a) while population size (measured as density, Pm^{-2}) decreases with time as a result of density-dependent death from crowding and natural, size-dependent mortality (Fig 2b). These competing effects lead to a humped function of total harvestable biomass, Ω, over time, with the peak occurring well before prawns grow to their full size (Fig 2c). Ten-year cumulative profits also have a single peak, which is determined by both the profit per cycle and the number of cycles possible within the 10-year time frame (Fig 2d). Cumulative profits are maximized by harvesting well before the peak in harvestable biomass occurs, indicating more, smaller harvests maximize profit over time.

Table 3.3.1: Optimal stocking and harvesting parameters for each prawn species reported as median (interquartile range).

Parameter	Definition	*M. vollenhovenii*	*M. rosenbergii*
$\boldsymbol{P_{0_{opt}^{sp}}}$	Optimal stocking density	2.4 Pm^{-2}	2.6 Pm^{-2}
$\boldsymbol{L_0}$	Stocking size of juveniles	$40mm$	$40mm$
$\boldsymbol{T_{opt}^{sp}}$	Optimal harvest time	260 $days$ (228 – 331)	165 $days$ (146 – 192)
$\boldsymbol{L(T_{opt}^{sp})}$	Mean length at harvest	$167mm$ (161 – 175)	$167mm$ (161 – 174)
$\boldsymbol{P(T_{opt}^{sp})}$	Prawns harvested	1056 (850 – 1236)	1559 (1434 – 1662)
$\boldsymbol{Y(T_{opt}^{sp}, P_{0_{opt}^{sp}})}$	Commercial yield per harvest	28 kg (21 – 36)	41 kg (34 – 49)
$\boldsymbol{n^{sp}}$	Number of cycles in 10 years	14 (11 – 16)	22 (19 – 25)
$\boldsymbol{CP_{opt}^{sp}}$	Cumulative profits over 10 years	\$1891 (\$856 – \$3486)	\$5403 (\$3380 – \$8075)

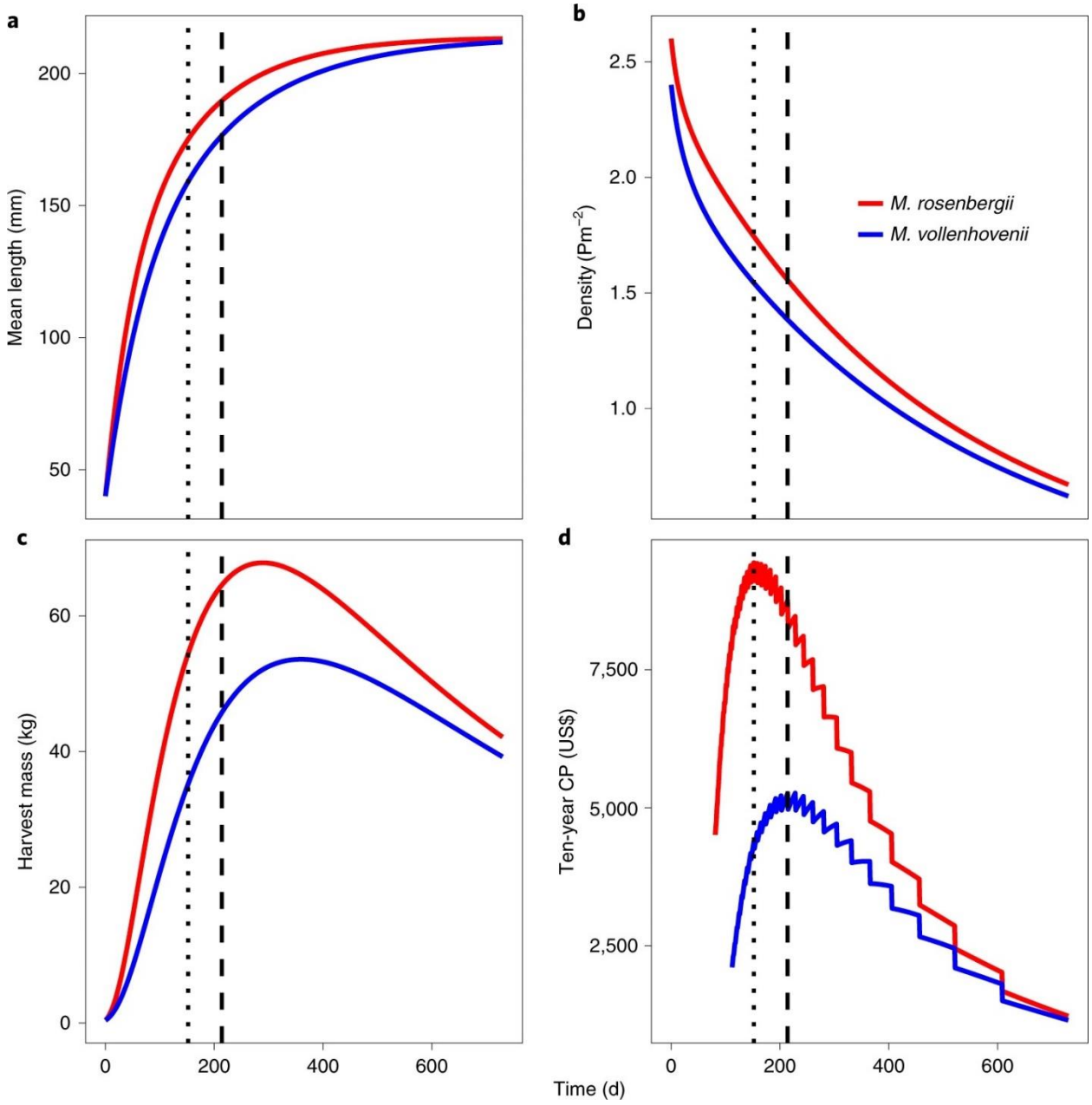

Figure 3.3.1: Prawn aquaculture model dynamics. Prawn aquaculture model dynamics. Two-year aquaculture cycles for *M. rosenbergii* (red lines) and *M. vollenhovenii* (blue lines) under optimal management showing how prawns grow in length over time (bottom-left), but decrease in density (top-left). This leads to a single peak in harvest mass (top-right), but harvesting actually occurs prior to the peak in order to maximize ten-year cumulative profits (bottom-right) by sacrificing profit-per-cycle for completing more aquaculture cycles. Vertical dashed lines indicate time at which harvest would occur for each species (small dashes – *M. rosenbergii*, large dashes – *M. vollenhovenii*). Harvest of the slower-growing *M. vollenhovenii* occurs later as they take longer to grow in size and biomass. Here, following [105], the cost *c* for a juvenile prawn is \$0.10 with $L_0 = 40mm$ (~0.35g per juvenile prawns) and the selling price is $\wp = \$12/kg$. Other parameters set as in Table 1.

The surface of values (P_0, T, CP^{sp}) resulting from the grid search to identify optimal management for each species is shown in Figure 3. As expected, profits associated with

aquaculture of the faster growing *M. rosenbergii* are higher. Considering parametric uncertainty, the peak estimate of median cumulative profit for *M. rosenbergii* occurs at $P_0 = 2.9\ Pm^{-2}$ and $T_{opt}^{ros} = 173\ days$ (IQR: $146 - 192$), producing $CP_{opt}^{ros} = \$5364$ ($\$3192 - \$8111$) per $1{,}000\ m^2$ enclosure. The same estimates for *M. vollenhovenii* are$P_0 = 2.5\ Pm^{-2}$,$T_{opt}^{vol} = 260\ days$ $(228 - 331)$, and $CP_{opt}^{vol} = \$1738$ ($\$704 - \$3394$). Cumulative profits are still feasible at much higher stocking densities for each species with $CP_{opt}^{ros} > 0$ at stocking densities as high as $P_0 = 6.5\ Pm^{-2}$ and $CP_{opt}^{vol} > 0$ at stocking densities up to $P_0 = 5.95\ Pm^{-2}$. Additional outputs from the aquaculture model that describe stock structure and aquaculture performance at optimal management are reported in Table 1.

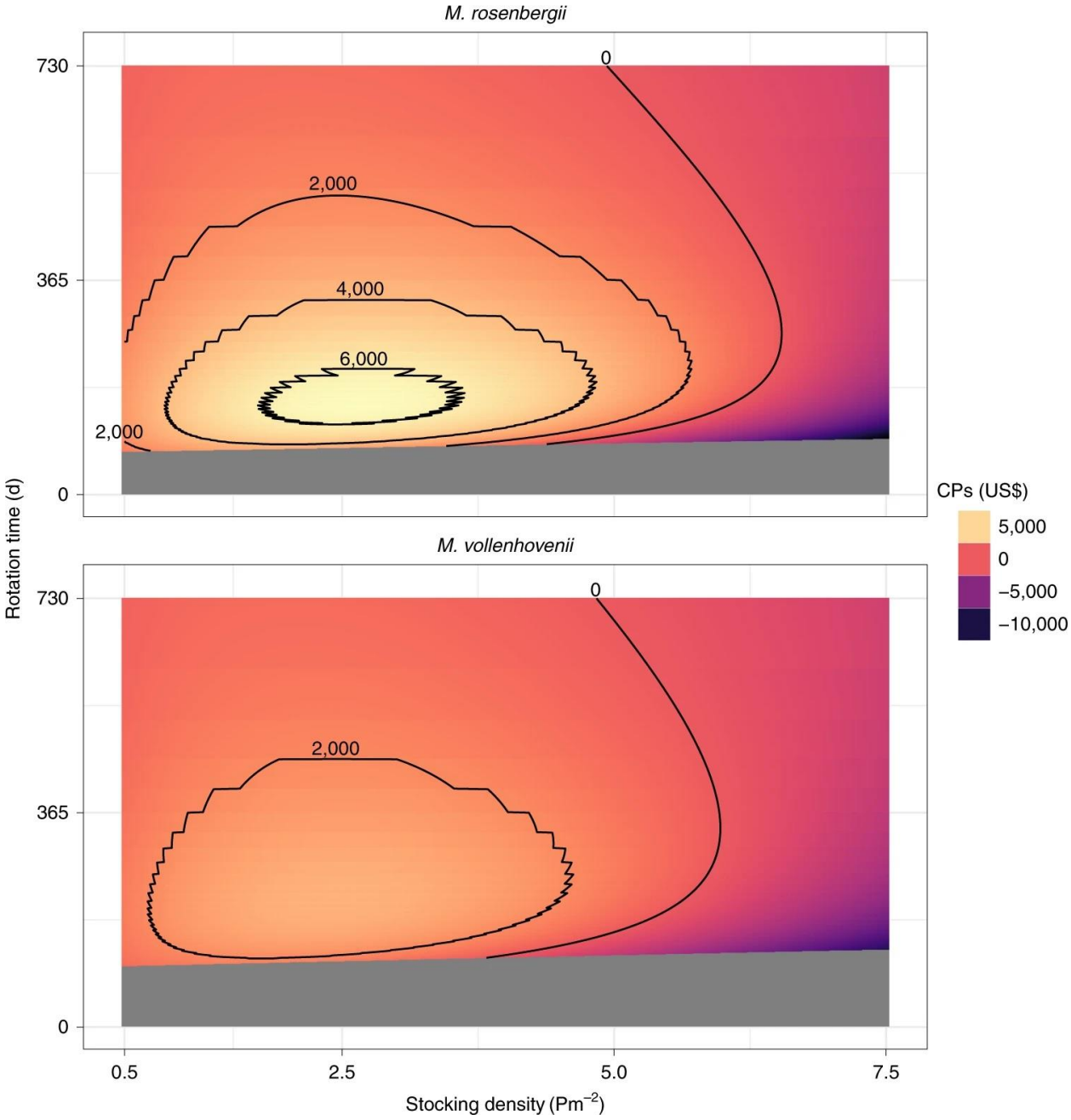

Figure 3.3.2: Grid search to identify optimum management decisions for each prawn species. CP^{sp} generated by the aquaculture model for each species across a range of potential stocking densities and rotation times. The grey regions indicate regions where harvesting is not feasible due to prawns not having reached a sufficient marketable size (30 g), due to insufficient time to grow and density-dependent growth rates. The contours indicate regions of CP^{sp} corresponding to the labelled value in 2018 US$.

Simulation of the integrated model reveals comparable performance of prawn intervention strategies to MDA strategies. As in previous analyses [45,78], annual MDA alone produces a pattern of gradually decreasing worm burden over time characterized by repeated rebound in infection following MDA (Fig 3.4A, purple line). The prawn-only intervention causes mean worm burden to gradually decline towards 0, eventually reducing worm burden to comparable levels by year

10 (Fig 3.4A, blue line). The combined MDA and prawn intervention leads to a rapid decline in mean worm burden that nearly reaches 0 by year 10 (Fig 3.4A, gold line).

These patterns can be explained by the underlying snail infection dynamics. Under MDA intervention, the snail population persists through repeated rounds of MDA and even increases due to the reduced influence of infection on fecundity and mortality of the snail population (Fig 3.4B). Most importantly, infected snails continue to shed infectious cercariae—albeit at lower levels—even as adult worms are removed from the treated human population through repeated MDA (Fig 3.4B). Interventions in which prawns are introduced at profit-maximizing densities cause rapid declines in the snail population and near elimination of infective snails (Fig 3.4C). Extirpation of the entire snail population is prevented due to the assumption of a Holling's type III (S-shaped) functional response that produces decreased rates of predation at low snail density and immigration from an unaffected reservoir population (see Fig S3 for snail infection dynamics without immigration and under a Holling's type II, logarithmic-shaped, functional response). Even though the entire snail population is not extirpated, transmission is effectively halted due to near elimination of the infected snail population (Fig 3.4C). Meanwhile, mean worm burden decreases slowly due to natural worm mortality (Fig 3.4a, blue line) or quickly in the presence of MDA (Fig 3.4a, gold line). This heavy reduction in transmission coupled with the benefits of MDA translates to near elimination of the parasite by year 10. Regardless of the intervention, ceasing efforts to control transmission after 10 years results in rapid returns towards pre-intervention snail populations and community-level mean worm burdens (Fig 3.4A-C).

Comparison of total DALYs lost over 10-year simulation periods under each intervention shows comparable performance of the prawn-only intervention and MDA, and substantial additional DALYs averted when combining MDA with prawn intervention. Without intervention a median 324 (IQR: 119 – 502) DALYs are lost to *S. haematobium* infection. Annual MDA and profit-maximizing prawn stocking perform comparably with 160 (IQR: 54 – 285) total DALYs lost with annual MDA and 184 (IQR: 70 – 294) total DALYs lost with prawns; representing 51% and 43% DALYs averted, respectively. Integrated interventions utilizing both MDA and prawn stocking reduce median DALYs lost to 83 (IQR: 30 – 137), representing a 74% reduction in *S. haematobium* related disability.

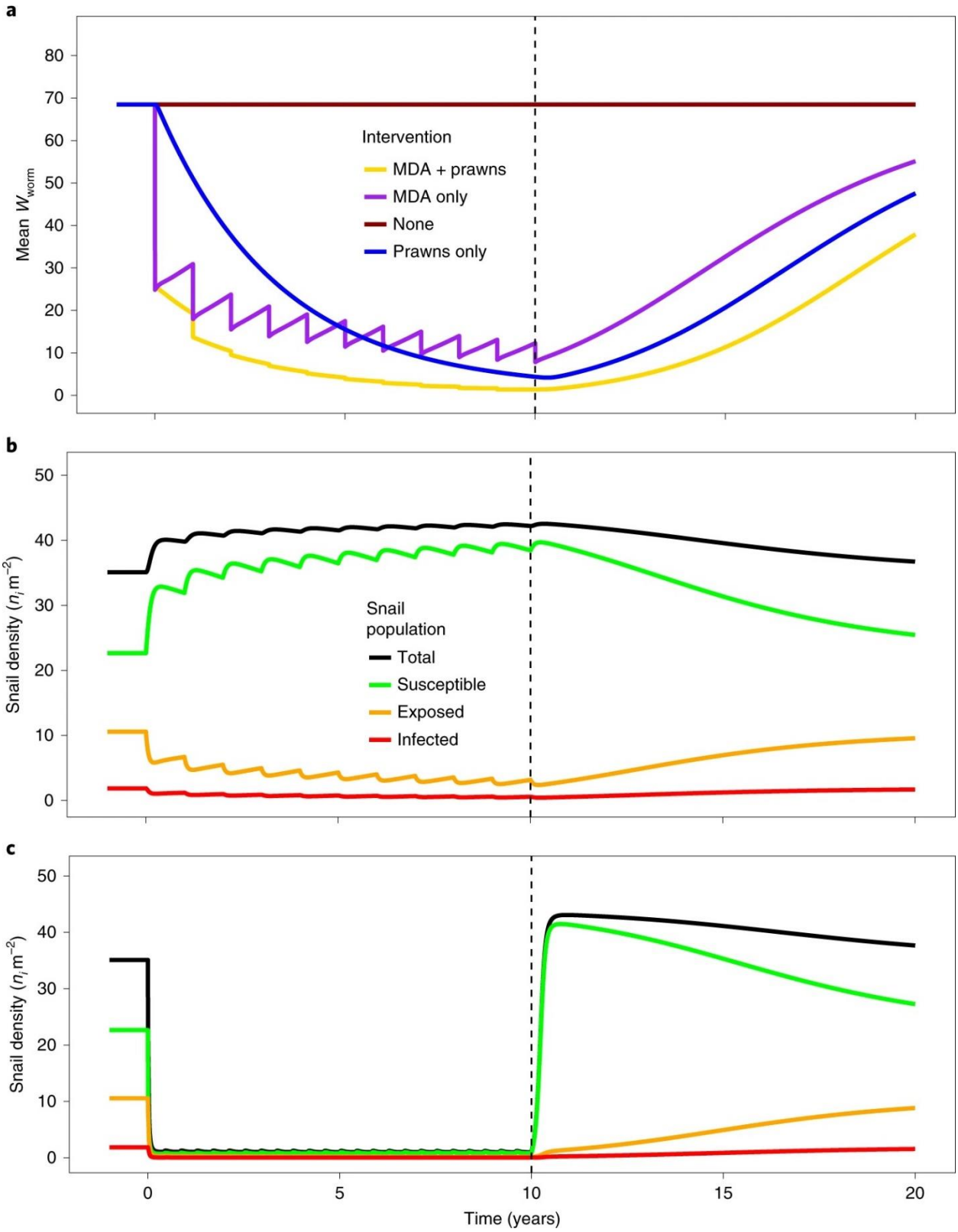

Figure 3.3.3: Outputs of the integrated model under different intervention scenarios implemented over ten years, followed by ten years of no intervention. a, Worm burden trajectories under no intervention (maroon), annual MDA

only (purple), prawn stocking of M. rosenbergii under optimum management (blue), and both annual MDA and prawn stocking (gold). b,c, Snail infection dynamics under the MDA-only intervention (b) and prawn stocking intervention (c). Outputs from M. volenhovenii interventions are not shown as they approximately mirror those of M. rosenbergii, since the profit-maximizing stocking densities of both species result in maximum reductions in the snail population.

3.4 Discussion, conclusions, and caveats

Small-scale, extensive prawn aquaculture such as that considered here offers a profitable and sustainable method to improve food production, reduce schistosomiasis transmission, and increase revenues for small-scale subsistence farmers, especially when paired with ongoing efforts such as rice cultivation [97]. In areas of high food insecurity, malnutrition, and endemic schistosomiasis—conditions which reinforce each other and often result in "poverty traps" [121,122]—the development of prawn aquaculture in transmission sites may be a solution for co-benefits of disease control and sustainable development.

To meet goals for schistosomiasis reduction set out by the World Health Organization (WHO) of morbidity control by 2020 and local elimination as a public health problem by 2025, additional control strategies are needed [74,94]. These results build on an increasing body of evidence indicating consumption of snails by predator species such as *Macrobrachium* prawns can be an effective method for combating schistosomiasis transmission to people [45,86,123]. Specifically, by targeting the environmental reservoir of schistosome parasites, prawns can reduce reinfection rates that undermine the effects of MDA campaigns in high transmission settings. By deploying prawn aquaculture with MDA, effective control—in which the schistosome parasite is suppressed in both human hosts and intermediate host snails—can be achieved. Furthermore, the use of prawns for snail control, as opposed to molluscicides that may have non-target effects on species other than schistosome-bearing snails, represents a more sustainable approach to schistosomiasis control.

Prawn interventions combined with established extensive aquaculture methods can also be profitable if carefully managed. Drawing on economic studies of existing aquaculture practices [91,105], we develop—to our knowledge—the first dynamic model of prawn aquaculture to investigate optimal management practices. The model suitably simulates prawn stocking in a large enclosure or rice paddy, and the length of optimal cycles coincides with typical rice harvesting timelines [97]. This system produces short- and long-term profits, implying the potential for a sustainable, community-driven intervention, given the right capital investment and incentive programs.

Under optimal management, extensive aquaculture of either *M. rosenbergii* or *M. vollenhovenii* leads to both profits and reductions of the snail population. The optimal stocking densities of each species are above the potential threshold of approximately $2\ Pm^{-2}$ necessary for local snail extirpation as identified in previous work [45], though our conservative inclusion of snail migration and a Holling's type III functional response restricts such an outcome in this analysis. While this estimate of the threshold stocking density necessary for snail extirpation is based on a number of realistic assumptions regarding prawn mortality, snail population dynamics and behavior, and prawn predation of snails, stocking densities at least three times higher than this are still

economically viable. Alternative funding mechanisms (e.g. that maximize the potential for snail control rather than for profit) may therefore be worth exploring.

Achieving these stocking densities may be challenging in sub-Saharan Africa where >90% of the global burden of schistosomiasis is found [95] and where strategies to complement ongoing MDA are most needed. Juvenile *M. rosenbergii* are readily available for purchase, and protocols for ideal rearing and management for aquaculture of this species have been established during 50 years of domestication [90,91]. Similar protocols for the African native *M. vollenhovenii* are still under development. Profits appear to be highly sensitive to parameters that regulate prawn growth, meaning continued research and development into *M. vollenhovenii* aquaculture—including nursery and hatchery protocols, better understanding of their growth and social structure, and selective breeding—may eventually provide comparable profits to *M. rosenbergii*, especially given the rapid expansion of aquaculture technologies and practices globally in recent years [124,125].

Stocking *M. rosenbergii* in coastal regions where it is non-native should be approached with caution to avoid the establishment of an alien population with potentially unintended ecological consequences on local biodiversity. Establishment of aquaculture biotechnologies for either all-male [126–128] or all-female [129] populations that do not rely on genetically modified organisms (GMOs) suggest possible strategies to prevent invasions. Moreover, recent laboratory experiments have ruled out the possibility of cross-fertilization between mature female *M. vollenhovenii* and male *M. rosenbergii*, demonstrating that male-only progeny of *M. rosenbergii* may be safely used for extensive aquaculture and schistosomiasis control in western Africa where *M. rosenbergii* is non-native [128,130].

Extensive sensitivity analyses reveal that key model outcomes, including profit generated by the aquaculture portion of the model and DALYs lost from the integrated model, are robust to uncertainty in key parameters governing profit estimation and the influence of prawn interventions on DALYs lost. Aquaculture performance—in terms of cumulative profits—is most sensitive to parameters governing somatic growth, which have been estimated from available literature, and supported by expert opinion [100,104]. This finding also suggests that if stock improvement or advances in husbandry practices can increase average prawn condition or size, i.e. by supplementing feeds, further increases in profit may be possible. Selective harvesting methods that only remove market-size prawns, leaving the remaining stock to continue to grow, may also improve aquaculture performance. However, such selective harvesting may require additional investment e.g. in nets with different mesh sizes or pumps to drain waterbodies and further inspect prawns. Harvesting all prawns in a single batch, as is assumed in these analyses, is therefore considered the easiest management strategy to implement.

Optimal aquaculture practices are also sensitive to the market price of adult prawns and the stocking cost of juvenile prawns, implying that optimal management may be influenced by fluctuations in market factors that may influence price and cost of harvested and stocked prawns. Profit generated from selling harvested prawns is based on reasonable assumptions of prices in premium markets, though the actual selling price in subsistence economies might be lower and

contingent on market access and local demand. However, the fixed cost sensitivity analysis demonstrates profitability is possible even with substantial additional costs associated with prawn stocking, and profitability persists across a wide range of stocking densities for each species. These results together assuage concerns that such market vagaries would impair success of the proposed system and suggest that prawn aquaculture can be economically viable even under non-optimal densities.

Surveys to identify potential prawn intervention sites, including rice paddies, ponds, and water contact sites that can be enclosed with a net, would also be needed on a local scale. Such sites would require water quality compatible with prawn survival, therefore activities such as laundry, car washing, and the use of insecticides on nearby crops would have to be limited [110,131]. Still other sources of additional prawn mortality such as disease outbreaks or predation by waterbirds, fish, amphibians or reptiles are also possible, though extensive aquaculture would still be profitable with mortality rates as high as five times natural mortality. Barring catastrophic events, this suggests that the proposed system should be resilient to such perturbations. Additional studies assessing prawn life expectancy, escapement rate, growth performance, changes in water quality, and potential changes in human behavior which might affect aquaculture performance and/or snail abundance, transmission rates, and epidemiologic outcomes should be pursued.

Prawn predation of the snail population as modeled here is also based on a number of assumptions including the Holling's type III functional response and the prawn attack rate penalty. The type III functional response likely represents a conservative estimate of the relationship between prawn predation and snail density as it does not allow for the potential extirpation of the snail population. This necessitates combining the prawn intervention with MDA to be effective in reaching elimination targets. A wide range of attack rate penalties that regulate the number of snails consumed per prawn per day were also tested, as no prior estimates of prawn predation efficiency in non-laboratory settings were identified. Effective control is feasible even when penalizing the attack rate by an order of magnitude (implying a substantially reduced attacked rate).

Regarding schistosomiasis transmission dynamics, recent findings suggest non-linearities in the human-to-snail force of infection may decrease the efficacy of MDA and lead to faster post-MDA rebounds of schistosomiasis [79]. While this may alter the effects of MDA in our simulations, we believe it strengthens the argument for strategies that explicitly target the intermediate host snail population, such as the prawn intervention proposed here. The model also makes simplifying assumptions that should be investigated in future research: that production of infectious cercariae, and human contact with water containing infectious cercariae both occur only in the site where prawns are stocked. Previous analyses have investigated the role of human movement and passive cercarial transport e.g. in river currents [111], but these processes have not been incorporated here due to the existing complexity of the model and the lack of adequate data to quantify these phenomena in this setting. The effectiveness of the prawn intervention is expected to be reduced if people are frequently exposed to schistosome cercariae at or from other transmission sites.

Another recent finding suggests that snail control can actually lead to increased human risk of *Schistosoma* infection if the snail population is limited by resource competition prior to "weak" control efforts [132]. In this scenario, remaining snails with higher per-capita resource availability may produce more cercariae. Given the large magnitude of snail reductions at the proposed prawn densities modeled here—even given the conservative Holling's III functional response—this effect is believed unlikely in our scenarios.

Finally, our model lacks seasonality, which may affect both schistosomiasis transmission and prawn growth as e.g. temperature and rainfall fluctuate through the year, especially in sub-tropical and near-temperate regions where schistosomiasis is still endemic, such as in northern Africa [133–135]. However, the assumption of a constant and large snail population carrying capacity represents a worst case scenario, and introducing seasonal variation would likely not alter the results presented here. Furthermore, in regions where transmission predominately occurs in ephemeral ponds during the rainy season, prawn aquaculture is likely not a viable approach [134].

This bioeconomic analysis shows that an integrated intervention strategy that utilizes both MDA and a profitable prawn aquaculture system can successfully control schistosomiasis while generating profit. Since the intervention is driven by a profitable business model, it may be sustainable purely through market incentives, and thereby reduce the need for external support from donors or public health agencies. Subsidies are expected to be necessary only in the event that *M. rosenbergii* aquaculture is not suitable for the region, and obtaining large quantities of *M. vollenhovenii* juveniles is infeasible or expensive. Research and development for this system is indeed ongoing in Senegal, which will aid future analyses of the effectiveness and feasibility of this promising integrated strategy.

3.5 Appendix

Epidemiologic model equations

$$\frac{dN_{S1}}{dt} = \xi N_{S1}^{E} + f\left(1 - \frac{N}{K}\right)\left(N_{S2} + N_{S3} + z(N_{E2} + N_{E3})\right) - (\mu_1 + g_1 + \psi_{S1}P + \xi + \beta M)N_{S1} \quad \text{(S1)}$$

$$\frac{dN_{S2}}{dt} = \xi N_{S2}^{E} + g_1 N_{S1} - \psi_{S2}P - (\mu_2 + g_2 + \xi + \beta M)N_{S2} \quad \text{(S2)}$$

$$\frac{dN_{S3}}{dt} = \xi N_{S3}^{E} + g_2 N_{S2} - \psi_{S3}P - (\mu_3 + \xi + \beta M)N_{S3} \quad \text{(S3)}$$

$$\frac{\mathrm{dN_{E1}}}{dt} = \xi N_{E1}^{E} + \beta M H N_{S1} - \psi_{E1}P - (\mu_1 + g_1 + \xi + \sigma)N_{E1} \quad \text{(S4)}$$

$$\frac{\mathrm{dN_{E2}}}{dt} = \xi N_{E2}^{E} + \beta M H N_{S2} - \psi_{E2}P - (\mu_2 + g_2 + \xi + \sigma)N_{E2} \quad \text{(S5)}$$

$$\frac{dN_{E3}}{dt} = \xi N_{E3}^{E} + \beta M H N_{S3} - \psi_{E3}P - (\mu_3 + \xi + \sigma)N_{E3} \quad \text{(S6)}$$

$$\frac{dN_{I1}}{dt} = \xi N_{I1}^{E} + \sigma N_{E1} - \psi_{I1} P - (g_1 + \mu_1 + \mu_I + \xi) N_{I1} \quad \text{(S7)}$$

$$\frac{dN_{I2}}{dt} = \xi N_{I2}^{E} + \sigma N_{E2} + g_1 N_{I1} - \psi_{I2} P - (g_2 + \mu_2 + \mu_I + \xi) N_{I2} \quad \text{(S8)}$$

$$\frac{dN_{I3}}{dt} = \xi N_{I3}^{E} + \sigma N_{E3} + g_2 N_{I2} - \psi_{I3} P - (\mu_3 + \mu_I + \xi) N_{I3} \quad \text{(S9)}$$

$$\frac{dW_t}{dt} = \lambda(N_{I1} + \theta_1 N_{I2} + \theta_2 N_{I3}) - (\mu_W + \mu_H) W_t \quad \text{(S10)}$$

$$\frac{dW_u}{dt} = \lambda(N_{I1} + \theta_1 N_{I2} + \theta_2 N_{I3}) - (\mu_W + \mu_H) W_u \quad \text{(S11)}$$

MDA Implementation and DALYs estimation

The model tracks treated and untreated segments of the population by dividing the worm burden based on MDA coverage, such that total worm burden is a weighted average of each population: $W = cvrg W_t + (1 - cvrg) W_u$. When MDA is implemented, mean worm burden in the treated compartment is reduced by $W_t(1 - eff)$. We assume the dispersion parameter of the negative binomial distribution (φ) in each population is constant over the simulation period. To estimate the total number of individuals with heavy and light egg burdens, H_{hi} and H_{lo}, respectively, we first sample $n = H * cvrg$ draws from a negative binomial distribution with mean W_t and dispersion φ to represent the distribution of adult worms in the treated segment of the human population. Similarly, we sample $n = H * (1 - cvrg)$ draws from a negative binomial distribution with mean W_u and dispersion φ to represent the distribution of adult worms in the untreated segment of the human population. We then convert these individual level adult worm counts, denoted W_h, to estimates of egg burden, denoted B_h, as: $B_h = 0.5 W_h \phi(W_h) \mathcal{E}$ where $0.5 W_h \phi(W_h)$ provides an estimate of the number of mated female (i.e. egg producing) worms and $\mathcal{E}$ is an estimate of *S. haematobium* eggs per 10mL urine per mated adult female worm from [136]. With the full distribution of B_h, we can then estimate the number of individuals with heavy (> 50 eggs per 10mL urine, H_{hi}) and light ($0 <$eggs per 10mL urine ≤ 50, H_{lo}) *S. haematobium* burdens as defined by WHO guidelines and subsequently estimate DALYs as in equation (10).

Sensitivity Analyses

Global sensitivity analyses using latin hypercube sampling and partial rank correlation coefficients (LHS-PRCC) were conducted to determine the sensitivity of key model outcomes to parameteric uncertainty. Latin hypercube sampling is first performed over parameter ranges in Tables S3.1-S3.3 to generate a set of 1,000 candidate sets. These parameter sets are used to derive estimates of uncertainty in model simulations. Furthermore, global sensitivity analysis using LHS-PRCC [137,138] is performed with optimal cumulative profit (CP_{opt}^{sp}) as the outcome in the prawn aquaculture model, equilibrium infected snail density (N_I) and mean worm burden (W) absent prawn or MDA interventions as the outcomes in the epidemiologic model, and total DALYs accumulated through simulated 10-year combined MDA and prawn interventions as the

outcome in the integrated model. Briefly, PRCC estimates the correlation between a model parameter and a model outcome by first rank-transforming parameters drawn from an LHS scheme and the corresponding model outputs, then removing the linear effects of all other model parameters on the parameter of interest and the outcome, and finally measuring the linear relationship between the rank-transformed parameter and outcome residuals [137]. Monotonicity of the relationship between model outputs and all parameters was assessed via scatterplots prior to conducting LHS-PRCC sensitivity analyses.

Two additional sensitivity analyses are performed to identify profitability thresholds for the prawn aquaculture model. In the first, fixed costs, c_f, in the range $\$0 - \$1{,}000$ are added to the per-cycle profit calculation (Equation (7); such that total cost for each cycle is $-(cP_0 + c_f)$) to represent additional costs that may be incurred with each aquaculture cycle such as labor, transport of prawns, and nursery costs leading up to stocking. In the second, the prawn mortality rate, μ_P, is multiplied up to 10 times the estimated natural rate to account for additional sources of prawn loss that may be incurred due to predation, escape, or other sources of mortality, such as disease or poor water quality.

Profitability of the prawn aquaculture system and reductions in schistosomiasis burden associated with prawn introductions are robust to model assumptions and parameters (Figs S3.1 and S3.2). The addition of fixed costs associated with each aquaculture cycle and additional sources of mortality reveal aquaculture of *M. rosenbergii* remains profitable with fixed costs of up to $\$550$ per cycle (Fig S3.2) and mortality rates up to 5.2 times higher than the baseline estimate (Fig S3.3). Aquaculture of *M. vollenhovenii* remains profitable with fixed costs of up to $\$400$ per cycle (Fig S3.2) and mortality rates up to 3.6 times higher than the baseline estimate (Fig S3.3). Global sensitivity analysis using Latin hypercube sampling and partial rank correlation coefficients shows that the parameters of the model that govern prawn growth dynamics (L_∞, κ) and parameters governing estimates of discounted profits $(\delta, \wp)$ are most correlated with 10-year cumulative profits (Fig S3.1B)

Exploration of snail infection dynamics under prawn interventions also reveals that the Holling's type III functional response and the inclusion of snail migration represent conservative structural model assumptions. Figure S4 shows that snail extirpation is only possible when both of these assumptions are relaxed. Parameters governing snail predation by prawns (ϵ, n) are also shown to have moderate influence on estimates of 10-year cumulative DALYs lost (Fig S3.1A).

Key outcomes from the epidemiologic model, including equilibrium estimates of infected snail density (I) and mean worm burden (W) and of DALYs lost over 10-year intervention periods, are mostly influenced by epidemiologic parameters, rather than parameters governing prawn population or predation dynamics (Fig S3.1A & S3.1C). Parameter sets in which the MDA-only intervention was superior to the prawn-only intervention in terms of DALYs averted were also compared. The MDA-only intervention is superior when the coverage and efficacy are high, while the prawn-only intervention performs better when the snail population carrying capacity (K) is higher (Fig S3.5).

Supplementary Tables

Table S3.1: Parameters of the prawn aquaculture model and ranges used in the global sensitivity analysis

Parameter	Value & Units	Description	Source	Range
L_∞	$214\ mm$	Maximum length used in von Bertalanffy growth equation	[104]	[184, 234]
κ	$0.0034\frac{mm}{day}$	Growth rate of *Macrobrachium vollenhovenii*	[104,139]	[0.0078, 0.012]
	$0.0104\frac{mm}{day}$	Growth rate of *Macrobrachium rosenbergii*	[101]	
γ	$3.5 \times 10^{-6}\ g^{-1}$	Density dependent growth reduction	[98]	$[3.5 \times 10^{-6}, 6.5 \times 10^{-6}]$
a_P	0.00244	Allometric parameter for *Macrobrachium* length-weight conversion	[100]	[0.066, 0.081]
b_P	3.55	Allometric parameter for *Macrobrachium* length-weight conversion		[3.46, 3.64]
μ_P†	$0.0061\frac{P}{day}$	Daily prawn mortality rate	[104,139]	[0.0054, 0.012]
d	-0.382	Size-dependent mortality scaling coefficient	[103]	[-0.461, -0.289]
ω	$5.5 \times 10^{-9}\ g^{-1}$	Density dependent mortality factor	[98]	$[7.5 \times 10^{-9}, 3.5 \times 10^{-9}]$
$\mathcal{p}$	$\frac{\$12}{kg}$	Price per kg of harvested market-size prawns	[105,140,141]	[11, 22]
δ	$\frac{1.99 \times 10^{-4}}{day}$	Discount rate	(7% annual)	[3%, 20%]
c†	$\frac{\$0.10}{P}$	Cost of a stocked juvenile prawn	[105]	[0.045, 0.12]

† See additional sensitivity analyses

Table S3.2: Parameters of the schistosomiasis epidemiologic model

Parameter	Value & Units	Description	Source	Range
f	$0.26\, N_{S1} day^{-1}$	Per-capita recruitment rate of reproductive snails	45	[0.06, 0.36]
K	$50 \frac{N}{m^2}$	Snail population carrying capacity	142	[25, 75]
z	0.5	Proportion of pre-patent snails that reproduce	113	[0.25, 1]
μ_1	$\frac{1}{50}\ day^{-1}$	Mortality rate of snails in size class 1	143,144	[25, 100]
μ_2	$\frac{1}{75}\ day^{-1}$	Mortality rate of snails in size class 2		[50, 125]
μ_3	$\frac{1}{100}\ day^{-1}$	Mortality rate of snails in size class 3		[75, 150]
μ_I	$\frac{1}{10}\ day^{-1}$	Mortality rate of snails in infection class I	113	[7, 20]
ξ	$\frac{1}{5}\ year^{-1}$	Migration rate of snails	145	[0, 1]
g_1	$\frac{1}{37}\ day^{-1}$	Growth rate of snails in size class 1	146	[20, 60]
g_2	$\frac{1}{62}\ day^{-1}$	Growth rate of snails in size class 2		[40, 100]
σ	$\frac{1}{50}\ day^{-1}$	Pre-patent period; transition rate of snails in infection class E to infection class I	147	[30, 70]
$m^{\dagger}$	0.8	Infectious miracidia produced per mated adult female worm	45	[0.5, 1.5]
$\beta^{\dagger}$	4×10^{-7}	Pre-patent snails produced per infectious miracidia		$[2.0 \times 10^{-7}, 8 \times 10^{-7}]$
$\lambda^{\dagger}$	7.5×10^{-6}	Adult worms produced per infectious cercaria shed by infected snails		$[5.0 \times 10^{-6}, 1.0 \times 10^{-5}]$
θ_1	1.31	Increased relative production of infectious cercariae by snails in class N_{I2}	114	[1, 5]
θ_2	7.88	Increased relative production of infectious cercariae by snails in class N_{I3}		[2, 10]
φ	0.08	Clumping parameter of the negative binomial distribution	110	[0.01, 0.3]
μ_W	$\frac{1}{3.3}\ year^{-1}$	Mortality rate of adult worms	45	[2, 4]
μ_H	$\frac{1}{60}\ year^{-1}$	Mortality rate of humans harboring adult worms		[50, 70]
DW_{hi}	0.05	Disability weight associated with heavy *S. haematobium* egg burden	78,148	[0.03, 0.15]
DW_{lo}	0.014	Disability weight associated with heavy *S. haematobium* egg burden	78,148	[0.003, 0.03]
eff	0.85	MDA efficacy		[0.75, 0.95]
$cvrg$	0.75	MDA coverage		[0.5, 0.95]

$\mathcal{E}^{\dagger}$	3.6	Eggs produced per 10mL urine per mated adult female worm	[149]	[2, 5]

† Units provided in description

Table S3.3: Parameters regulating snail predation of snails, linking the aquaculture model to the epidemiologic model

Parameter	Value & Units	Description	Source	Range
a_N	0.19	Allometric parameter for snail shell width-weight conversion	[87]	[0.1, 0.3]
b_N	2.54	Allometric parameter for snail shell width-weight conversion		[2, 3]
α_m	0.91	Parameter to estimate prawn attack rate from prawn-snail biomass ratio		[0.5, 1.5]
T_{h_m}	0.39	Parameter to estimate prawn handling time from prawn-snail biomass ratio		[0.2, 0.5]
n	2	Exponent of Holling's type III functional response	[110]	[1.1, 4]
ϵ	0.1	Prawn predation attack rate penalty associated with searching for prey in wildlife rather than laboratory conditions	Estimated as 10% of laboratory-determined rates with wide range investigated in sensitivity analysis	[0.01, 1]

Supplementary Figures

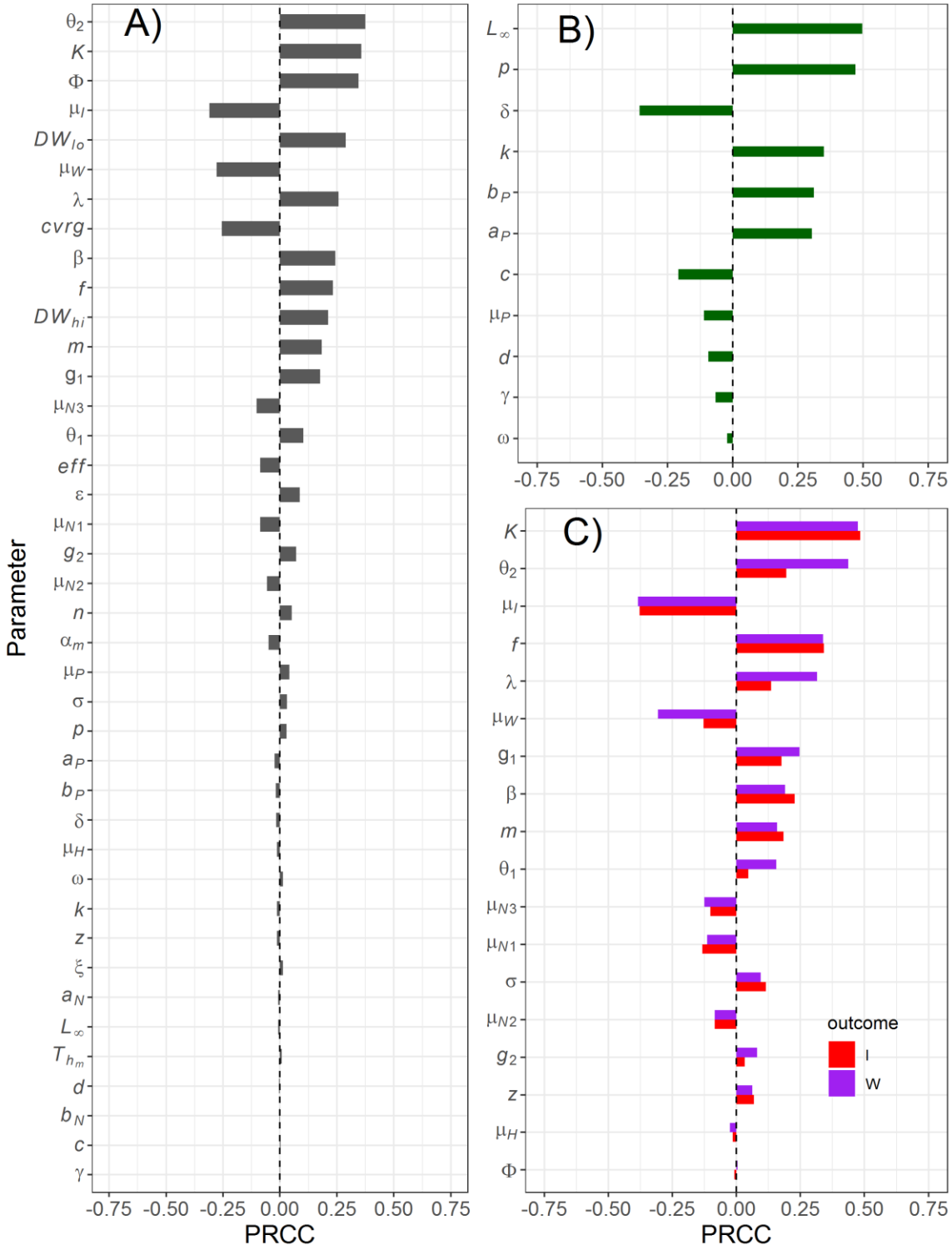

Supplementary Figure S3.1: Sensitivity of key model outcomes to model parameters assessed with LHS-PRCC. Sensitivity to all parameters of DALYs lost following 10 years of combined MDA and prawn intervention (A), cumulative 10-year profit sensitivity to prawn aquaculture parameters (B), and sensitivity of mean worm burden and

equilibrium infected snail density to epidemiologic parameters (C). Parameter definitions and baseline values can be found in supplementary tables 1-3.

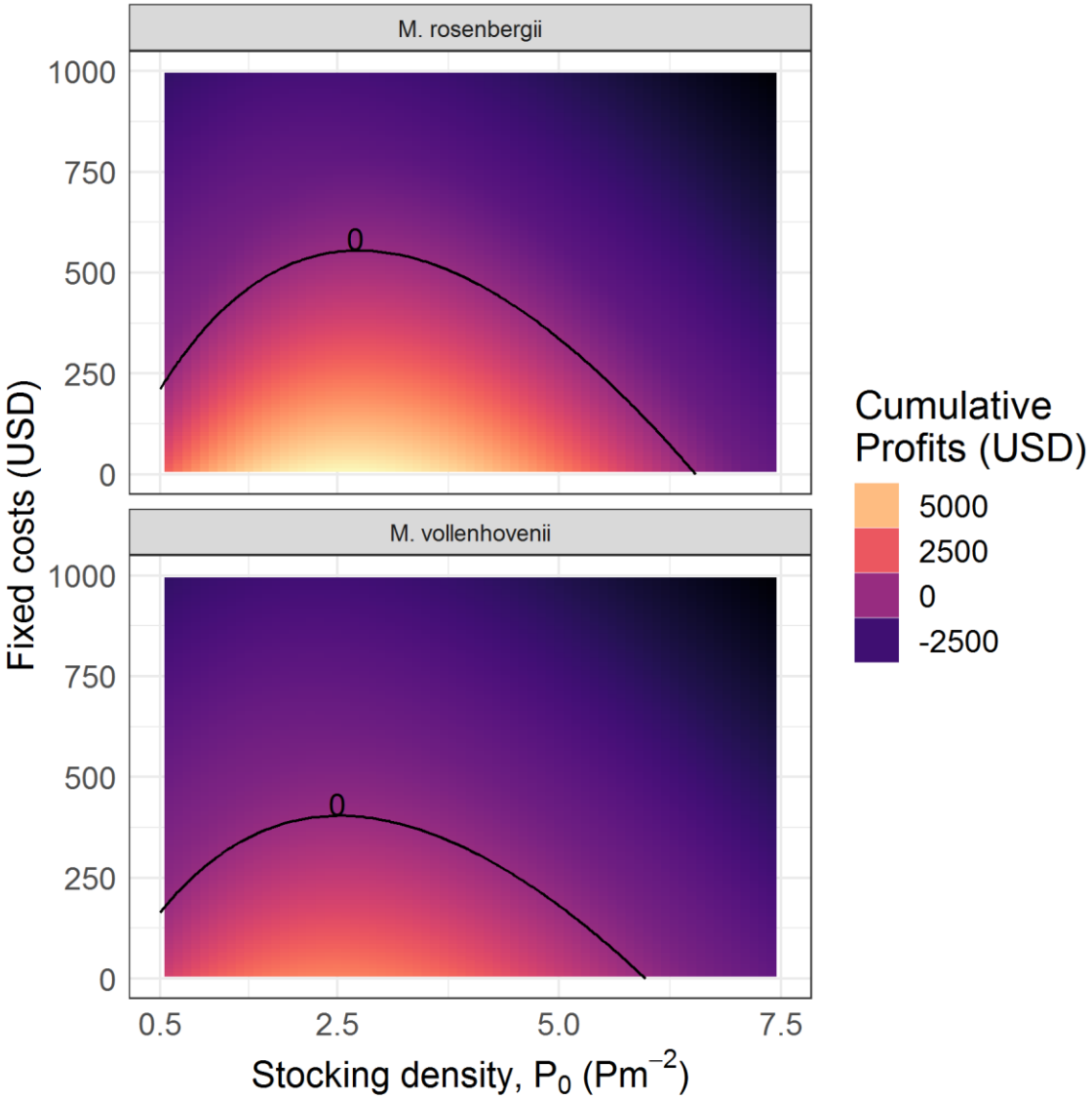

Supplementary Figure S3.2: Sensitivity analysis investigating the influence of fixed costs incurred each aquaculture cycle on profits generated by the prawn aquaculture model. Color indicates the 10-year cumulative profits generated by optimal management with stocking at the density indicated on the x-axis. The black line delineates the maximum boundary of profitability.

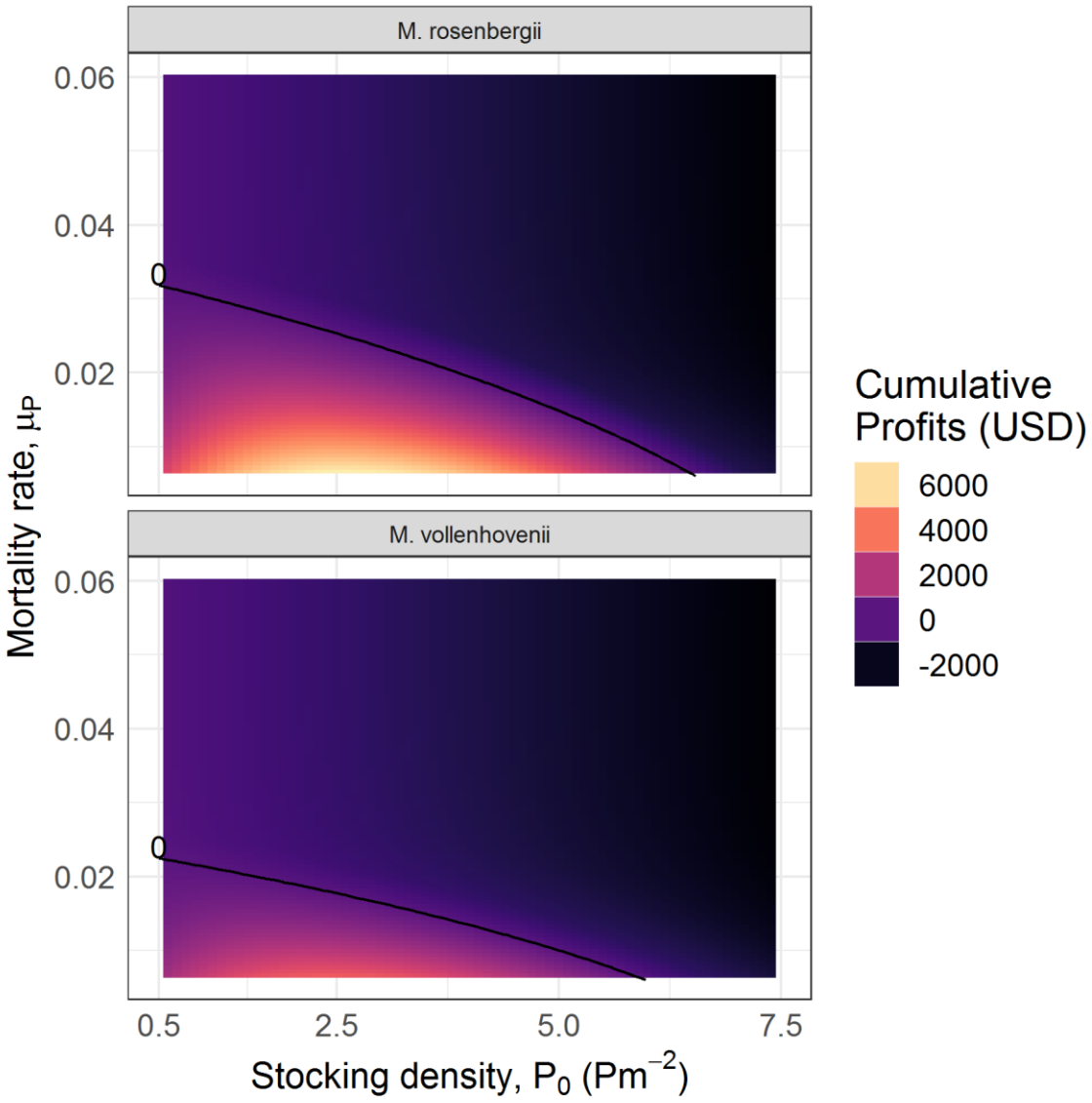

Supplementary Figure S3.3: Sensitivity analysis investigating the influence of increased mortality rates (baseline $\mu_P = 0.006$) on profits generated by the prawn aquaculture model. Color indicates the 10-year cumulative profits generated by optimal management with stocking at the density indicated on the x-axis. The black line delineates the maximum boundary of profitability.

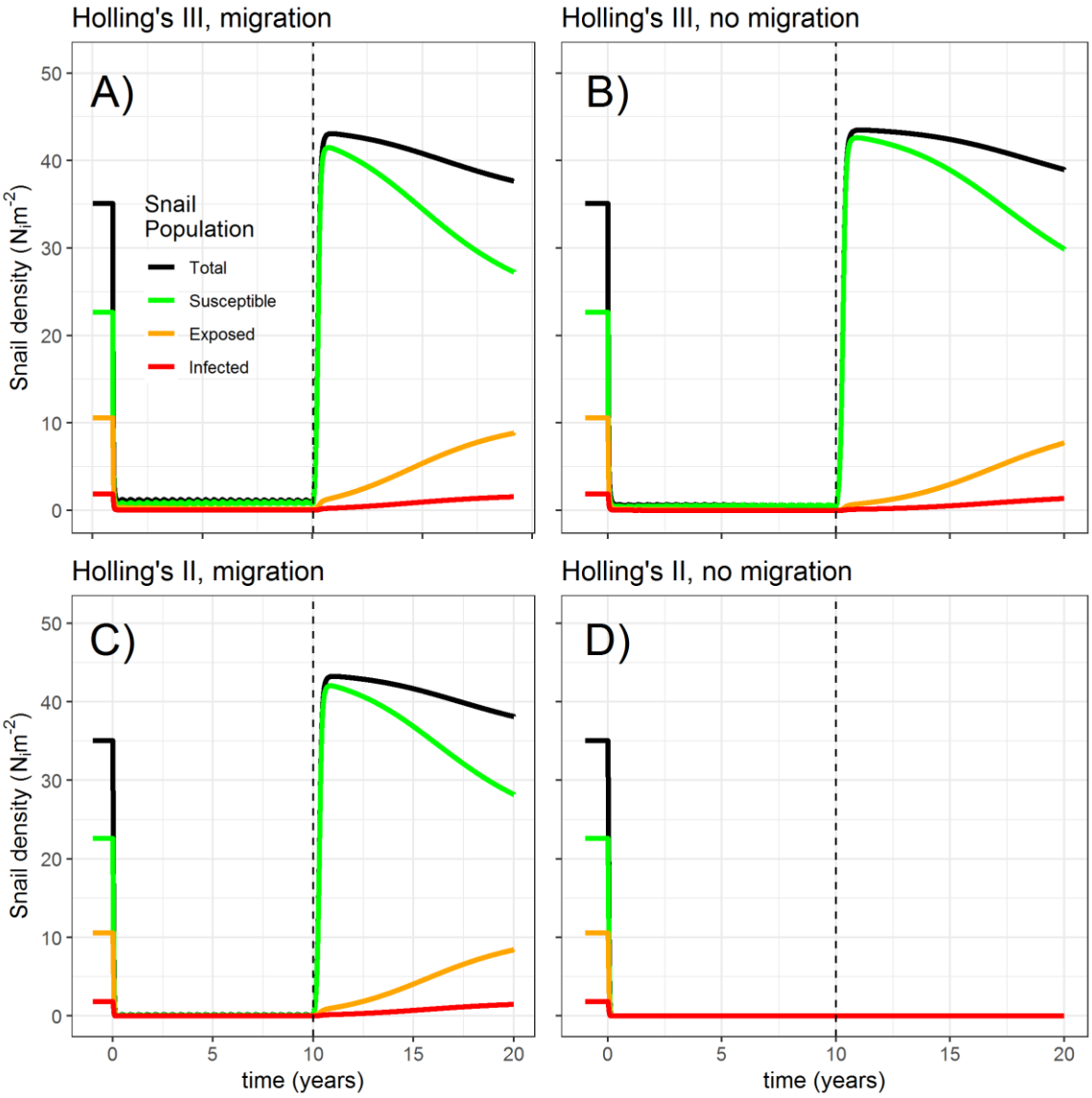

Supplementary Figure S3.4: Sensitivity analysis investigating the influence of the predation functional response and migration on snail infection dynamics. The model is simulated assuming a type III functional response and migration from an external source (A), a type III functional response with no migration (B), a type II functional response with migration (C), and a type II functional response with no migration (D). Simulations indicate that as long as migration is present or predation dynamics follow a type III response (indicating decreased predation rates at low densities due to e.g. prey switching or the presence of prey refugia) the snail population rapidly reestablishes after prawn interventions are discontinued.

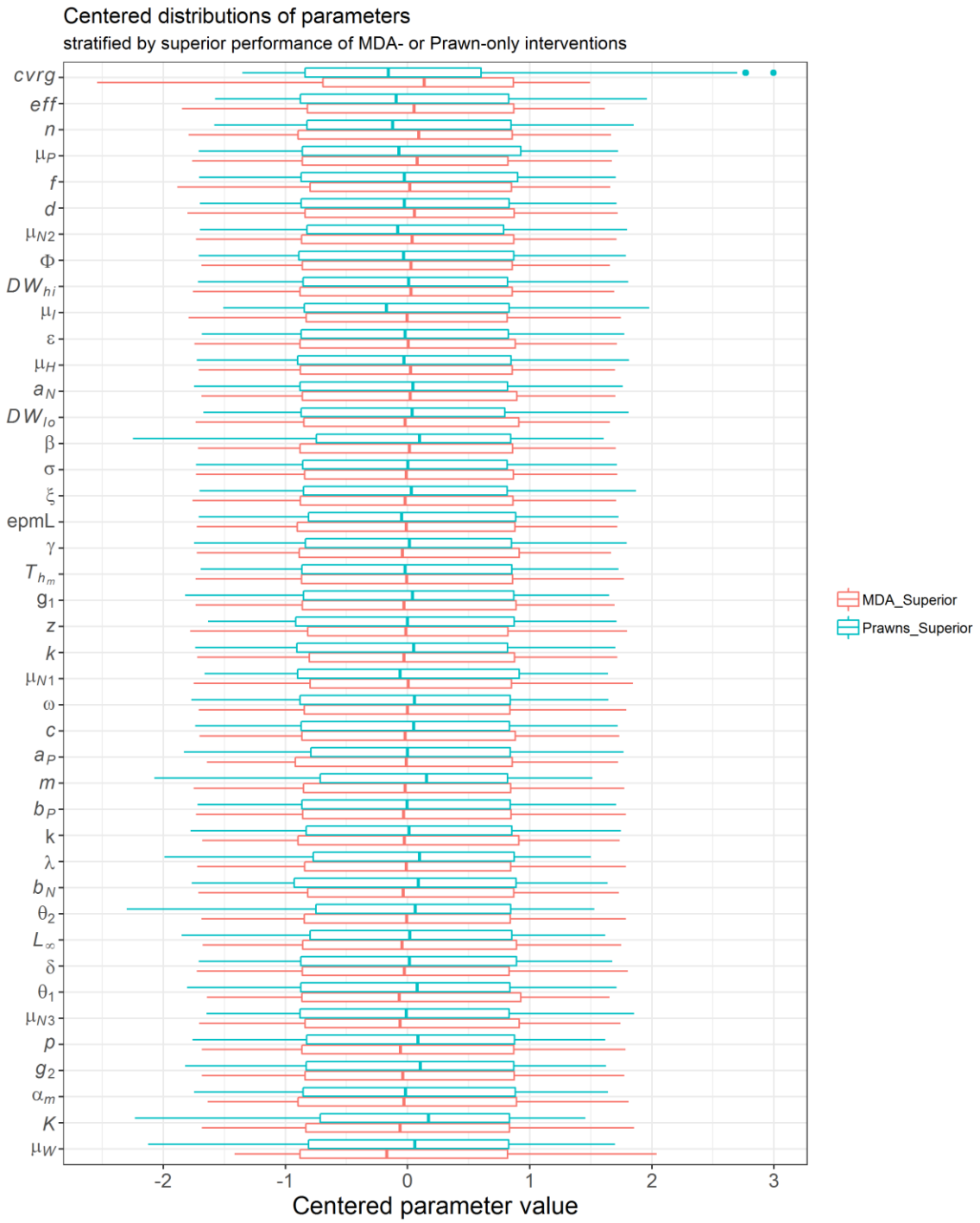

Supplementary Figure S3.5: Centered distributions of model parameters stratified by whether more DALYs were averted in MDA-only or in Prawn-only intervention simulations compared to no intervention simulations. Comparisons show that the MDA intervention tends to perform superior when MDA coverage (*cvrg*) and efficacy (*eff*) are higher and when infected snail and prawn mortality are higher (μ_I and μ_P, respectively). The prawn intervention performs notably better when the snail population carrying capacity (K) is higher.

Chapter 4: Reaching the breakpoint: Density dependence, connectivity, and the importance of non-pharmaceutical interventions

4.1 Breakpoints and their relevance to control and elimination

Attempts to control and eliminate schistosomiasis and other helminthiases globally have frequently run into challenges. Vaccines remain elusive, and non-human components of transmission including disease vectors, intermediate hosts, and other environmental reservoirs cause rapid reinfection following treatment. These dynamics frequently thwart treatment efforts, making persistent hotspots and repeated treatments common. [15,150] Transmission intensity and reinfection can be reduced by targeting environmental reservoirs of transmission, improving water access, sanitation, and hygiene (WASH) in affected populations, and changing behaviors that contribute to infection and transmission. However, these non-pharmaceutical interventions are rarely pursued concurrently with treatment campaigns, hampering the long-term prospect of successful control and elimination.

Schistosome parasites transition between human and intermediate snail hosts via two free-living, host-seeking larval forms: miracidia (shed by humans, infect snails) and cercariae (shed by snails, infect humans). Current control strategies rely on preventive chemotherapy by mass drug administration (MDA) to treat high-risk populations. School-aged children (SAC; ages 5-14) are frequently targeted for MDA as they are both at high risk for infection and are easily reached. Community-based MDA strategies that seek to treat adults and pre-school aged children in addition to SAC are also pursued, but reaching these populations can be logistically challenging. [151,152] In many areas, these MDA-based strategies have reduced schistosomiasis infection levels as measured by overall prevalence, prevalence of heavy infections, and individual parasite burdens. [153] However, schistosomiasis prevalence in many communities remains stable even after multiple years of MDA, and more than 200 million people still require treatment. [8,13–15,154]

Control strategies based on MDA are essential to reduce morbidity associated with infection, but they also affect transmission of the parasite. Treated individuals with fewer parasites will contribute less to transmission. Suppressing transmission through MDA or other means is further facilitated by positive density dependence arising from the dioecious nature of adult schistosomes. Approaching elimination, low worm burdens among the human population are hypothesized to cause mate limitation among the adult parasite population, producing a transmission breakpoint, below which sub-replacement transmission occurs (also known as a strong Allee effect).

Frequent, widespread MDA may reduce the parasite population below the breakpoint. Elimination is possible if schistosome worm burdens in the human population are suppressed below the breakpoint, e.g. via widespread treatment of infected individuals with MDA. However, negative density dependent processes such as density dependent fecundity also affect schistosomiasis transmission, making the breakpoint harder to reach. [155,156] In addition, the highly overdispersed nature of parasite burdens among definitive human hosts, as explored in

Chapter 2, make strong positive density dependence less likely, as a limited number of heavily infected individuals may be sufficient to sustain transmission.

Non-pharmaceutical interventions (NPIs) have an indirect effect on morbidity, but may be more effective in reducing transmission. By targeting other components of the schistosome life cycle, they are not influenced by density dependencies among the adult parasite population that complicate the effects of MDA on transmission. Molluscicide and habitat remediation to reduce the intermediate host snail population were critical to the successful elimination of schistosomiasis in areas of northern Africa, South America, and east Asia. [157] Integrated control strategies that draw on snail control, MDA, education campaigns and behavior changes, agricultural mechanization, and WASH improvements may be more effective at achieving long term goals of schistosomiasis control such as elimination. [17,19,20,158]

The success of both NPIs and MDA is further hampered by sources of infection outside of the human population that is explicitly targeted in control efforts. Zoonotic transmission of human-bovine schistosome hybrids is increasingly recognized as an important aspect of transmission in sub-Saharan Africa, [81] and both human movement and hydrological connectivity may perturb local control efforts. [159,160] These external sources of infection have been identified as key drivers of ongoing transmission and barriers to successful elimination of schistosomiasis. [82,160,161]

Analyzing ongoing control efforts in light of these sources of transmission resilience is challenging in part due to the lack of a generalizable framework to simultaneously quantify the effects of NPIs, MDA, and their interaction. [20] Here, we present such a framework that focuses on estimation and manipulation of the effective reproduction number, $R_e(W)$. Estimates of $R_e(W)$ are developed in the context of external sources of infection such as zoonotic reservoirs or connected foci of transmission and density dependencies in the parasite population, measured via the mean worm burden, W, in the targeted human population. We estimate the breakpoint mean worm burden, W_{bp}, using model parameters estimated from human and intermediate host snail infection data from ongoing studies in the lower Senegal River basin. We show that W_{bp} is reduced and even disappears—making elimination theoretically impossible—with modest external infectious input, but can be recovered through NPIs that improve WASH conditions, alter human behavior, or reduce the intermediate host snail population. We present methods to estimate the MDA coverage necessary to reduce the population mean worm burden below the breakpoint, demonstrating how integrated strategies that incorporate NPIs and MDA interact. We conclude with simulations from a stochastic individual-based model of schistosomiasis transmission in which we compare control strategies in different transmission and intervention scenarios with respect to their estimated probability of achieving elimination.

4.2 Models and methods used to estimate breakpoints and their manipulation through interventions

Epidemiologic Data

We use data from a set of communities in the lower Senegal River basin where ongoing studies on the effects of prawn introduction and vegetation removal on schistosomiasis transmission are

taking place. [45,47,162] Data consists of a baseline egg burden survey conducted in 2016 measuring individual mean *Schistosoma haematobium* eggs/10mL urine among SAC in 12 communities. Egg burdens were assessed using a 2x1 sampling approach with two slide reads per urine sample and the mean of these two samples was used as the individual burden. Annual double-dose school-based MDA in which two doses of praziquantel were administered to all SAC three weeks apart was conducted following parasitological surveys in 2016, 2017, and 2018. Concomitant snail sampling in each community was conducted with summary measures of snail habitat, abundance, and infection prevalence described previously. [47] Human population characteristics, snail densities, and baseline worm burden and aggregation estimates are listed in table 1.

The model

Intermediate host snail infection dynamics

The schistosomiasis transmission model represents susceptible-exposed-infected (state variables S, E, and I respectively) infection dynamics among the intermediate host snail population, **N**, in order to account for the delay (pre-patent period, $1/\sigma$) between infection ($S \to E$) and active shedding of cercariae (patency, $E \to I$).

$$\frac{dS}{dt} = f_N(S+E) - \mu_N S - \Lambda(W)S$$

$$\frac{dE}{dt} = \Lambda(W)S - (\mu_N + \sigma)E$$

$$\frac{dI}{dt} = \sigma E - \mu_I I$$

Infected snails, I, do not reproduce due to parasitic castration and the snail population growth rate, f_N, is logistic with max reproduction rate, r, and carrying capacity, K, giving $f_N = r(1 - N/K)$. Snail infection dynamics are linked to the human population via the human-to-snail force of infection, $\Lambda(W)$, described further below.

Human infection dynamics

Human infectionas the mean worm burden (state variable W) in the human population, assumed to be negative binomially distributed with clumping parameter κ.

$$\frac{dW}{dt} = \lambda(I) - (\mu_W + \mu_H)W$$

Human infection dynamics are linked to the intermediate host snail population via the snail-to-human force of infection, $\lambda(I)$, modeled as the product of cercarial density, C, exposure rate, ω_2, and the probability of a cercarial contact resulting in an adult worm infection, α. Infected snails shed cercariae at daily rate θ, giving $C = \theta I$ and $\lambda(I) = \alpha\omega_2\theta I$.

Human-to-snail FOI, $\Lambda(W)$

Snail FOI, Λ, is estimated as the product of total miracidial density per snail, M/N , and the probability of infection per miracidial contact, β. Miracidial density generated by the local worm population (M^L) is estimated as the product of mean egg output, $\mathcal{E}(W) = 0.5WHmU$, egg viability, v, and the contamination rate, ω_1, with additional model parameters defined in Table 1. The influence of density dependencies and external miracidial input from connected sources of infection are described further below.

Model fit and parameter estimation

We use baseline measures of the community mean egg burden measured in eggs/10mL urine to estimate baseline dispersion, κ, and mean worm burden. Given the lack of recent interventions in study area, the baseline measure of W is interpreted as the endemic equilibrium worm burden, W_{eq}, for each community. In addition, we incorporate estimates of the total snail abundance (N_{eq}) and infected snail abundance (I_{eq}) derived previously [159] for these same communities to estimate infected snail prevalence (I_P). From these inputs, we subsequently solve for K, Λ, β, ω_1, and ω_2 for each community assuming equilibrium conditions as described in the SI.

Density dependencies and external sources of infection

Assuming a 1:1 sex ratio and negative binomially distributed adult worms, density dependent functions representing the mating probability, $\Phi(W, \kappa)$, and density-dependent fecundity, $\rho(W, \kappa, \gamma)$, are estimated as described previously. [23,24] The mating probability is the only source of positive density dependence affecting schistosomiasis transmission, therefore its estimation is critical when estimating elimination thresholds such as the breakpoint. Assuming male and female parasites are distributed together from the same negative binomial distribution, the mating probability can be estimated as a function of the W and κ [23]:

$$\phi(W, \kappa) = 1 - \frac{\left(1 - \frac{W}{W + \kappa}\right)^{1+\kappa}}{2\pi} \int_0^{2\pi} \frac{(1 - \cos(x))\, dx}{\left(1 + \frac{W\cos(x)}{W + \kappa}\right)^{1+\kappa}}$$

While κ is often considered constant, previous analyses of the distribution of estimated worm counts within definitive human host populations have shown that the dispersion parameter varies predictably as a function of the overall mean worm burden and can change quite dramatically following reductions in the worm burden such as those induced by MDA. [117,163][CITE chapter 2] In particular, κ decreases, implying more skewed distributions in which fewer individuals harbor more worms, as W decreases. This leads to an increase in the mating probability relative to an assumption of constant κ even as worm populations decrease due to MDA or other interventions. Simulations with constant κ are therefore compared to those in which κ varies according to a logarithmic function of the mean worm burden:

$$\kappa(W) = 1 - e^{aW^b}$$

with parameterization of a and b presented in detail in the SI.

As the parasite population approaches elimination, negative density dependent processes are also relaxed, increasing transmission and thus introducing further resilience to elimination. Density dependent fecundity acting on the mean egg output per mated female worm is therefore included as a function of W, κ, and γ as described previously :

$$\rho(W,\gamma,\kappa) = \left(1 + \frac{(1-e^{-\gamma})W}{\kappa}\right)^{(-\kappa+1)}$$

Finally, we represent external sources of infection that contribute miracidia to the local infection system. We consider the addition of external miracidial input, M^E, from socially or hydrologically connected human sources or zoonotic reservoirs in terms of a single parameter, $\mathcal{F}$, representing the proportion of the total miracidial population at equilibrium produced externally, e.g. $M_{eq}^T = M_{eq}^L(W_{eq})(1+\mathcal{F})$ and $M_{eq}^E = \mathcal{F}M_{eq}^L$.

Next, to allow M^E to vary as a function of the local worm burden, W, (therefore functioning similar to a density dependence), we express $\mathcal{F}(W)$ as:

$$\mathcal{F}(W) = \frac{y}{W+z}$$

representing external miracidial input as a function of the local worm burden, $M^T(W) = M^L(W)\mathcal{F}(W)$. Parameters y and z are estimated by solving:

$$\mathcal{F}(W_{eq}) = 1 + \mathcal{F} = \frac{y}{W_{eq}+z}$$
$$\mathcal{F}(W_{bp}) = 1 + \mathcal{F}\mathcal{F}_{bp} = \frac{y}{W_{bp}+z}$$

in which the additional parameter $\mathcal{F}_{bp}$ is the ratio of locally generated miracidia at W_{eq} compared to the worm burden breakpoint (W_{bp}, described further below) such that $M_{bp}^T = M_{bp}^L(1+\mathcal{F}\mathcal{F}_{bp})$. Incorporating density dependencies and external miracidial input into the snail FOI thus gives:

$$\Lambda(W,\mathcal{F}) = \left(\beta 0.5WHmU\phi\left(W,\kappa(W)\right)\rho\left(W,\gamma,\kappa(W)\right)v\omega_1\mathcal{F}(W)\right)N^{-1}$$

Reproduction numbers

Basic reproduction number

We estimate R_0 as a baseline estimate of infection intensity in each community considering the relative rates of change of each infection class in the absence of density dependencies:

$$R_0 = \frac{\Lambda N^*}{(\mu_N+\sigma)} \times \frac{\sigma}{\mu_I} \times \frac{\lambda}{(\mu_W+\mu_H)} = \frac{\Lambda N^* \sigma\lambda}{\mu_I(\mu_N+\sigma)(\mu_W+\mu_H)}$$

Assuming linear human-to-snail FOI, $\Lambda = \beta M/N$, and no external miracidial input, $\mathcal{F} = M^E = 0$, we thus have:

$$R_0 = \frac{\beta 0.5HmUv\omega_1\sigma\alpha\theta\omega_2}{\mu_I(\mu_N+\sigma)(\mu_W+\mu_H)}$$

While with $\mathcal{F} > 0$:

$$R_0 = \frac{\beta 0.5 HmUv\omega_1(1+\mathcal{F})\sigma\alpha\theta\omega_2}{\mu_I(\mu_N+\sigma)(\mu_W+\mu_H)}$$

demonstrating that R_0 scales linearly with increasing external input.

Effective reproduction number

The effective reproduction number, R_e, for schistosomiasis is defined as the number of mated adult female worms produced by a single adult female worm over the course of her lifetime. Unlike the basic reproduction number, R_0, R_e changes as a function of the current level of infection, here measured in terms of the mean worm burden, W. We can estimate the effective reproduction number from the rate of worm burden change as described previously [24]:

$$\frac{dW}{dt} = \lambda - (\mu_H + \mu_W)W$$

$$\frac{dW}{dt} = (\mu_H + \mu_W)W\left(\frac{\lambda(W)}{(\mu_H+\mu_W)W} - 1\right)$$

$$\frac{dW}{dt} = (\mu_H + \mu_W)W(R_e(W) - 1)$$

$$R_e(W) = \frac{\lambda(W)}{(\mu_H+\mu_W)W}$$

Where $(\mu_H + \mu_W)$ is the mean lifespan of an adult worm accounting for both worm and human host mortality and $\lambda(W)$ is the worm acquisition rate or snail-to-human FOI, which is a function of the exposure coefficient, ω_2, probability of worm acquisition given exposure, α, and cercarial concentration estimated as a function of cercarial shedding and the infected snail population size.

Assuming fast snail relative to human infection dynamics as is common, we can express $R_e(W)$ in terms of the equilibrium snail population size, N, and snail FOI, Λ, both in terms of W (details in SI):

$$R_e(W) = \frac{\alpha\omega_2\theta\sigma N(W)}{W(\mu_H+\mu_W)\left(\frac{\mu_I(\mu_N+\sigma)}{\Lambda(W)} + \mu_I + \sigma\right)}$$

$$N(W) = K\left(1 - \frac{\mu_N + \Lambda(W)}{r\left(1 + \frac{\Lambda(W)}{\mu_N+\sigma}\right)}\right)$$

We estimate $R_e(W)$ across $W \in \{0.0001, 100\}$ in order to characterize the $R_e(W)$ profile for every community, both with constant and dynamic κ.

Breakpoint estimation and effects of non-pharmaceutical interventions

The breakpoint worm burden population size, W_{bp}, is an unstable equilibrium at which each female worm replaces herself perfectly, i.e. $R_e(W_{bp}) = 1$, therefore the breakpoint can be estimated numerically using rootsolving or searching algorithms with the above equations for $R_e(W)$ and $N(W)$ given a set of estimated model parameters (Table 1). We estimate W_{bp} for both constant and dynamic κ to quantify the influence of dynamic aggregation on W_{bp}. In addition, we estimate W_{bp} across a range of values of $\mathcal{F}$, representing external miracidial input, to determine how the breakpoint varies with external infection inputs.

Obviously from the $R_e(W)$ equations above, a number of parameters affect $R_e(W)$ and thus W_{bp}, but we focus on four in particular due to their interpretation in relation to NPIs: 1) K, the snail population carrying capacity, modifiable through habitat remediation, vegetation removal, or other efforts to induce permanent alterations to the intermediate host snail habitat; 2) μ_N, the snail population mortality rate, modifiable through molluscicide, biocontrol, or other emerging technologies such as gene drives; 3) ω_1, the human contamination coefficient, modifiable through improved sanitation and behavior changes that reduce the proportion of eggs produced by the human population that interact with the snail population; and 4) ω_2, the human exposure coefficient, modifiable through targeted education, behavior change, or improved water infrastructure and access that reduces water contact. We estimate W_{bp} for every community across a range of each of these parameters in order to quantify the influence of NPIs on the breakpoint.

Interaction of mass drug administration and non-pharmaceutical interventions to reach the breakpoint

Another useful outcome is the MDA coverage necessary to reach the breakpoint. We can model MDA as a reduction in the mean worm burden following MDA in terms of the MDA coverage, Ψ, and drug efficacy, ϵ:

$$W_{t+1} = (1 - \epsilon)\Psi W_t + (1 - \Psi)W_t$$

If the goal is to reduce the worm burden below the breakpoint (i.e. $W_{t+1} < W_{bp}$) with MDA, we can estimate the coverage required as:

$$\Psi = \frac{W_t - W_{bp}}{\epsilon W_t}$$

As is standard, $\epsilon = 0.94$, representing 94% clearance of adult *S. haematobium* worms following treatment with praziquantel is assumed. [23] This simple estimation reveals the critical role of the magnitude of the breakpoint mean worm burden and its determinants discussed above in reaching elimination: for any $W_{bp} < \epsilon W_t$, elimination is not feasible from a single MDA (e.g. $\Psi > 1$). Even for moderate pre-treatment to breakpoint worm burden ratios, extremely high levels of treatment coverage that have proved impractical in real-world settings may be necessary. To demonstrate the role of NPIs in enhancing the effectiveness of MDA interventions

and the probability of reducing W below W_{bp}, Ψ is estimated across a range of values of K, μ_N, ω_1, and ω_2. In addition, we estimate Ψ across these NPI parameters and values of external miracidial input $\mathcal{F}$ to quantify the importance of NPIs in reducing transmission arising from external sources that presumed unaffected by MDA.

Stochastic individual-based model simulating control strategies and probability of elimination as a metric of potential success

A stochastic, individual based version of the model (IBM) is next used to simulate infection dynamics under different transmission and intervention scenarios. The IBM explicitly tracks individual male and female worm burdens and stochastically generates miracidial (M) and cercarial (C) concentrations from human egg output and snail shedding, respectively. The human susceptibility parameter, α, is drawn from a gamma distribution with the same mean as in Table 1 and variance estimated from prior work. [57] Introducing this variability in α leads to aggregation dynamics similar to those incorporated into the mean model. Mass drug administration is incorporated into the model with coverage Ψ and individual compliance correlation, $\mathcal{C}$, as described in a similar IBM developed for lymphatic filariasis. [56]

For each community, the model is first simulated for three years with annual MDA and compared to epidemiological data collected at baseline (used to parameterize the model as described above and in the SI) and two follow-up surveys for model validation. Next, simulations continue MDA and incorporate additional NPIs for ten years. Finally, one year of transmission with no intervention is simulated at the end of which outcomes are assessed. In line with WHO definitions, [8] a simulation is defined to achieve "elimination as a public health problem" if the prevalence of heavy infections is <1% at the end of the year long follow-up, achieve "transmission interruption" if no incident cases (i.e. no increase in mean worm burden) occurs in the one year of no-intervention follow up, and achieve "outright elimination" if $W = 0$ at the end of the follow up period. For each community and intervention strategy, 1000 model iterations are simulated to estimate the probability of each control outcome (estimated as the proportion of simulations resulting in that outcome) associated with each of the following interventions: annual MDA at 60% coverage, biannual snail control with 80% efficacy, annual 5% reduction in the environmental carrying capacity of the snail population representing habitat remediation, annual 5% reduction in mean human contamination (ω_1), and annual 5% reduction in mean human exposure (ω_2).

Table 1: Constant parameters, input data across all 12 communities, and estimated parameters for 12 communities used in estimation and modeling

Constant Parameters

α	m	μ_W	μ_H	γ	U	v	r	μ_N	σ	μ_I	θ	b
0.002	5	$\frac{1}{3.3 \times 365}$	$\frac{1}{60 \times 365}$	0.001	120	0.08	0.15	1/60	0.025	0.1	200	0.36

Input Data*

	DF	DT	GK	LR	MB	ME	MG	MO	MT	NE	NM	ST
H	1300	1500	400	1623	1120	1852	761	1316	833	1542	771	866
W_{eq}	13.7	35.5	26.8	30.7	12.7	51.1	26.4	5.4	39.0	25.5	11.1	46.7
κ	0.13	0.21	0.20	0.23	0.12	0.21	0.17	0.07	0.18	0.08	0.09	0.45
N_{eq}	6994	51982	7057	60327	93016	25940	130	13668	75962	68116	80090	55816
I_{eq}	15	63	15	771	99	967	0	752	623	144	170	2395
I_P	0.002	0.001	0.002	0.013	0.001	0.037	0.002	0.055	0.008	0.002	0.002	0.043

Estimated Parameters*

	DF	DT	GK	LR	MB	ME	MG	MO	MT	NE	NM	ST
K	7880	58532	7952	68534	104726	30056	146	16079	7880.2	58532	7952	68534
$\Lambda^{\dagger}$	0.36	0.2	0.36	2.28	0.18	7.64	0.36	12.66	1.43	0.36	0.36	0.2
$\omega_1{}^{\dagger}$	2.03	1.24	3.93	0.09	0.28	0.12	210.54	0.02	0.14	0.39	2.03	1.24
$\omega_2{}^{\dagger}$	2.03	1.24	3.93	0.09	0.28	0.12	210.54	0.02	0.14	0.39	2.03	1.24
a	-0.053	-0.066	-0.068	-0.074	-0.051	-0.056	-0.055	-0.041	-0.053	-0.066	-0.068	-0.074

* Community abbreviations: DF – Diokoul Fall, DT – Diokhor Tack, GK – Guidik, LR – Lampsar, MB – Mbakhana, ME – Mbane, MG – Merina Guewel, MO – Mbarigo, MT – Malla Tack, NE – Ndiawdoune, NM – Ndiol Maure, ST – Syer Tack

† All values multiplied by 10^3

4.3 Breakpoint estimates and their signifance

Estimating W_{bp}

Table 1 shows baseline characteristics of each community including human population, baseline snail densities, and parasite burdens as well as the model parameters estimated from these baseline values. The mean baseline worm burden across all communities was 27.07 (range 5.43 - 51.09 among individual communities) and baseline infected snail prevalence varied from 0.11%

to 5.5%. Basic reproduction numbers assuming no external miracidial input ($M^E = 0$) are shown in Figure 1c and ranged from 1.27 to 1.73.

Figure 1a shows the $R_e(W)$ profiles for every community both with constant and dynamic treatment of the aggregation parameter, κ. All $R_e(W)$ profiles exhibit a distinct unimodal shape with two equilibria at $R_e(W) = 1$: the lower, unstable equilibrium at the breakpoint, W_{bp}, and the higher, stable equilibrium at the endemic equilibrium, W_{eq}. The breakpoint mean worm burden, W_{bp}, was more strongly correlated with R_0 (r^2=0.65) than the baseline mean worm burden (r^2=0.15), and ranged from 0.46 to 5.37 assuming constant aggregation and from 0.12 to 3.91 when allowing κ to vary as a function of W (Fig 1c). Estimates of dynamic aggregation parameter a are shown in table 1 and the relationship between κ and W across all communities used to estimate dynamic aggregation parameter b is showing in supplementary figure 1. The mean shift in W_{bp} attributable to dynamic aggregation was -1.19 (range -2.23 - -0.12).

Figure 1b shows estimates of the breakpoint across values of the external miracidial input fraction $\mathcal{F}$, for every community assuming constant aggregation. Corresponding $R_e(W)$ profiles are shown in supplementary figure 2. At $\mathcal{F} = 0.1$ (external miracidial input is equivalent to 10% of local miracidial production), the shift in W_{bp} ranged from -3.66 to -0.22, averaging -1.81. At $\mathcal{F} = 1.0$ (external miracidial input is equivalent to local miracidial production), W_{bp} is exceedingly small, averaging just 0.14 (range 0.04 - 0.21), which represents an average shift of -2.79 (range -5.19 - -0.43).

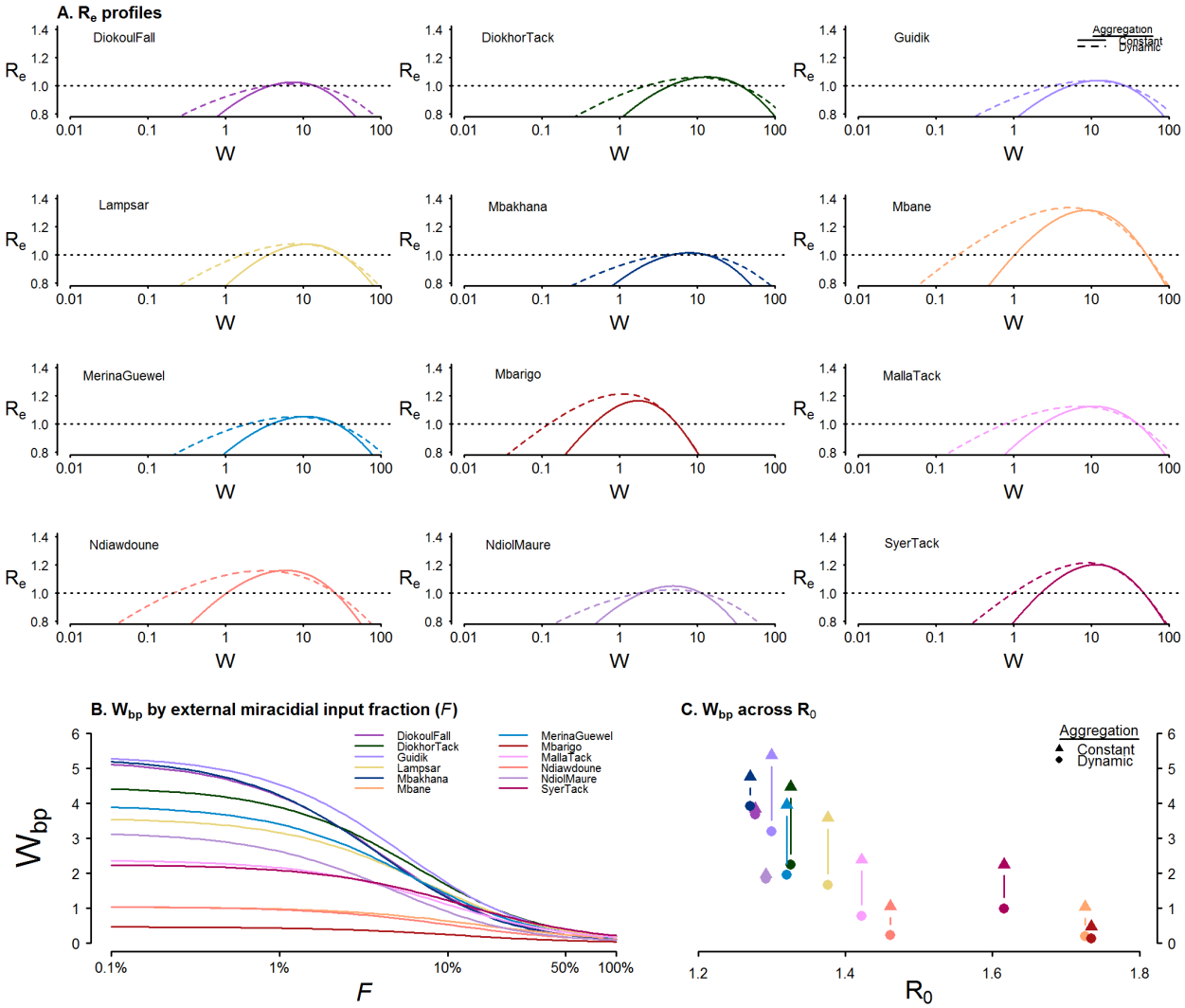

Figure 4.3.1: Effective reproduction numbers, $R_e(W)$, and the effect of external infection and dynamic aggregation on estimates of the breakpoint, W_{bp}. A) Effective reproduction number profiles for all twelve Senegalese communities assuming constant (solid line) and dynamic (dashed line) aggregation in which the dispersion parameter is allowed to vary as a function of the mean worm burden (see main text). Also shown by the horizontal dotted line is the critical threshold at $R_e = 1$. The upper intersection at which $R_e = 1$ is the endemic equilibrium estimated from epidemiological data, and the lower intersection is W_{bp} estimated from epidemiological data and additional model parameters in Table 1. The shift in the breakpoint from constant to dynamic aggregation is also reflected in panel C. B) Estimates of W_{bp} across external miracidial input values ($\mathcal{F}$, see main text). C) Estimates of W_{bp} across R_0, showing lower (less achievable) values of W_{bp} as R_0 increases, and decreasing estimates of W_{bp} when aggregation is dynamic, even as R_0 remains constant.

Altering W_{bp} through NPIs

Figure 2 shows the breakpoint across changes in model parameters that can be targeted via NPIs, demonstrating that W_{bp} can be manipulated through interventions targeting these parameters. In particular, W_{bp} increases, making it more attainable, as the snail population carrying capacity (K) is reduced (Fig 2a), as the snail mortality rate (μ_N) is increased (Fig 2b), and as the human contamination parameter (ω_1, a key component of the snail FOI) or the human exposure

parameter (ω_2), a key component of the human FOI) are reduced (Fig 2c and 2d, respectively). Given sufficient intervention on these parameters, transmission can also be reduced such that $\max(R_e(W)) < 1$, implying sub-replacement transmission and eventual elimination barring perturbations that increase transmission or introduce parasites in some form. In figure 2, this is displayed as parameters exceeding the y axis limit, demonstrating an exceedingly large W_{bp}.

There is also substantial between-community and between-parameter variability in the effect of NPIs on W_{bp}. Interventions acting on K have little effect on W_{bp} until reaching 60% or greater reductions, while minimal increases in W_{bp} even at 90% reductions are estimated for communities with low baseline W_{bp} (Fig 2a). The same communities with greatly increased W_{bp} due to reduced K also respond to increases in snail mortality, μ_N, though at smaller relative alterations to the parameter value, implying that interventions that increase snail mortality rather than reducing the snail population carrying capacity may be more efficient in increasing W_{bp} (Fig 2b). Similarly, smaller relative alterations of human contamination (ω_1) and exposure (ω_2) are necessary to increase W_{bp} for most communities, and all but 1 community achieves $\max(R_e(W)) < 1$ if either parameter is reduced by 20% (Fig 2c and 2d).

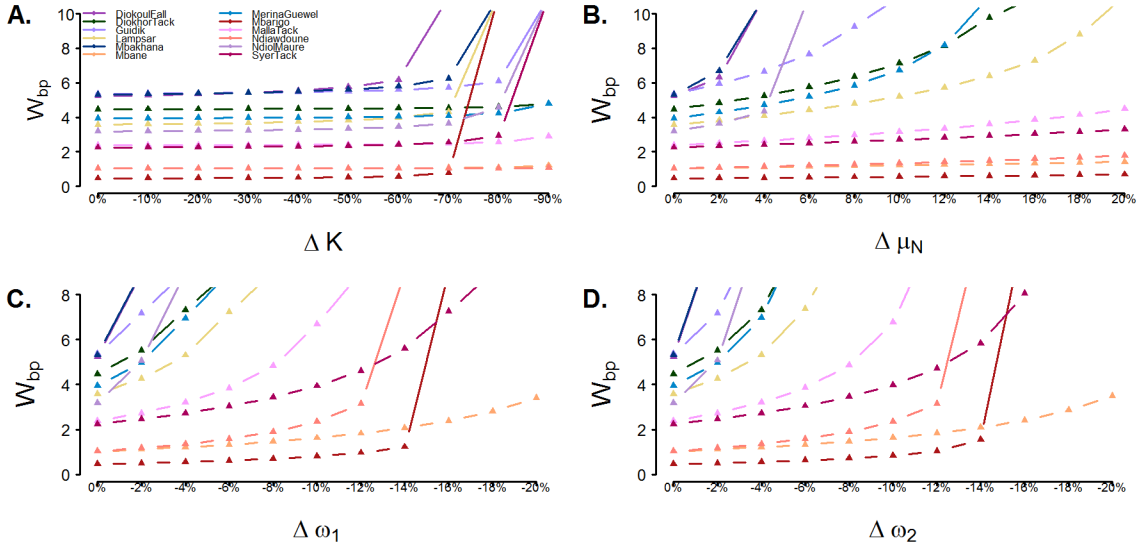

Figure 4.3.2: Worm burden breakpoint (W_{bp}) as function of model parameters targeted by specific interventions. A) reductions in the snail population carrying capacity (model parameter K), B) increases in the snail mortality rate (μ_N), C) reductions in the human-to-snail force of infection via improved sanitation (ω_1), D) reductions in the snail-to-human force of infection via reduced water contact (ω_2). Points that exceed the y axis limit indicate reductions in transmission that reduce all values of $R_e(W)$ below 1 (equivalent to $R_0 < 1$), therefore there is no breakpoint and elimination would be expected without further intervention or perturbation.

Reaching W_{bp} with MDA and NPIs

MDA coverage to reach W_{bp}

These parameter reductions, which lead to increases in W_{bp}, also make MDA more likely to result in sustained reductions in W or elimination. However, external miracidial input is also

expected to reduce W_{bp} and increase $R_e(W)$, making sustained reductions and elimination more difficult to achieve. Figure 3 shows the MDA coverage (Ψ) necessary to reduce the population mean worm burden from W_{eq} to W_{bp} assuming praziquantel efficacy of 94% across the same parameters shown in Figure 2 as well as external miracidial input fractions ($\mathcal{F}$) from $0 - 1.0$. As $\mathcal{F}$ increases, Ψ approaches and even exceeds 1.0, implying that MDA alone is unable to reduce the worm burden below the breakpoint in a single round. However, lower, more achievable MDA coverage is recovered by parameter changes representing NPIs along the y axis in Figure 3.

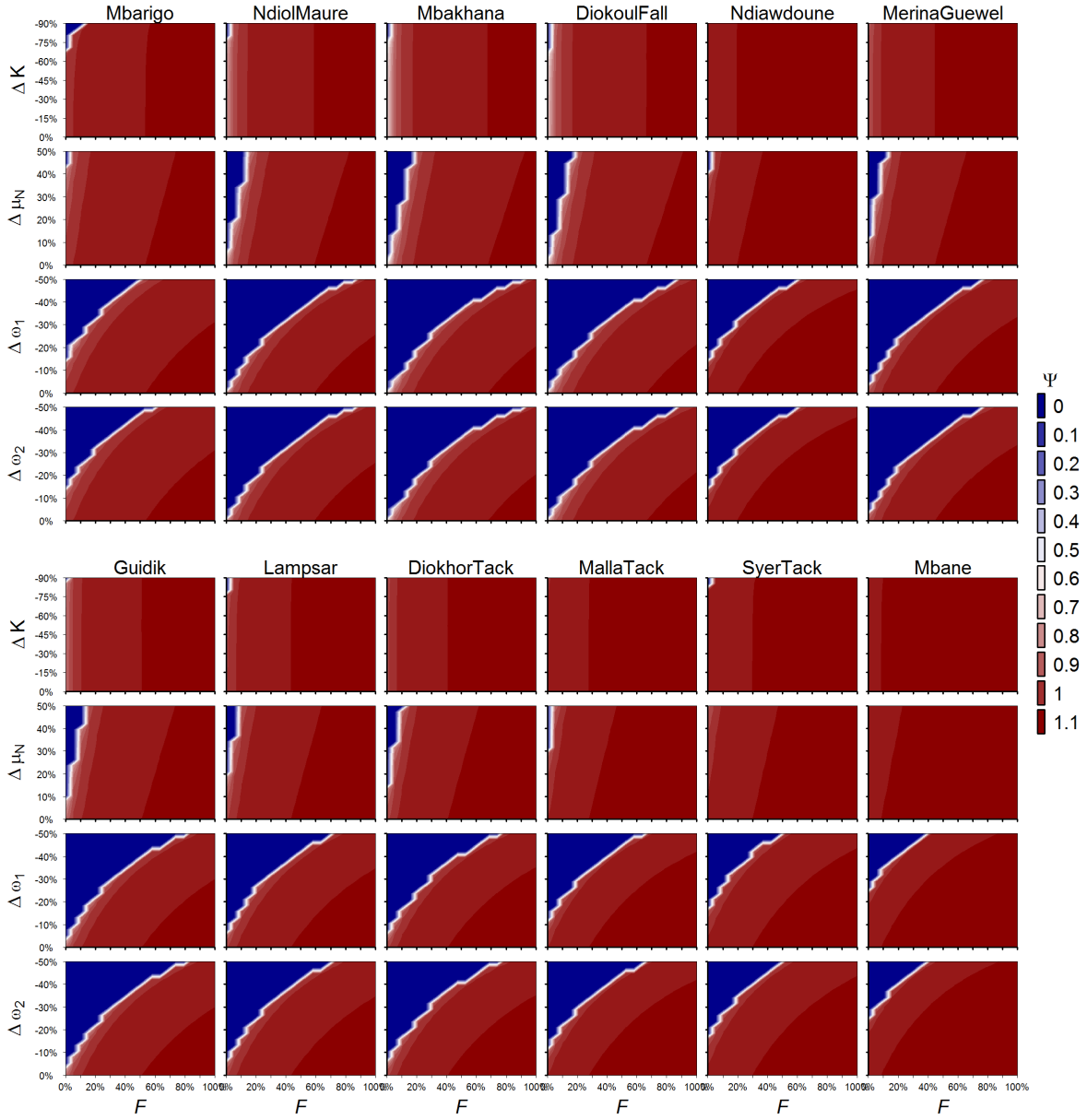

Figure 4.3.3: MDA treatment coverage, Ψ, necessary to reach the breakpoint as function of model parameters (K, μ_N, ω_1 and, ω_2) that can be targeted through non-pharmaceutical interventions and external miracidial input

fractions $\mathcal{F}$. Infiltration of blue shades moving from left to right in each heatmap represents parameter space in which NPIs (Y axis) can recover breakpoints that are reachable via MDA even in the presence of higher external miracidial inputs (X axis).

Probability of achieving key elimination targets

To test the hypothesis that supplementing MDA with NPIs is more likely to achieve key public health targets such as morbidity reduction and transmission control *in silico*, we conducted simulations of an individual based model for 10 year intervention periods comparing MDA-only interventions with MDA in addition to snail control, snail habitat reduction, contamination reduction (sanitation improvement), or exposure reduction interventions. Table 2 shows the probability of achieving key public health outcomes including elimination as a public health problem, $P(E_{php})$ and transmission control, $P(TC)$ for every community across these interventions and external miracidial input fractions, $\mathcal{F} \in (0.01,0.1,1.0)$. No simulations resulted in total elimination, i.e. $P(E_{tot}) = 0$, therefore more detailed results are not shown for this outcome.

Probability of elimination as a public health problem ($P(E_{php})$)

The probability of achieving elimination as a public health problem with MDA alone was high across all communities and interventions when connectivity was low ($\mathcal{F} = 0.01$), with $P(E_{php}) = 1$ for all interventions for all but two communities. Estimates of $P(E_{php})$ for the MDA-only intervention in these two communities were still greater than 0.9 (Mbane $P(E_{php}) = 0.92$; Syer Tack $P(E_{php}) = 0.98$) and were increased to 1.0 when adding supplemental snail control (μ_N), contaminaion reduction (ω_1), or exposure reduction interventions (ω_2).

Increasing site connectivity via the external miracidial fraction parameter to 10% ($\mathcal{F} = 0.1$) decreased the median $P(E_{php})$ in the MDA-only intervention across all communities to 0.97, though the range was $0 - 1$. Adding snail control resulted in a 0.09 mean increase in $P(E_{php})$ (range $0 - 0.55$), habitat reduction a mean 0 change (range $-0.02 - 0.04$), contamination reduction a mean 0.07 increase (range $0 - 0.44$), and exposure reduction a mean 0.15 increase (range $0 - 0.7$).

When increasing the external miracidial fraction parameter to 100% ($\mathcal{F} = 1.0$, implying miracidia contributed from external sources are equally abundant to those produced locally), $P(E_{php})$ in the MDA-only intervention simulations was ≤ 0.10 for all but two communities, but was increased by a mean of 0.1 (range $0 - 0.54$) by adding the snail control intervention, 0 (range $-0.02 - 0$) by the habitat reduction intervention, 0.03 (range $0 - 0.16$) by the contamination reduction intervention, and 0.2 (range $0 - 0.97$) by the exposure reduction intervention.

Probability of transmission control ($P(TC)$)

The probability of achieving the more stringent definition of transmission control (no increase in mean worm burden, W, during the simulated year of follow-up with no intervention), was lower across all communities, particularly when connectivity was increased ($\mathcal{F} > 0.01$). In the highest

connectivity scenario ($\mathcal{F} = 1.0$), transmission control was not achieved ($P(TC) = 0$) across all communities and interventions.

In the lowest connectivity scenario ($\mathcal{F} = 0.01$), the median probability of achieving transmission control was 0.52 and ranged from $0 - 0.96$ across all communities. Adding snail control resulted in a 0.11 mean increase in $P(TC)$ (range -0.01 $-$ 0.32), habitat reduction a mean 0 change (range -0.05 $-$ 0.02), contamination reduction a mean 0.21 increase (range $0 - 0.56$), and exposure reduction a mean 0.33 increase (range $0.03 - 0.82$).

In the intermediate connectivity scenario ($\mathcal{F} = 0.1$), transmission control was not possible with MDA alone in any community, and adding snail control or snail habitat reduction interventions did not result in an increase in the probability of achieving transmission control ($P(TC) = 0$). However, adding contamination reduction resulted in a 0.01 probability of transmission control in Mbarigo, and adding exposure reduction resulted in 4 communities with $P(TC) > 0$, with a mean 0.04 increase (range $0 - 0.25$) in $P(TC)$ across all communities.

Table 4.3.2: Outcomes of stochastic individual-based model simulations. Columns are stratified by the outcome assessed: $P(E_{php})$ – probability of elimination as a public health problem, $P(TC)$ – probability of transmission control; and further stratified by the implemented intervention (*MDA* – mass drug administration at 60% coverage and 80% between-round correlation only, μ_N – MDA plus biannual snail control, K – MDA plus 5% annual reduction in snail population carrying capacity, ω_1 – MDA plus 5% annual reduction in human contamination parameter that connects human egg output to snail population, and ω_2 – MDA plus 5% annual reduction in the human exposure parameter that connects infected snail cercarial output to the human population) and. Results for $P(E_{tot})$ – probability of total elimination, are not shown as no simulations with inputs as described in the table and main text resulted in total elimination of the local parasite population. Rows are stratified for each of the twelve communities and by external miracidial input fraction, $\mathcal{F} \in (0.01, 0.1, 1.0)$.

	$P(E_{php})$					$P(TC)$				
	MDA	μ_N	***K***	ω_1	ω_2	***MDA***	μ_N	***K***	ω_1	ω_2
Diokoul Fall										
$\mathcal{F} = 0.01$	1.00	1.00	1.00	1.00	1.00	0.96	0.95	0.96	0.97	0.99
$\mathcal{F} = 0.1$	1.00	1.00	1.00	1.00	1.00	0.00	0.00	0.00	0.00	0.01
$\mathcal{F} = 1$	0.01	0.26	0.01	0.04	0.98	0.00	0.00	0.00	0.00	0.00
DiokhorTack										
$\mathcal{F} = 0.01$	1.00	1.00	1.00	1.00	1.00	0.15	0.43	0.12	0.69	0.97
$\mathcal{F} = 0.1$	0.69	0.99	0.73	0.98	1.00	0.00	0.00	0.00	0.00	0.00
$\mathcal{F} = 1$	0.00	0.00	0.00	0.00	0.00	0.00	0.00	0.00	0.00	0.00
Guidik										
$\mathcal{F} = 0.01$	1.00	1.00	1.00	1.00	1.00	0.60	0.73	0.61	0.80	0.92
$\mathcal{F} = 0.1$	0.92	0.99	0.93	0.99	1.00	0.00	0.00	0.00	0.00	0.00
$\mathcal{F} = 1$	0.00	0.00	0.00	0.00	0.00	0.00	0.00	0.00	0.00	0.00
Lampsar										
$\mathcal{F} = 0.01$	1.00	1.00	1.00	1.00	1.00	0.25	0.53	0.25	0.81	0.99
$\mathcal{F} = 0.1$	0.95	1.00	0.96	1.00	1.00	0.00	0.00	0.00	0.00	0.00
$\mathcal{F} = 1$	0.00	0.00	0.00	0.00	0.00	0.00	0.00	0.00	0.00	0.00
Mbakhana										
$\mathcal{F} = 0.01$	1.00	1.00	1.00	1.00	1.00	0.94	0.96	0.95	0.96	0.99
$\mathcal{F} = 0.1$	1.00	1.00	1.00	1.00	1.00	0.00	0.00	0.00	0.00	0.04
$\mathcal{F} = 1$	0.10	0.64	0.10	0.24	1.00	0.00	0.00	0.00	0.00	0.00

	$P(E_{php})$					$P(TC)$				
	MDA	μ_N	K	ω_1	ω_2	***MDA***	μ_N	K	ω_1	ω_2
Mbane										
$\mathcal{F} = 0.01$	0.92	1.00	0.94	1.00	1.00	0.00	0.00	0.00	0.00	0.04
$\mathcal{F} = 0.1$	0.00	0.00	0.00	0.00	0.10	0.00	0.00	0.00	0.00	0.00
$\mathcal{F} = 1$	0.00	0.00	0.00	0.00	0.00	0.00	0.00	0.00	0.00	0.00
Merina Guewel										
$\mathcal{F} = 0.01$	1.00	1.00	1.00	1.00	1.00	0.65	0.77	0.60	0.87	0.95
$\mathcal{F} = 0.1$	0.99	1.00	0.99	1.00	1.00	0.00	0.00	0.00	0.00	0.00
$\mathcal{F} = 1$	0.00	0.00	0.00	0.00	0.00	0.00	0.00	0.00	0.00	0.00
Mbarigo										
$\mathcal{F} = 0.01$	1.00	1.00	1.00	1.00	1.00	0.90	0.91	0.92	0.91	0.96
$\mathcal{F} = 0.1$	1.00	1.00	1.00	1.00	1.00	0.00	0.00	0.00	0.01	0.25
$\mathcal{F} = 1$	1.00	1.00	1.00	1.00	1.00	0.00	0.00	0.00	0.00	0.00
Malla Tack										
$\mathcal{F} = 0.01$	1.00	1.00	1.00	1.00	1.00	0.05	0.21	0.06	0.47	0.81
$\mathcal{F} = 0.1$	0.29	0.84	0.27	0.73	0.99	0.00	0.00	0.00	0.00	0.00
$\mathcal{F} = 1$	0.00	0.00	0.00	0.00	0.00	0.00	0.00	0.00	0.00	0.00
Ndiawdoune										
$\mathcal{F} = 0.01$	1.00	1.00	1.00	1.00	1.00	0.44	0.75	0.45	0.93	0.98
$\mathcal{F} = 0.1$	1.00	1.00	1.00	1.00	1.00	0.00	0.00	0.00	0.00	0.00
$\mathcal{F} = 1$	0.00	0.00	0.00	0.00	0.00	0.00	0.00	0.00	0.00	0.00
Ndiol Maure										
$\mathcal{F} = 0.01$	1.00	1.00	1.00	1.00	1.00	0.93	0.92	0.91	0.93	0.97
$\mathcal{F} = 0.1$	1.00	1.00	1.00	1.00	1.00	0.00	0.00	0.00	0.00	0.14
$\mathcal{F} = 1$	0.48	0.88	0.46	0.64	1.00	0.00	0.00	0.00	0.00	0.00
Syer Tack										
$\mathcal{F} = 0.01$	0.98	1.00	0.99	1.00	1.00	0.00	0.01	0.00	0.04	0.31
$\mathcal{F} = 0.1$	0.00	0.05	0.00	0.02	0.51	0.00	0.00	0.00	0.00	0.00
$\mathcal{F} = 1$	0.00	0.00	0.00	0.00	0.00	0.00	0.00	0.00	0.00	0.00

4.4 Discussion

We present a series of modeling analyses to estimate the worm burden breakpoint for communities in the lower Senegal River basin, the site of one of the largest ever outbreaks of schistosomiasis that continues today. This represents, to our knowledge, the first effort to quantify worm burden breakpoints and explore their sensitivity to model parameters that can be altered through non-pharmaceutical interventions. We find that even modest reductions to these parameters can increase the breakpoint, making it easier to reach through MDA, and thus increasing the feasibility pf achieving key public health objectives including morbidity reduction and transmission control.

However, the probability of achieving these outcomes is greatly reduced when the snail force of infection is influenced by external sources of infection. Mass drug administration in particular is rendered less effective as reductions in the local worm population have less of an effect on transmission in a more connected environment. Sufficient transmission reduction to reach elimination targets in such environments is possible via non-pharmaceutical interventions that target the intermediate host snail population or reduce human exposure.

The addition of non-pharmaceutical interventions to a routine annual MDA campaign is found to increase the probability of achieving transmission control and elimination as a public health

problem. Snail control (affecting model parameter μ_N) and exposure reduction (model parameter ω_2) are particularly effective at increasing the success of simulated interventions, particularly when external sources of transmission are low. Snail habitat reduction (model parameter K) is found to be less effective, reflecting the amplifying nature of the parasite whereby small numbers of infected snails produce large numbers of cercariae that cause infection in humans. Contamination reduction (model parameter ω_1) is also found to be less effective, particularly when external sources of infection are high. This exemplifies the key role of connectivity in determining elimination feasibility, as reducing local contamination is met with decreasing returns in terms of reductions in the snail force of infection if external sources are sufficient to maintain snail infections.

These results imply that supplementing MDA efforts with snail control and interventions aimed at reducing human exposure to schistosome-contaminated freshwater bodies may be more successful at achieving sustainable schistosomiasis control. Particularly in hotspots that have a history of not responding to MDA-based strategies, we advocate for the addition of NPIs which serve to reduce $R_e(W)$, thus increasing the breakpoint (W_{bp}) and reducing the bounce back rate following MDA treatments. [20,152,164,165] Snail control, improvements in sanitation, education, and other behavioral changes were critical components of previous successes in controlling and eliminating schistosomiasis. [77] Our analyses contribute to explaining why these NPIs are integral to achieving sustainable reductions in transmission, and provide a quantitative framework to explore the joint contributions of MDA and NPIs in different transmission environments.

We seek to capture key sources of heterogeneity in the human and parasite populations including variability in human susceptibility to infection, high correlation in compliance between MDA events, demographic stochasticity in the parasite population, and highly variable egg production by mated parasite pairs and cercarial production by infected snails. Despite these efforts, additional sources of variability affecting the efficacy of NPIs and the influence of external sources of infection are likely to influence transmission in the real world. Individual heterogeneity in behaviors contributing to both exposure and contamination are important to schistosomiasis transmission dynamics and are also likely to vary through time. [166,167] Additional sources of temporal heterogeneity such as seasonality may also be considered in the future, along with corresponding considerations of the timing of MDA and NPIs.

The modeling analyses considered here also build on a fairly cursory conception of an external source of infection, in that they only consider contributions of primary larval miracidia to the local dynamics of interest. While it is has been demonstrated that both cercariae [161] and snails [145] can be transported between hydrologically connected sites, we assume here that miracidial production by systematically untreated individuals outside of the modeled population or zoonotic sources are more important to capturing transmission dynamics. Furthermore, a simple formulation of the snail force of infection was chosen here for analytic tractability in the reproduction number and breakpoint analyses, but simulations incorporating non-linear snail force of infection dynamics derived previously [79] will be pursued in future analyses.

Moving forward, it is essential to develop strategies that make real the NPIs that result in the parameter reductions modeled here. A recent large scale trial comparing biannual MDA to biannual MDA plus a snail control intervention and biannual MDA plus a behavioral intervention in the low transmission setting of Zanzibar found evidence that these supplemental interventions were effective in further reducing transmission, though the differences did not reach significance. [43] Meanwhile, with a goal of elimination and control by 2023 for schistosomiasis, soil-transmitted helminths, lymphatic filariasis, and trachoma, Kenya's Ministry of Health has recently implemented a national "breaking transmission strategy". [168] This national campaign has objectives to expand WASH-based interventions, mainstream behavior change as an intervention to combat schistosomiasis and other NTDs, and increase MDA coverage. This also highlights the added benefit of NPIs to reduce transmission of NTDs other than schistosomiasis in areas where co-endemicity occurs.

Recent findings make the successful development and implementation of NPIs even more important to achieving near-term goals of schistosomiasis control and elimination. Though praziquantel remains a cheap, safe, and effective treatment, development of widespread resistance in the future remains a concern in Senegal and more broadly. [37,169,170] Indeed the effectiveness of the drug itself in killing adult parasites is being revisited as findings from genetic analyses and more sensitive diagnostic assays have suggested that the true efficacy of the drug in killing adult schistosomes may be lower than previously estimated. [54,171] Identification of hybrid *S. bovis* and *S. haematobium* [81] strains and infected rodents [82] that are capable of sustaining transmission also suggest that external sources of infection capable of sustaining snail infections even as human treatment is successful—such as those considered in the modeling analyses here—are a substantial challenge to elimination. Future efforts to quantify just how much these sources of miracidia contribute to transmission would aid in the parameterization of future modeling analyses.

Finally, broader challenges to controlling and eliminating schistosomiasis and other helminthiases remain. Positive feedback loops between helminth infection and poverty—so-called poverty traps—are pernicious products of global economic systems that exploit many nations in the global south where NTDs remain pervasive. [50,121,152] In addition, climate change is expected to shift the geographic range of schistosomiasis, with net increases in the number of people at risk likely. [172] Global food production and the expansion of industrialized agricultural practices into schistosomiasis-endemic areas are also expected to complicate efforts to control and eliminate schistosomiasis and other NTDs. [110,173–175]

In conclusion, we show that NPIs are a critical component of schistosomiasis elimination efforts. By increasing the breakpoint, NPIs compliment MDA to increase the likelihood of sustainable reductions in schistosomiasis transmission. Integrated control strategies that incorporate MDA and NPIs should be pursued to combat present and future challenges to achieving elimination of schistosomiasis and other helminthiases

4.5 Supplementary Information

Solving for model parameters

Human to Snail FOI (Λ)

Beginning with the basic schistosomiasis model with $S-E-I$ infection dynamics and logistic population growth among the intermediate host snail population we have three ODEs and one simple relation between each infection class and the total snail population, N:

$$\frac{dS}{dt} = f_N(S+E) - (\mu_N + \Lambda)S$$

$$\frac{dE}{dt} = \Lambda S - (\mu_N + \sigma)E$$

$$\frac{dI}{dt} = \sigma E - \mu_I I$$

$$N = S + E + I$$

Where Λ is the human-to-snail force of infection (FOI). We can first solve for the snail population carrying capacity, K, assuming known intrinsic reproduction rate, r, and mortality rate, μ_N, and input equilibrium snail abundance, N_{eq}:

$$K = N_{eq}\left(1 - \frac{\mu_n}{r}\right)$$

Next, at equilibrium infection dynamics, $\frac{dS}{dt} = \frac{dE}{dt} = \frac{dI}{dt} = 0$ we have:

$$E_{eq} = \frac{\Lambda S_{eq}}{\mu_N + \sigma}$$

$$I_{eq} = \frac{\sigma E_{eq}}{\mu_I} = \frac{\sigma \Lambda \mathrm{S_{eq}}}{\mu_I(\mu_N + \sigma)}$$

and therefore:

$$N_{eq} = S_{eq}\left(1 + \frac{\Lambda}{\mu_N + \sigma} + \frac{\sigma\Lambda}{\mu_I(\mu_N + \sigma)}\right)$$

In addition, we can solve equation 1 representing susceptible snail dynamics for N^* in terms of Λ as:

$$N_{eq}(\Lambda) = K\left(1 - \frac{\mu_N + \Lambda}{r\left(1 + \frac{\Lambda}{\mu_N + \sigma}\right)}\right)$$

Which gives:

$$S_{eq} = \frac{K\left(1 - \frac{\mu_N + \Lambda}{r\left(1 + \frac{\Lambda}{\mu_N + \sigma}\right)}\right)}{1 + \frac{\Lambda}{\mu_N + \sigma} + \frac{\sigma\Lambda}{\mu_I(\mu_N + \sigma)}}$$

and

$$I_{eq} = \frac{K\sigma\Lambda\left(1 - \frac{\mu_N + \Lambda}{r\left(1 + \frac{\Lambda}{\mu_N + \sigma}\right)}\right)}{(\mu_I(\mu_N + \sigma))\left(1 + \frac{\Lambda}{\mu_N + \sigma} + \frac{\sigma\Lambda}{\mu_I(\mu_N + \sigma)}\right)}$$

Which simplifies to:

$$I_{eq} = \frac{K\sigma\left(1 - \frac{\mu_N + \Lambda}{r\left(1 + \frac{\Lambda}{\mu_N + \sigma}\right)}\right)}{\left(\frac{\mu_I(\mu_N + \sigma)}{\Lambda} + \mu_I + \sigma\right)} = \frac{\sigma N_{eq}}{\left(\frac{\mu_I(\mu_N + \sigma)}{\Lambda} + \mu_I + \sigma\right)}$$

Therefore with infected snail prevalence, $I_P = I_{eq}/\mathrm{N_{eq}}$, and other snail population and infection parameters as inputs, we can estimate Λ as:

$$I_P = \frac{\sigma}{\frac{\mu_I(\mu_N + \sigma)}{\Lambda} + \mu_I + \sigma}$$

$$\Lambda = \frac{\mu_I(\mu_N + \sigma)}{\frac{\sigma}{I_P} - \mu_I - \sigma}$$

Human exposure ($\boldsymbol{\omega_1}$) and contamination ($\boldsymbol{\omega_2}$)

From I_{eq}, we can next estimate the equilibrium cercarial concentration, $C_{eq} = I_{eq}\theta$. Taking α, the mean probability of infection given cercarial exposure as known [55,57,58], we can thus solve for ω_1 from:

$$\omega_1 = \frac{W_{eq}(\mu_H + \mu_W)}{\alpha C_{eq}}$$

With ω_1, we next make the assumption that $\omega_1 = \omega_2$, in line with previous modeling work assuming behaviors contributing to both exposure and contamination are closely related [79], therefore we can estimate the equilibrium, locally generated miracidial concentration, $M_{eq}^{L} = 0.5W_{eq}H\Phi\left(W_{eq}, \kappa\right)\rho\left(W_{eq}, \kappa, \gamma\right)mUv\omega_2$ and solve for β assuming linear human-to-snail FOI:

$$\beta = \frac{\Lambda N_{eq}}{M_{eq}^{L}}$$

In the presence of external miracidial inputs, β can simply be estimated by substituting M_{eq}^{T} for M_{eq}^{L} in the above.

Dynamic aggregation parameters

To estimate the dynamic aggregation parameters, a and b, of the function $\kappa(W) = 1 - e^{aW^b}$, we first use all estimates of W and κ estimated from the 12 Senegalese communities (below, Supp Fig 1) to estimate the best global estimate of b. We then solve for a for each community given its equilibrium worm burden, W_{eq}, and dispersion parameter and use the resulting equation to model the response of κ to W for each community as W is perturbed.

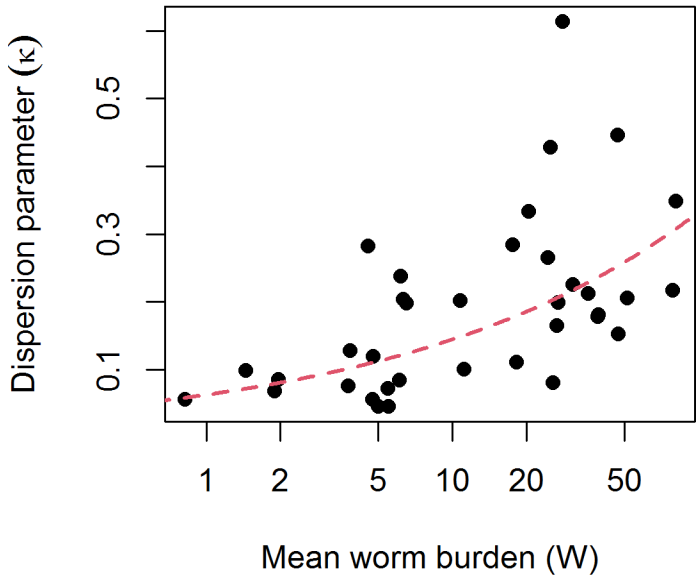

Supplementary Figure 1: Relationship between mean worm burden (W) and worm burden dispersion parameter (κ) with best fit line used to derive the dynamic aggregation parameter, b.

Individual-based model

Snail infection dynamics proceed as in the mass action model and are linked to human infection dynamics first via cercarial shedding by the infected snail population, I, where $C = \theta I$ gives the total number of cercariae produced and $C_{i,t} = \text{Pois}(\omega_2 C)$ gives stochastic individual, i, cercarial exposures. The exposure parameter ω_2 is here considered constant across individuals, but could also be made to vary between individuals by drawing from e.g. a gamma distribution. Individual worm acquisition, sex determination, and death are determined at each time step, t, as a function of cercarial exposure, $C_{i,t}$, individual susceptibility, α_i, and adult worm mortality rate, μ_W:

$$W_{i,t+1} \sim W_{i,t} + \sum_{C_{i,t}} B(1, e^{-\alpha_i}) - \sum_{W_{i,t}} B(1, 1 - e^{-\mu_W})$$

$$W_{f_{i,t+1}} \sim W_{f_{i,t}} + \sum_{W_i} B(1, 0.5) - \sum_{W_{f_{i,t}}} B(1, 1 - e^{-\mu_W})$$

$$W_{m_{i,t+1}} \sim W_{i,t} - W_{f_{i,t}} - \sum_{W_{m_{i,t}}} B(1, 1 - e^{-\mu_W})$$

The number of mated pairs and their stochastic egg output are then estimated as:

$$W_{\phi,t} \sim \min\left(W_{m_{i,t}}, W_{f_{i,t}}\right)$$

$$\mathcal{E}_{i,t} \sim \sum_{W_{\phi,t}} NB(mW_{\phi_i}, \kappa_\phi)$$

And the link back to the snail population is made via estimation of the number of miracidia, M_t, interacting with the snail population, where ω_1 is again assumed constant but could be made to vary on an individual level:

$$M_t = \sum_i \mathcal{E}_{i,t} \omega_1 U v$$

$R_e(W)$ profiles for different external miracidial input fractions ($\mathcal{F}$)

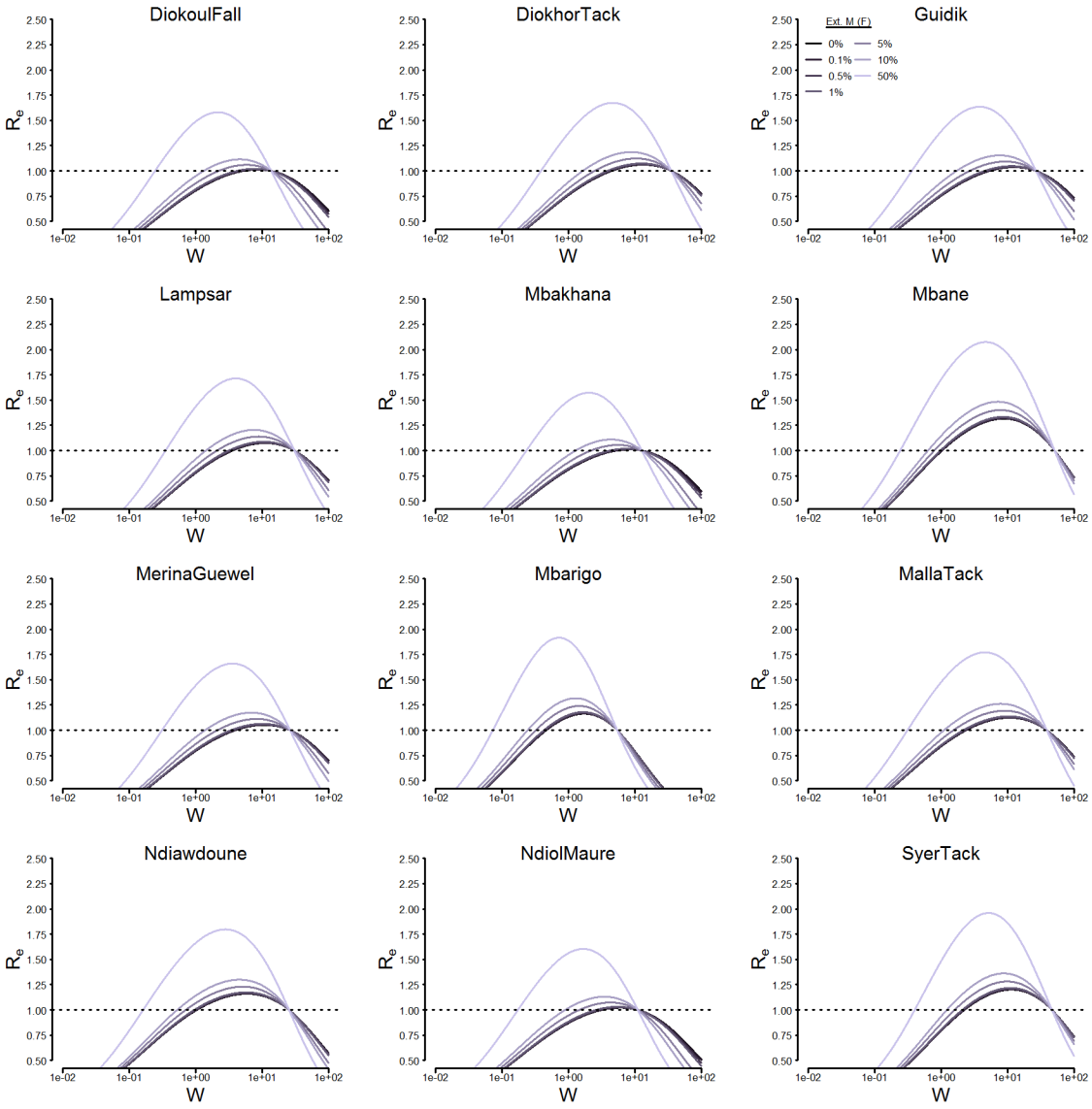

Supplementary Figure 2: Effective reproduction number, $R_e(W)$, profiles across different values of the external miracidial input fraction, $\mathcal{F}$.

Chapter 5: Conclusions

As the global conversation shifts towards elimination for schistosomiasis and other NTDs, a better understanding of the processes and strategies that contribute to elimination will be essential. Here I have used schistosomiasis as a study system to better understand the effects of positive density dependence and breakpoint phenomena on helminthiases transmission and to elucidate the role of positive density dependence in global elimination efforts. I have developed a novel dynamic model of schistosomiasis that explicitly accounts for adult parasite mating dynamics to better investigate transmission dynamics approaching elimination. Using the model, I have identified schistosomiasis control strategies that take advantage of positive density

dependent mate limitation to alter the breakpoint, making it easier to achieve elimination. This model is made freely available in the open-source R statistical programming language as an R package at https://github.com/cmhoove14/Schisto_IBM to facilitate its further use. Indeed, all code and data necessary to reproduce the analyses conducted for this dissertation are freely available on github at https://github.com/cmhoove14. This accessibility is representative of my commitment to promoting and practicing reproducible workflows to increase trust and transparency in science.

As with most analyses, the preceding chapters raise just as many questions as they provide answers. I look forward to continuing and building on these analyses but here would like to provide some conclusive remarks for the work and what comes next. Chapter 2 on aggregation dynamics has important implications for the theory presented in Chapter 4, but also has more practical implications for ongoing control and elimination campaigns. Individuals who remain infected and continue to contribute to transmission are likely not being reached through traditional MDA or other treatment routes. This makes continued MDA in elimination settings potentially less cost-effective as many treatments may be allocated to individuals who are no longer infected nor contributing to further transmission. Identifying individuals who do remain infected and treating them will require more boots-on-the-ground investigative epidemiology, more sensitive diagnostics, and more integrated approaches to control such as those proposed in Chapters 3 and 4.

Presuming aggregation dynamics are in part driven by individual heterogeneity in susceptibility to infection, the ability to identify individuals at high risk for infection would also be valuable. I will explore the impact of such a diagnostic and treatment strategies that build on it to more explicitly target high-risk individuals in future analyses. In addition, I have begun researching the immunology of helminthiases more generally and hope to build on this knowledge to identify measurable determinants of helminth susceptibility that could be assessed on a population level.

Chapters 3 and 4 advocate for an expanded view of schistosomiasis control and elimination that integrates novel and “old-school” interventions with MDA-based strategies. I do not mean to detract from the importance of MDA as a backbone to any control strategy. The reductions in morbidity, particularly among school-aged children, associated with MDA are essential for the long term health of these populations. But if we are to meet the ambitious target of schistosomiasis elimination in the next decade, we will have to broaden our thinking. In Chapter 3, I have proposed a novel intervention that uses prawn aquaculture to combat schistosomiasis via biocontrol of the intermediate host snail population. The proposed intervention also has co-benefits as prawns are a valuable food commodity that can serve both as a food source and as a generator of revenue for producers. I have been excited to track the progress of an aquaculture facility being built in Senegal by collaborators on this project and am hopeful that the proposed intervention may soon become a reality. At such time, there will be plenty of additional measurement and analysis to be done to validate the modeling analyses performed here in the field.

In Chapter 4, I have collated ecological theory, environmental health perspectives on the importance of exposure and risk as key determinants of health, and mathematical simulation in an attempt to clarify how I believe schistosomiasis elimination should be pursued. I believe the main contribution of this work is to provide a quantifiable target, the breakpoint, for elimination. Many preceding analyses have proposed MDA coverages and reductions in transmission necessary to achieve elimination, but elimination in these analyses is frequently ill-defined. By measuring the breakpoint, I here am able to place a number on an elimination target. Furthermore, I show that it can be manipulated through non-pharmaceutical interventions to make it easier to achieve, and I present methods for estimating the precise number of treatments that may be necessary to achieve it. I hope to build on the connections I have made through this dissertation with researchers at the Schistosomiasis Consortium for Operational Research and Evaluation (SCORE) and elsewhere to apply this thinking in the field.

5.1 Future directions: vaccination, development, and decolonization

It is impossible to spend four years at Berkeley and not be convinced of the universal importance of the social determinants of health. Yet, this perspective is often lacking when considering how best to control and eliminate schistosomiasis and other NTDs. This leads to what I see as a sense of complacency and lack of innovation in this global health space. The ultimate product of this is an excessive reliance on what intuition tells us should be easy fixes. Treat people, and we should control and ultimately eliminate the disease. If treating people fails, treat more people or treat them more frequently. But decades of evidence and the theory explored in this dissertation show that this mantra is far from a panacea. This should lead us to ask what the real, sustainable solution is, and do everything in our power to get there. I believe there are two answers that are quite simple in concept, but exceedingly difficult in practice.

The first answer is vaccination. Vaccines have been humanity's predominant weapon against infectious diseases for the past century and have led to unprecedented improvements in life expectancy and public health, often for pennies on the dollar.[176] Various vaccines for schistosomiasis and other NTDs are in development,[172] but parasitic diseases pose unique challenges for vaccine development. Parasites are complex, multicellular organisms that have co-evolved with *Homo sapiens* and our ancestors for millennia, all the while "learning" how best to evade our immune systems. The first known case of schistosomiasis, for instance, was identified from skeletal remains in modern-day Syria from nearly 10,000 years ago.[177] Given that vaccines generally seek to train our immune systems to recognize and combat infections before experiencing the real causative agent, this is problematic. Arming the immune system with more tools to fight a parasite that already has defenses against those tools is a losing battle.

Despite this, there is ample evidence that vaccination against schistosomiasis could work. Adults are generally less heavily infected than children in highly endemic areas, perhaps due to the effects of acquired immunity.[24,57] A population of heavily exposed individuals in Brazil also appear to be entirely immune to schistosomiasis,[178] further suggesting that the human immune system can adequately subdue schistosome parasites. In Chapter 2, I explore variation in individual susceptibility as a potential driver of aggregation dynamics, but determining what

produces this variability, and deriving methods for quantifying it, are exciting next steps. Ultimately, I believe this will rely on measuring immune function in some way, and I look forward to exploring this area of research in the future. Identifying these drivers of individual variability also has implications for successful vaccination development, particularly if some fundamental characteristic of immune function causes this variability. Determining what makes some individuals more susceptible and others more resilient could prove valuable in the manufacturing of future vaccines against schistosomiasis and other helminthiases.

The second answer—bringing us back to the social determinants of health—is development. Areas that have successfully eliminated schistosomiasis on a broad scale—Japan, Brazil, China, Caribbean island nations, and some nations of the Middle East and northern Africa—have experienced widespread concomitant development. This brings about improvements in sanitation and hygiene, reductions in exposure associated with farming and other pastoral activities that require water contact, and improved access to healthcare. These improvements are directly in line with the types of non-pharmaceutical interventions I advocate in Chapter 4. These improvements lead to enduring reductions in transmission intensity—quantifiable by R_0—that can eventually lead to environments that are not suitable for transmission, particularly combined with widespread treatment via MDA.

Also demonstrated in Chapter 4 is the barrier between elimination and endemic infection—quantifiable by the breakpoint—is exceedingly low in presence of high connectivity and a suitable environment for transmission. The recent outbreak and apparent establishment of endemic schistosomiasis in southern Europe on the island of Corsica is exemplary of this. It appears as though a single infected individual shedding miracidia in an area with suitable snail hosts was able to cause an outbreak of schistosomiasis in a tourist area where many people spent extended time in the same water bodies.[9] But the outbreak in Corsica was quickly recognized and investigated, and the affected individuals were diagnosed and treated in an easily accessible healthcare system. Contrast this with the situation in most of sub-Saharan Africa where schistosomiasis is highly endemic. A child may exhibit symptoms of acute schistosomiasis that go untreated, eventually subsiding into more manageable day-to-day symptoms such as hematuria, and the child will hopefully be treated in a school-based national deworming program at some point in their future. However, that child then returns to an unaltered environment which caused their infection in the first place, thus continuing an endless cycle of treatment and reinfection.[179]

The broader social, political, and economic drivers of these systems are beyond my realm of expertise, but I feel compelled to express my beliefs here, regardless. The globalized world in which we live has undoubtedly brought about tremendous innovation and prosperity. Indeed, it has brought about tremendously successful companies such as Merck which have the capability to manufacture and distribute millions of doses of praziquantel to sub-Saharan Africa every year to treat individuals with schistosomiasis. But the benefits of these systems are increasingly aggregated at the very top of society. Individuals and whole societies that have historically been exploited or neglected continue to be oppressed.

This has led to emerging calls to decolonize global health.[180,181] These calls are based on the remnants of western colonial systems that were built on white supremacy and white saviorism and still permeate global health institutions. The majority of the funding, leadership, ideas, and institutions that drive global health strategies and decision making are western-focused. Decolonizing global health would shift some of the power to institutions that are better integrated with the people whose lives and livelihoods are at stake, including national and regional governments, non-governmental organizations led by and organized by black, indigenous, and other people of color (BIPOC), and non-western academic institutions.[181] Decolonization would also amplify the voice of BIPOC and other marginalized groups within institutions such as the World Health Organization and the Gates Foundation which increasingly drive global health strategies.

Decolonizing global health is an essential part of development and of eliminating NTDs such as schistosomiasis because disease and development are intrinsically linked. Positive feedback loops between schistosomiasis and poor living conditions lead to "poverty traps" that are difficult to break. [121,122,166,182] Another emerging theme of my work not represented in this dissertation is an investigation of the effects of agrochemical pollution on schistosomiasis ecology and epidemiology.[110,162,173] Given historical links between agricultural improvements and development, I look forward to further investigations and collaborations on the complex links between schistosomiasis, agricultural expansions, and development.

I began my career in public health, and specifically in the environmental determinants of infectious disease, seven years ago. It was mostly unintentional and driven by a feeling that I was not spending enough time outside, having moved from bucolic Manchester, Tennessee to bustling Atlanta, Georgia for college. Slowly, but with increasing clarity, a career that merged my passions for the outdoors, for math, and for helping others began to take shape. I am fortunate that these past seven years have felt like the beginning of a career, rather than a septennial toil of endless studying. However, I also am glad that my chosen vocation in academia allows and invites a fair amount of toiling in books, for there is no limit to the virtue of knowledge.

References

1. U Olveda, D. Bilharzia: Pathology, Diagnosis, Management and Control. *Trop. Med. Surg.* **01**, 135 (2013).
2. Feldmeier, H., Krantz, I. & Poggensee, G. Female Genital Schistosomiasis as a Risk-Factor for the Transmission of HIV. *Int. J. STD AIDS* **5**, 368–372 (1994).
3. Hotez, P. J. *et al.* Female genital schistosomiasis and HIV/AIDS: Reversing the neglect of girls and women. *PLoS neglected tropical diseases* **13**, e0007025 (2019).
4. Tchuem Tchuenté, L.-A. *et al.* Evaluation of Circulating Cathodic Antigen (CCA) Urine-Tests for Diagnosis of Schistosoma mansoni Infection in Cameroon. *PLoS Negl. Trop. Dis.* **6**, e1758 (2012).
5. Coulibaly, J. T. *et al.* Accuracy of Urine Circulating Cathodic Antigen (CCA) Test for Schistosoma mansoni Diagnosis in Different Settings of Côte d'Ivoire. *PLoS Negl. Trop. Dis.* **5**, e1384 (2011).
6. Kremsner, P. G. *et al.* Circulating anodic and cathodic antigen in serum and urine from schistosoma haematobium-infected cameroonian children receiving praziquantel: A longitudinal study. *Clin. Infect. Dis.* **18**, 408–413 (1994).
7. GBD 2017 Disease and Injury Incidence and Prevalence Collaborators, S. L. *et al.* Global, regional, and national incidence, prevalence, and years lived with disability for 354 diseases and injuries for 195 countries and territories, 1990-2017: a systematic analysis for the Global Burden of Disease Study 2017. *Lancet (London, England)* **392**, 1789–1858 (2018).
8. World Health Organization. Schistosomiasis: progress report 2001 - 2011, strategic plan 2012 - 2020. (2013).
9. Boissier, J. *et al.* Outbreak of urogenital schistosomiasis in Corsica (France): an epidemiological case study. *Lancet Infect. Dis.* **16**, 971–979 (2016).
10. French, M. D. *et al.* Schistosomiasis in Africa: Improving strategies for long-term and sustainable morbidity control. *PLoS Negl. Trop. Dis.* **12**, e0006484 (2018).
11. Fenwick, A. & Jourdan, P. Schistosomiasis elimination by 2020 or 2030? *Int. J. Parasitol.* **46**, 385–388 (2016).
12. Toor, J. *et al.* Predicted Impact of COVID-19 on Neglected Tropical Disease Programs and the Opportunity for Innovation. *Clin. Infect. Dis.* (2020). doi:10.1093/cid/ciaa933
13. Landouré, A. *et al.* Significantly Reduced Intensity of Infection but Persistent Prevalence of Schistosomiasis in a Highly Endemic Region in Mali after Repeated Treatment. *PLoS Negl. Trop. Dis.* **6**, e1774 (2012).
14. Koukounari, A. *et al. Schistosoma haematobium* Infection and Morbidity Before and After Large-Scale Administration of Praziquantel in Burkina Faso. *J. Infect. Dis.* **196**, 659–669 (2007).
15. Kittur, N. *et al.* Persistent Hot spots in Schistosomiasis Consortium for Operational Research and Evaluation Studies for Gaining and Sustaining Control of Schistosomiasis after Four Years of Mass Drug Administration of Praziquantel. *Am. J. Trop. Med. Hyg.* tpmd190193 (2019). doi:10.4269/ajtmh.19-0193
16. Colley, D. G. *et al.* Defining Persistent Hotspots: Areas That Fail to Decrease

Meaningfully in Prevalence after Multiple Years of Mass Drug Administration with Praziquantel for Control of Schistosomiasis. *Am. J. Trop. Med. Hyg.* **97**, 1810–1817 (2017).
17. Liu, Y. *et al.* Interruption of schistosomiasis transmission in mountainous and hilly regions with an integrated strategy: a longitudinal case study in Sichuan, China. *Infect. Dis. Poverty* **6**, 79 (2017).
18. Rea, C. *et al.* An Integrated Strategy for Transmission Control of Schistosoma japonicum in a Marshland Area of China: Findings from a Five-Year Longitudinal Survey and Mathematical Modeling. *Am. J. Trop. Med. Hyg.* **85**, 83–88 (2011).
19. Yang, Y. *et al.* Integrated control strategy of schistosomiasis in The People's Republic of China: Projects Involving agriculture, water conservancy, forestry, sanitation and environmental modification. *Adv. Parasitol.* **92**, 237–268 (2016).
20. Liang, S., Abe, E. M. & Zhou, X.-N. Integrating ecological approaches to interrupt schistosomiasis transmission: opportunities and challenges. *Infect. Dis. Poverty* **7**, 124 (2018).
21. Allee, W. C. & Bowen, E. S. Studies in animal aggregations: Mass protection against colloidal silver among goldfishes. *J. Exp. Zool.* **61**, 185–207 (1932).
22. Stephens, P. A., Sutherland, W. J. & Freckleton, R. P. What Is the Allee Effect? *Oikos* **87**, 185 (1999).
23. May, R. M. Togetherness among Schistosomes: its effects on the dynamics of the infection. *Math. Biosci.* **35**, 301–343 (1977).
24. Anderson, R. M. R. M. & May, R. M. R. M. *Infectious Diseases of Humans*. (Oxford University Press, 1991).
25. Krkošek, M., Connors, B. M., Lewis, M. A. & Poulin, R. Allee effects may slow the spread of parasites in a coastal marine ecosystem. *Am. Nat.* **179**, 401–12 (2012).
26. Cox, R. *et al.* Mate limitation in sea lice infesting wild salmon hosts: the influence of parasite sex ratio and aggregation. *Ecosphere* **8**, e02040 (2017).
27. Arakala, A. *et al.* Estimating the elimination feasibility in the 'end game' of control efforts for parasites subjected to regular mass drug administration: Methods and their application to schistosomiasis. *PLoS Negl. Trop. Dis.* **12**, e0006794 (2018).
28. Drake, J. M. & Griffen, B. D. Early warning signals of extinction in deteriorating environments. *Nature* **467**, 456–459 (2010).
29. Boettiger, C., Mangel, M. & Munch, S. Avoiding tipping points in fisheries management through Gaussian process dynamic programming. *Proc. R. Soc. B Biol. Sci.* **282**, 20141631 (2015).
30. Sugeno, M. & Munch, S. B. A semiparametric Bayesian method for detecting Allee effects. *Ecology* **94**, 1196–1204 (2013).
31. Boissier, J. & Mone, H. Experimental observations on the sex ratio of adult Schistosoma mansoni , with comments on the natural male bias. *Parasitology* **121**, 379–383 (2000).
32. Mone, H. & Boissier, J. Sexual Biology of Schistosomes. *Adv. Parasitol.* **57**, 89–189 (2004).
33. Popiel, I. Male-stimulated female maturation in Schistosoma: A review. *J. Chem. Ecol.* **12**, 1745–1754 (1986).

34. Lu, D.-B., Deng, Y., Ding, H., Liang, Y.-S. & Webster, J. P. Single-sex schistosome infections of definitive hosts: Implications for epidemiology and disease control in a changing world. *PLOS Pathog.* **14**, e1006817 (2018).
35. Morand, S., Pointier, J.-P., Borel, G. & Theron, A. Pairing Probability of Schistosomes Related to Their Distribution Among the Host Population. *Ecology* **74**, 2444–2449 (1993).
36. Pica-Mattoccia, L. & Cioli, D. Sex- and stage-related sensitivity of Schistosoma mansoni to in vivo and in vitro praziquantel treatment. *Int. J. Parasitol.* **34**, 527–533 (2004).
37. Danso-Appiah, A. & De Vlas, S. J. Interpreting low praziquantel cure rates of Schistosoma mansoni infections in Senegal. *Trends Parasitol.* **18**, 125–129 (2002).
38. Webster, J. P. *et al.* Genetic Consequences of Mass Human Chemotherapy for Schistosoma mansoni: Population Structure Pre- and Post-Praziquantel Treatment in Tanzania. *Am. J. Trop. Med. Hyg.* **83**, 951–957 (2010).
39. Barbosa, L. M. *et al.* Repeated praziquantel treatments remodel the genetic and spatial landscape of schistosomiasis risk and transmission. *Int. J. Parasitol.* **46**, 343–350 (2016).
40. Gower, C. M. *et al.* Phenotypic and genotypic monitoring of Schistosoma mansoni in Tanzanian schoolchildren five years into a preventative chemotherapy national control programme. *Parasit. Vectors* **10**, 593 (2017).
41. Huyse, T. *et al.* Regular treatments of praziquantel do not impact on the genetic make-up of Schistosoma mansoni in Northern Senegal. *Infect. Genet. Evol.* **18**, 100–105 (2013).
42. Lelo, A. E. *et al.* No Apparent Reduction in Schistosome Burden or Genetic Diversity Following Four Years of School-Based Mass Drug Administration in Mwea, Central Kenya, a Heavy Transmission Area. *PLoS Negl. Trop. Dis.* **8**, e3221 (2014).
43. Knopp, S. *et al.* Evaluation of integrated interventions layered on mass drug administration for urogenital schistosomiasis elimination: a cluster-randomised trial. *Lancet Glob. Heal.* **7**, e1118–e1129 (2019).
44. Knopp, S. *et al.* A 5-Year intervention study on elimination of urogenital schistosomiasis in Zanzibar: Parasitological results of annual cross-sectional surveys. *PLoS Negl. Trop. Dis.* **13**, e0007268 (2019).
45. Sokolow, S. H. *et al.* Reduced transmission of human schistosomiasis after restoration of a native river prawn that preys on the snail intermediate host. *Proc. Natl. Acad. Sci. U. S. A.* **112**, 9650–9655 (2015).
46. Savaya Alkalay, A. *et al.* The prawn Macrobrachium vollenhovenii in the Senegal River basin: towards sustainable restocking of all-male populations for biological control of schistosomiasis. *PLoS Negl. Trop. Dis.* **8**, e3060 (2014).
47. Wood, C. L. *et al.* Precision mapping of snail habitat provides a powerful indicator of human schistosomiasis transmission. *Proc. Natl. Acad. Sci.* **116**, 23182 LP – 23191 (2019).
48. Haggerty, C. J. E. *et al.* Aquatic macrophytes and macroinvertebrate predators affect densities of snail hosts and local production of schistosome cercariae that cause human schistosomiasis. *PLoS Negl. Trop. Dis.* **14**, e0008417 (2020).
49. World Health Organization. *Ending the neglect to attain the Sustainable Development Goals: A road map for neglected tropical diseases 2021–2030*. (2020).
50. Spear, R., Zhong, B. & Liang, S. Low Transmission to Elimination: Rural Development as

a Key Determinant of the End-Game Dynamics of Schistosoma japonicum in China. *Trop. Med. Infect. Dis.* **2**, 35 (2017).

51. Anderson, R. M., Turner, H. C., Farrell, S. H., Yang, J. & Truscott, J. E. What is required in terms of mass drug administration to interrupt the transmission of schistosome parasites in regions of endemic infection? *Parasites and Vectors* **8**, 553 (2015).
52. Faust, C. L. *et al.* Schistosomiasis Control: Leave No Age Group Behind. *Trends in Parasitology* **36**, 582–591 (2020).
53. Adriko, M. *et al.* Low Praziquantel Treatment Coverage for Schistosoma mansoni in Mayuge District, Uganda, Due to the Absence of Treatment Opportunities, Rather Than Systematic Non-Compliance. *Trop. Med. Infect. Dis.* **3**, (2018).
54. Faust, C. L. *et al.* Two-year longitudinal survey reveals high genetic diversity of Schistosoma mansoni with adult worms surviving praziquantel treatment at the start of mass drug administration in Uganda. *Parasites and Vectors* **12**, 607 (2019).
55. Carlton, E. J., Hubbard, A., Wang, S. & Spear, R. C. Repeated Schistosoma japonicum Infection Following Treatment in Two Cohorts: Evidence for Host Susceptibility to Helminthiasis? *PLoS Negl. Trop. Dis.* **7**, e2098 (2013).
56. Irvine, M. A. *et al.* Modelling strategies to break transmission of lymphatic filariasis - aggregation, adherence and vector competence greatly alter elimination. *Parasit. Vectors* **8**, 547 (2015).
57. Wang, S. & Spear, R. C. Exploring the Contribution of Host Susceptibility to Epidemiological Patterns of Schistosoma japonicum Infection Using an Individual-Based Model. *Am. J. Trop. Med. Hyg.* **92**, 1245–1252 (2015).
58. Wang, S. & Spear, R. C. Exposure versus Susceptibility as Alternative Bases for New Approaches to Surveillance for Schistosoma japonicum in Low Transmission Environments. *PLoS Negl. Trop. Dis.* **10**, e0004425 (2016).
59. Toor, J. *et al.* Determining post-treatment surveillance criteria for predicting the elimination of Schistosoma mansoni transmission. *Parasit. Vectors* **12**, 437 (2019).
60. Kittur, N., Castleman, J. D., Campbell, C. H., King, C. H. & Colley, D. G. Comparison of Schistosoma mansoni Prevalence and Intensity of Infection, as Determined by the Circulating Cathodic Antigen Urine Assay or by the Kato-Katz Fecal Assay: A Systematic Review. *Am. J. Trop. Med. Hyg.* **94**, 605–610 (2016).
61. Knopp, S. *et al.* Urogenital schistosomiasis elimination in Zanzibar: Accuracy of urine filtration and haematuria reagent strips for diagnosing light intensity Schistosoma haematobium infections. *Parasites and Vectors* **11**, 552 (2018).
62. Bradley, D. J. & May, R. M. Consequences of helminth aggregation for the dynamics of schistosomiasis. *Trans. R. Soc. Trop. Med. Hyg.* **72**, 262–273 (1978).
63. Person, B. *et al.* Community co-designed schistosomiasis control interventions for school-aged children in Zanzibar. *J. Biosoc. Sci.* **48**, S56–S73 (2016).
64. Celone, M. *et al.* Increasing the reach: Involving local Muslim religious teachers in a behavioral intervention to eliminate urogenital schistosomiasis in Zanzibar. *Acta Trop.* **163**, 142–148 (2016).
65. Lloyd-Smith, J. O. Maximum Likelihood Estimation of the Negative Binomial Dispersion Parameter for Highly Overdispersed Data, with Applications to Infectious Diseases. *PLoS One* **2**, e180 (2007).

66. R Core Team. R: A language and environment for statistical computing. (2015).
67. Van Lieshout, L. *et al.* Analysis of Worm Burden Variation in Human Schistosoma mansoni Infections by Determination of Serum Levels of Circulating Anodic Antigen and Circulating Cathodic Antigen. *J. Infect. Dis.* **172**, 1336–1342 (1995).
68. Hubbard, A. *et al.* Estimating the distribution of worm burden and egg excretion of Schistosoma japonicum by risk group in Sichuan Province, China. *Parasitology* **125**, 221–31 (2002).
69. De Vlas, S. J., Van Oortmarssen, G. J., Habbema, J. D., Gryseels, B. & Polderman, A. M. A model for variations in single and repeated egg counts in schistosoma mansoni infections. *Parasitology* **104**, 451–460 (1992).
70. Csilléry, K., François, O. & Blum, M. G. B. Abc: An R package for approximate Bayesian computation (ABC). *Methods Ecol. Evol.* **3**, 475–479 (2012).
71. Halekoh, U., Højsgaard, S. & Yan, J. The R package geepack for generalized estimating equations. *J. Stat. Softw.* **15**, 1–11 (2006).
72. Wickham, H. *et al.* Welcome to the Tidyverse. *J. Open Source Softw.* **4**, 1686 (2019).
73. Klepac, P., Metcalf, C. J. E., McLean, A. R. & Hampson, K. Towards the endgame and beyond: complexities and challenges for the elimination of infectious diseases. *Philos. Trans. R. Soc. B Biol. Sci.* **368**, 20120137 (2013).
74. Toor, J. *et al.* Are We on Our Way to Achieving the 2020 Goals for Schistosomiasis Morbidity Control Using Current World Health Organization Guidelines? *Clin. Infect. Dis. Achiev. WHO Schistosomiasis Goals • CID* **2018**, 66
75. Colley, D. G., Andros, T. S. & Campbell, C. H. Schistosomiasis is more prevalent than previously thought: what does it mean for public health goals, policies, strategies, guidelines and intervention programs? *Infect. Dis. Poverty* **6**, 63 (2017).
76. Spear, R. C. *et al.* The challenge of effective surveillance in moving from low transmission to elimination of schistosomiasis in China. *Int. J. Parasitol.* **41**, 1243–7 (2011).
77. Sokolow, S. H. *et al.* Global assessment of schistosomiasis control over the past century shows targeting the snail intermediate host works best. *PLoS Negl. Trop. Dis.* **10**, e0004794 (2016).
78. Lo, N. C. *et al.* Impact and cost-effectiveness of snail control to achieve disease control targets for schistosomiasis. *Proc. Natl. Acad. Sci. U. S. A.* **115**, E584–E591 (2018).
79. Gurarie, D., Lo, N. C., Ndeffo-Mbah, M. L., Durham, D. P. & King, C. H. The human-snail transmission environment shapes long term schistosomiasis control outcomes: Implications for improving the accuracy of predictive modeling. *PLoS Negl. Trop. Dis.* **12**, e0006514 (2018).
80. Civitello, D. J. & Rohr, J. R. Disentangling the effects of exposure and susceptibility on transmission of the zoonotic parasite *Schistosoma mansoni*. *J. Anim. Ecol.* **83**, 1379–1386 (2014).
81. Webster, B. L., Diaw, O. T., Seye, M. M., Webster, J. P. & Rollinson, D. Introgressive Hybridization of Schistosoma haematobium Group Species in Senegal: Species Barrier Break Down between Ruminant and Human Schistosomes. *PLoS Negl. Trop. Dis.* **7**, e2110 (2013).

82. Rudge, J. W. *et al.* Identifying host species driving transmission of schistosomiasis japonica, a multihost parasite system, in China. *Proc. Natl. Acad. Sci. U. S. A.* **110**, 11457–62 (2013).
83. King, C. H., Sutherland, L. J. & Bertsch, D. Systematic review and meta-analysis of the impact of chemical-based mollusciciding for control of Schistosoma mansoni and S. haematobium transmission. *PLoS Negl. Trop. Dis.* **9**, e0004290 (2015).
84. Andrews, P., Thyssen, J. & Lorke, D. The biology and toxicology of molluscicides, bayluscide. *Pharmacol. Ther.* **19**, 245–295 (1982).
85. Dawson, V. K. Environmental fate and effects of the lampricide Bayluscide: a review. *J. Great Lakes Res.* **29**, 475–492 (2003).
86. Mkoji, G. M. *et al.* Impact of the crayfish *Procambarus clarkii* on *Schistosoma haematobium* transmission in Kenya. *Am. J. Trop. Med. Hyg.* **61**, 751–759 (1999).
87. Sokolow, S. H., Lafferty, K. D. & Kuris, A. M. Regulation of laboratory populations of snails (*Biomphalaria* and *Bulinus* spp.) by river prawns, *Macrobrachium* spp. (Decapoda, Palaemonidae): implications for control of schistosomiasis. *Acta Trop.* **132**, 64–74 (2014).
88. Roberts, J. K. & Kuris, A. M. Predation and control of laboratory populations of the snail Biomphalaria glabrata by the freshwater prawn Macrobrachium rosenbergii. *Ann. Trop. Med. Parasitol.* **84**, 401–12 (1990).
89. Islam, M. S. & Wahab, M. A. A review on the present status and management of mangrove wetland habitat resources in Bangladesh with emphasis on mangrove fisheries and aquaculture. *Hydrobiologia* **542**, 165–190 (2005).
90. Food and Agriculture Organization of the United Nations. *Report of the FAO Expert Workshop on the Use of Wild Fish and/or Other Aquatic Species as Feed in Aquaculture and its Implications to Food Security and Poverty Alleviation*. (Food and Agriculture Organization of the United Nations, 2008).
91. New, M. B., Valenti, W. C., Tidwell, J. H., D'Abramo, L. R. & Kutty, M. N. *Freshwater prawns : biology and farming*. (Blackwell Pub, 2010).
92. New, M. B., Valenti, W. C. & Wiley InterScience (Online service). *Freshwater prawn culture : the farming of Macrobrachium rosenbergii*. (Blackwell Science, 2000).
93. Levy, T. *et al.* All-female monosex culture in the freshwater prawn Macrobrachium rosenbergii – A comparative large-scale field study. *Aquaculture* **479**, 857–862 (2017).
94. WHO. *Schistosomiasis: progress report 2001–2011, strategic plan 2012–2020*. (2013).
95. Hotez, P. J. *et al.* The Global Burden of Disease Study 2010: Interpretation and Implications for the Neglected Tropical Diseases. *PLoS Negl. Trop. Dis.* **8**, e2865 (2014).
96. Balasubramanian, V., Sie, M., Hijmans, R. J. & Otsuka, K. Increasing Rice Production in Sub-Saharan Africa: Challenges and Opportunities. *Adv. Agron.* **94**, 55–133 (2007).
97. Ahmed, N. & Garnett, S. T. Sustainability of Freshwater Prawn Farming in Rice Fields in Southwest Bangladesh. *J. Sustain. Agric.* **34**, 659–679 (2010).
98. Ranjeet, K. & Kurup, B. M. Heterogeneous Individual Growth of Macrobrachium rosenbergii Male Morphotypes. *ICLARM Q.* **25**, (2002).
99. von Bertalanffy, L. A quantitative theory of organic growth (inquiries on growth laws. II). *Human Biology* **10**, 181–213 (1938).
100. Lalrinsanga, P. L. *et al.* Length Weight Relationship and Condition Factor of Giant

Freshwater Prawn Macrobrachium rosenbergii (De Man, 1879) Based on Developmental Stages, Culture Stages and Sex. *Turkish J. Fish. Aquat. Sci.* **12**, 917–924 (2012).

101. Sampaio, C. M. S. & Valenti, W. C. Growth Curves for Macrobrachium rosenbergii in Semi-Intensive Culture in Brazil. *J. WORLD Aquac. Soc.* **27**, (1996).
102. Lima, J. de F., Garcia, J. da S. & Silva, T. C. da. Natural diet and feeding habits of a freshwater prawn (Macrobrachium carcinus: Crustacea, Decapoda) in the estuary of the Amazon River. *Acta Amaz.* **44**, 235–244 (2014).
103. Lorenzen, K. The relationship between body weight and natural mortality in juvenile and adult fish: a comparison of natural ecosystems and aquaculture. *J. Fish Biol.* **49**, 627–647 (1996).
104. Nwosu, F. & Wolfi, M. Population dynamics of the Giant African River prawn Macrobrachium vollenhovenii Herklots 1857 (Crustacea, Palaemonidae) in the Cross River Estuary, Nigeria. *West African J. Appl. Ecol.* **9**, (2009).
105. Dasgupta, S. & Tidwell, J. H. A Breakeven Price Analysis of Four Hypothetical Freshwater Prawn, Macrobrachium rosenbergii, Farms Using Data from Kentucky. *J. Appl. Aquac.* **14**, 1–22 (2003).
106. Office of Management and Budget. *Discount Rates for Cost-Effectiveness Analysis of Federal Programs*. (2018).
107. Reed, W. J. Optimal harvesting models in forest management - a survey. *Nat. Resour. Model.* **1**, 55–79 (1986).
108. Karp, L., Sadeh, A. & Griffin, W. L. Cycles in Agricultural Production: The Case of Aquaculture. *Am. J. Agric. Econ.* **68**, 553 (1986).
109. Guttormsen, A. G. Faustmann in the Sea: Optimal Rotation in Aquaculture. *Marine Resource Economics* **23**, 401–410 (2008).
110. Halstead, N. T. *et al.* Agrochemicals increase risk of human schistosomiasis by supporting higher densities of intermediate hosts. *Nat. Commun.* **9**, 837 (2018).
111. Ciddio, M. *et al.* The spatial spread of schistosomiasis: A multidimensional network model applied to Saint-Louis region, Senegal. *Adv. Water Resour.* **108**, 406–415 (2016).
112. Lafferty, K. D. & Kuris, A. M. Parasitic castration: the evolution and ecology of body snatchers. *Trends Parasitol.* **25**, 564–572 (2009).
113. Mangal, T. D., Paterson, S. & Fenton, A. Effects of Snail Density on Growth, Reproduction and Survival of Biomphalaria alexandrina Exposed to Schistosoma mansoni. *J. Parasitol. Res.* **2010**, 1–6 (2010).
114. Chu, K. Y. & Dawood, I. K. Cercarial production from Biomphalaria alexandrina infected with Schistosoma mansoni. *Bull. World Health Organ.* **42**, 569–74 (1970).
115. Holling, C. S. The Components of Predation as Revealed by a Study of Small-Mammal Predation of the European Pine Sawfly. *Can. Entomol.* **91**, 293–320 (1959).
116. Soetaert, K., Petzoldt, T. & Setzer, R. W. Solving Differential Equations in R: Package deSolve. *J. Stat. Softw.* **33**, 1–25 (2010).
117. Lo, N. C. *et al.* Assessment of global guidelines for preventive chemotherapy against schistosomiasis and soil-transmitted helminthiasis: a cost-effectiveness modelling study. *Lancet Infect. Dis.* **16**, 1065–1075 (2016).
118. Beverton, R. J. H. & Holt, S. J. *On the Dynamics of Exploited Fish Populations*. (Springer

Netherlands, 1993). doi:10.1007/978-94-011-2106-4
119. Zwang, J. & Olliaro, P. L. Clinical Efficacy and Tolerability of Praziquantel for Intestinal and Urinary Schistosomiasis—A Meta-analysis of Comparative and Non-comparative Clinical Trials. *PLoS Negl. Trop. Dis.* **8**, e3286 (2014).
120. Lo, N. C. *et al.* Comparison of community-wide, integrated mass drug administration strategies for schistosomiasis and soil-transmitted helminthiasis: a cost-effectiveness modelling study. *Lancet Glob. Heal.* **3**, e629–e638 (2015).
121. Ngonghala, C. N. *et al.* Poverty, Disease, and the Ecology of Complex Systems. *PLoS Biol.* **12**, e1001827 (2014).
122. King, C. H. Parasites and poverty: The case of schistosomiasis. *Acta Trop.* **113**, 95–104 (2010).
123. Younes, A., El-Sherief, H., Gawish, F. & Mahmoud, M. Biological control of snail hosts transmitting schistosomiasis by the water bug, Sphaerodema urinator. *Parasitol. Res.* **116**, 1257–1264 (2017).
124. Asche, F. Farming the Sea. *Marine Resource Economics* **23**, 527–547 (2008).
125. Kumar, G. & Engle, C. R. Technological Advances that Led to Growth of Shrimp, Salmon, and Tilapia Farming. *Rev. Fish. Sci. Aquac.* **24**, 136–152 (2016).
126. Karplus, I. & Sagi, A. The Biology and Management of Size Variation. in *Freshwater Prawns* 316–345 (Wiley-Blackwell). doi:10.1002/9781444314649.ch16
127. Ventura, T. & Sagi, A. The insulin-like androgenic gland hormone in crustaceans: From a single gene silencing to a wide array of sexual manipulation-based biotechnologies. *Biotechnol. Adv.* **30**, 1543–1550 (2012).
128. Aflalo, E. D. *et al.* A novel two-step procedure for mass production of all-male populations of the giant freshwater prawn Macrobrachium rosenbergii. *Aquaculture* **256**, 468–478 (2006).
129. Levy, T. *et al.* A Single Injection of Hypertrophied Androgenic Gland Cells Produces All-Female Aquaculture. *Mar. Biotechnol.* **18**, 554–563 (2016).
130. Savaya-Alkalay, A. *et al.* Exploitation of reproductive barriers between Macrobrachium species for responsible aquaculture and biocontrol of schistosomiasis in West Africa. *Aquac. Environ. Interact.* **10**, 487–499 (2018).
131. Halstead, N. T., Civitello, D. J. & Rohr, J. R. Comparative toxicities of organophosphate and pyrethroid insecticides to aquatic macroarthropods. *Chemosphere* **135**, 265–271 (2015).
132. Civitello, D. J., Fatima, H., Johnson, L. R., Nisbet, R. M. & Rohr, J. R. Bioenergetic theory predicts infection dynamics of human schistosomes in intermediate host snails across ecological gradients. *Ecol. Lett.* **21**, 692–701 (2018).
133. Perez-Saez, J. *et al.* A Theoretical Analysis of the Geography of Schistosomiasis in Burkina Faso Highlights the Roles of Human Mobility and Water Resources Development in Disease Transmission. *PLoS Negl. Trop. Dis.* **9**, e0004127 (2015).
134. Perez-Saez, J. *et al.* Hydrology and density feedbacks control the ecology of intermediate hosts of schistosomiasis across habitats in seasonal climates. *Proc. Natl. Acad. Sci.* **113**, 6427–6432 (2016).
135. Sturrock, R. F. *et al.* Seasonality in the transmission of schistosomiasis and in populations

of its snail intermediate hosts in and around a sugar irrigation scheme at Richard Toll, Senegal. *Parasitology* **123**, 77–89 (2001).

136. Cheever, A. W., Kamel, I. A., Elwi, A. M., Mosimann, J. E. & Danner, R. Schistosoma mansoni and S. haemotobium infections in Egypt. II. Quantitative Parasitological Findings at Necrospy. *Am. J. Trop. Med. Hyg.* **26**, (1977).
137. Marino, S., Hogue, I. B., Ray, C. J. & Kirschner, D. E. A methodology for performing global uncertainty and sensitivity analysis in systems biology. *J. Theor. Biol.* **254**, 178–96 (2008).
138. Wu, J. *et al.* Sensitivity analysis of infectious disease models: methods, advances and their application. *J. R. Soc. Interface* **10**, 20121018 (2013).
139. Etim, L. & Sankare, Y. Growth and mortality, recruitment and yield of the fresh-water shrimp, Macrobrachium völlenhovenii, Herklots 1851 (Crustacea, Palaemonidae) in the Fahe reservoir, Côte d'Ivoire, West Africa. *Fish. Res.* **38**, 211–223 (1998).
140. Dasgupta, S. Economics of freshwater prawn farming in the United States. *South. Reg. Aquac. Cent.* **Nov**, 1–8 (2005).
141. Tidwell, J. H., D'Abramo, L. R., Coyle, S. D. & Yasharian, D. Overview of recent research and development in temperate culture of the freshwater prawn (Macrobrachium rosenbergii De Man) in the South Central United States. *Aquac. Res.* **36**, 264–277 (2005).
142. Woolhouse, M. E. J. & Chandiwana, S. K. Population biology of the freshwater snail *Bulinus globosus* in the Zimbabwe highveld. *J. Appl. Ecol.* **27**, 41–59 (1990).
143. Woolhouse, M. E. J. & Chandiwana, S. K. Population Biology of the Freshwater Snail Bulinus globosus in the Zimbabwe Highveld. *J. Appl. Ecol.* **27**, 41 (1990).
144. McCreesh, N. & Booth, M. The Effect of Increasing Water Temperatures on Schistosoma mansoni Transmission and Biomphalaria pfeifferi Population Dynamics: An Agent-Based Modelling Study (vol 9, e101462, 2014). *PLoS One* **9**, (2014).
145. Head, J. R. *et al.* Genetic Evidence of Contemporary Dispersal of the Intermediate Snail Host of Schistosoma japonicum: Movement of an NTD Host Is Facilitated by Land Use and Landscape Connectivity. *PLoS Negl. Trop. Dis.* **10**, e0005151 (2016).
146. McCreesh, N., Arinaitwe, M., Arineitwe, W., Tukahebwa, E. M. & Booth, M. Effect of water temperature and population density on the population dynamics of Schistosoma mansoni intermediate host snails. *Parasit. Vectors* **7**, 9 (2014).
147. Pflüger, W., Roushdy, M. Z. & El Emam, M. The prepatent period and cercarial production of Schistosoma haematobium in Bulinus truncatus (Egyptian field strains) at different constant temperatures. *Zeitschrift für Parasitenkd. (Berlin, Ger.* **70**, 95–103 (1984).
148. King, C. H., Dickman, K. & Tisch, D. J. Reassessment of the cost of chronic helmintic infection: a meta-analysis of disability-related outcomes in endemic schistosomiasis. *Lancet* **365**, 1561–1569 (2005).
149. Cheever, A. W. A quantitative post-mortem study of schistosomiasis mansoni in man. *Am. J. Trop. Med. Hyg.* **17**, (1977).
150. Pennance, T. *et al.* Urogenital schistosomiasis transmission on Unguja Island, Zanzibar: characterisation of persistent hot-spots. *Parasit. Vectors* **9**, 646 (2016).
151. Binder, S. *et al.* Lessons learned in conducting mass drug administration for

schistosomiasis control and measuring coverage in an operational research setting. *Am. J. Trop. Med. Hyg.* **103**, 105–113 (2020).
152. Ross, A. G. P. *et al.* A new global strategy for the elimination of schistosomiasis. *Int. J. Infect. Dis.* **54**, 130–137 (2017).
153. Phillips, A. E. *et al.* Evaluating the impact of biannual school-based and community-wide treatment on urogenital schistosomiasis in Niger. *Parasit. Vectors* **13**, 557 (2020).
154. Ahmed, A. M., El Tash, L. A., Mohamed, E. Y. & Adam, I. High levels of Schistosoma mansoni infections among school children in central Sudan one year after treatment with praziquantel. in *Journal of Helminthology* **86**, 228–232 (Cambridge University Press, 2012).
155. Medley, G. & Anderson, R. M. Density-dependent fecundity in schistosoma mansoni infections in man. *Trans. R. Soc. Trop. Med. Hyg.* **79**, 532–534 (1985).
156. Neves, M. I., Webster, J. P. & Walker, M. Estimating helminth burdens using sibship reconstruction. *Parasites and Vectors* **12**, 1–12 (2019).
157. Sokolow, S. H. *et al.* Global Assessment of Schistosomiasis Control Over the Past Century Shows Targeting the Snail Intermediate Host Works Best. *PLoS Negl. Trop. Dis.* **10**, e0004794 (2016).
158. Liang, S. *et al.* Environmental effects on parasitic disease transmission exemplified by schistosomiasis in western China. *Proc. Natl. Acad. Sci. U. S. A.* **104**, 7110–7115 (2007).
159. Perez-Saez, J. *et al.* A Theoretical Analysis of the Geography of Schistosomiasis in Burkina Faso Highlights the Roles of Human Mobility and Water Resources Development in Disease Transmission. *PLoS Negl. Trop. Dis.* **9**, e0004127 (2015).
160. Gurarie, D. *et al.* Connectivity sustains disease transmission in environments with low potential for endemicity: modelling schistosomiasis with hydrologic and social connectivities. *J. R. Soc. Interface* **6**, 495–508 (2009).
161. Spear, R. C. Internal versus external determinants of Schistosoma japonicum transmission in irrigated agricultural villages. *J. R. Soc. Interface* **9**, 272–282 (2012).
162. Hoover, C. M. *et al.* Modelled effects of prawn aquaculture on poverty alleviation and schistosomiasis control. *Nat. Sustain.* **2**, 611–620 (2019).
163. Gurarie, D. & King, C. H. Population biology of Schistosoma mating, aggregation, and transmission breakpoints: more reliable model analysis for the end-game in communities at risk. *PLoS One* **9**, e115875 (2014).
164. Stothard, J. R. *et al.* Towards interruption of schistosomiasis transmission in sub-Saharan Africa: developing an appropriate environmental surveillance framework to guide and to support 'end game' interventions. *Infect. Dis. Poverty* **6**, 10 (2017).
165. Arakala, A. *et al.* Estimating the elimination feasibility in the 'end game' of control efforts for parasites subjected to regular mass drug administration: Methods and their application to schistosomiasis. *PLoS Negl. Trop. Dis.* **12**, (2018).
166. Lund, A. J. *et al.* Unavoidable risks: Local perspectives on water contact behavior and implications for schistosomiasis control in an agricultural region of Northern Senegal. *Am. J. Trop. Med. Hyg.* **101**, 837–847 (2019).
167. Seto, E. Y. W., Lee, Y. J., Liang, S. & Zhong, B. Individual and village-level study of water contact patterns and Schistosoma japonicum infection in mountainous rural China.

Trop. Med. Int. Heal. **12**, 1199–1209 (2007).
168. Republic of Kenya Ministry of Health. *The Kenya national breaking transmission strategy for soil-transmitted helminthiases, schistosomiasis, lymphatic filariasis, and trachoma*.
169. Crellen, T. *et al.* Reduced Efficacy of Praziquantel Against Schistosoma mansoni Is Associated With Multiple Rounds of Mass Drug Administration. *Clin. Infect. Dis.* **63**, 1151–1159 (2016).
170. Bergquist, R., Utzinger, J. & Keiser, J. Controlling schistosomiasis with praziquantel: How much longer without a viable alternative? *Infect. Dis. poverty* **6**, 74 (2017).
171. Lamberton, P. H. L., Kabatereine, N. B., Oguttu, D. W., Fenwick, A. & Webster, J. P. Sensitivity and Specificity of Multiple Kato-Katz Thick Smears and a Circulating Cathodic Antigen Test for Schistosoma mansoni Diagnosis Pre- and Post-repeated-Praziquantel Treatment. *PLoS Negl. Trop. Dis.* **8**, e3139 (2014).
172. Yang, G. J. & Bergquist, R. Potential impact of climate change on schistosomiasis: A global assessment attempt. *Trop. Med. Infect. Dis.* **3**, (2018).
173. Hoover, C. M. *et al.* Effects of agrochemical pollution on schistosomiasis transmission: a systematic review and modelling analysis. *Lancet Planet. Heal.* **4**, e280–e291 (2020).
174. McCreesh, N., Nikulin, G. & Booth, M. Predicting the effects of climate change on Schistosoma mansoni transmission in eastern Africa. *Parasit. Vectors* **8**, 9 (2015).
175. Rohr, J. R. *et al.* Emerging human infectious diseases and the links to global food production. *Nat. Sustain.* **2**, 445–456 (2019).
176. Greenwood, B. The contribution of vaccination to global health: past, present and future. doi:10.1098/rstb.2013.0433
177. Anastasiou, E., Lorentz, K. O., Stein, G. J. & Mitchell, P. D. Prehistoric schistosomiasis parasite found in the Middle East. *The Lancet Infectious Diseases* **14**, 553–554 (2014).
178. Gazzinelli, A. *et al.* Exposure to Schistosoma mansoni infection in a rural area of Brazil. I: Water contact. *Trop. Med. Int. Heal.* **6**, 126–135 (2001).
179. Remais, J. V & Eisenberg, J. N. Balance between clinical and environmental responses to infectious diseases. *Lancet* **379**, 1457–1459 (2012).
180. Büyüm, A. M., Kenney, C., Koris, A., Mkumba, L. & Raveendran, Y. Decolonising global health: If not now, when? *BMJ Global Health* **5**, 3394 (2020).
181. Abimbola, S. & Pai, M. Will global health survive its decolonisation? *Lancet* **396**, 1627–1628 (2020).
182. Garchitorena, A. *et al.* Disease ecology, health and the environment: a framework to account for ecological and socio-economic drivers in the control of neglected tropical diseases. *Philos. Trans. R. Soc. B Biol. Sci.* **372**, 20160128 (2017).